EMBRYONIC ORIGIN OF THE OLFACTORY SENSORY SYSTEM: FATE MAP, LINEAGE ANALYSIS AND SPECIFICATION OF THE AVIAN OLFACTORY PLACODE

Thesis by

Sujata Bhattacharyya

In Partial Fulfillment of the Requirements

for the Degree of

Doctor of Philosophy

California Institute of Technology

Pasadena, California

2005

(Defended September 8, 2004)

Acknowledgements

Accomplishing a Ph.D. is at once a solitary yet collective experience. I would like to acknowledge all the people who have made this process a uniquely enriching and greatly edifying one. First and foremost, I will always be indebted to my thesis adviser, Marianne Bronner-Fraser for her tremendous support of my development as a scientist. She has given me the independence to pursue questions of interest to me while tempering it with practical advice when required. She has joyfully shared in all my little successes and believed in me at times when it was hard for me to believe in my own abilities. She accepts that life continues to happen even in the midst of a Ph.D. and has taught me the invaluable lesson of living life to the fullest even whilst pursuing with passion one's scientific ambitions. Her infectious optimism and endless patience astound me on a daily basis and I can only hope that these qualities have rubbed off on me.

Scott Fraser, David Anderson, Kai Zinn and Bruce Hay were members of my thesis committee who kept me focused on my goal and encouraged me to delve deeper in understanding the complexity of biological mechanisms. I am particularly grateful to Scott for finding time in his extremely busy schedule to teach me how to do single cell injections and to Bruce for teaching me the basics of molecular biology when I rotated through his lab many eons ago!

Special mention must be made of my immediate placode community for equipping me with much of my knowledge, tools and necessary constructive criticism to study placodes for my thesis work. This includes two former post-docs in the lab, Clare Baker and Andy Groves who have answered countless questions over the years and taught me to approach my work in a logical and clear-thinking manner. It has been a pleasure and a unique opportunity to work in close collaboration with Andrea Streit and Andrew Bailey, both in Pasadena and in London. Andrea has been an invaluable resource in the course of my work. Her clarity of thought, deep insight and elegant experiments inspire me to do better everyday. I am grateful to all of them for their guidance and warm friendship.

I have learnt much, both at the bench and through constructive discussions with innumerable members of the Bronner-Fraser lab, past and present. They have also made graduate school a fun and stimulating experience. Tanya Moreno and Dan Meulemans, fellow graduate students have helped troubleshoot experiments, been sympathetic ears when things looked bleak and always been fun to chat with, Laura Gammill, office-mate and mentor who has always been there right behind me (literally!) with practical advice on science and life, protocols, encouragement and Vietnamese food, Martin Garcia-Castro who took me under his wings when I first rotated in Marianne's lab and has since been keenly interested in and enthusiastic about my progress and Meyer Barembaum who has calmly and patiently answered all my questions over the years. My thanks also go to Tatjana Sauka-Spengler and Vivian Lee, mines of information who are willing to chat science and eat sushi any time of the day or night, Max Ezin for being my partner in learning single-cell injections and making movies, Martin and Meghan, my other office-mates who have made grad school an illuminating cultural journey as well, Lisa, my fitness guru, David, Sara, Anne, Ed, Maria-Elena, Katy, Peter, Yun, Carole, Jack and all the technicians (particularly Andrea Manzo and Matt Jones) for their help and support. A huge thanks to Mary Flowers for so gracefully handling the endless tedium of ordering and taking care of administrative matters that makes life in lab so much easier and to Gary Belford who has taught me the value of never updating to a new operating system on a Friday evening and for taking care of things when I have!

Finally, I am truly thankful for having a very supportive family and caring friends, here and at home. I am particularly grateful to my parents for being willing to send their only child half way around the world to achieve her dreams even if it meant a great personal loss to them. I owe much of who I am today to my mother who has always been a very strong role model and encouraged me to be the best I can, both as a person and as a scientist. And lastly, I would like to acknowledge the anchor in my life, my husband, Subhabrata Sanyal for taking six years of a long distance marriage in his stride, never waning in his support of my endeavours inspite of it and always wanting the best for me! There were times I thought I wouldn't make it, but with him by my side, that has never been an option.

Abstract

Coordinating the generation of myriad cell types within the developing nervous system is an exquisite and intensely studied puzzle. The entire vertebrate peripheral nervous system derives from two multipotential cell types in the embryo: neural crest and placodes**. Neurogenic placodes** are focal ectodermal thickenings present in stereotypic positions in the head. Their derivatives are responsible for much of our sensory perceptions in the craniofacial region. The **olfactory placode** which gives rise to the olfactory epithelium mediates our sense of smell. Its derivatives include the regenerating olfactory sensory neurons, gonadotropin releasing hormone neurons, olfactory ensheathing glial cells and the basal and supporting cells. While we have some clues to the molecular mechanisms driving its differentiation into the various cell types mentioned above, little is known about the source and induction of the olfactory placode precursor cells in the early embryo.

To trace definitively the origin of the olfactory placode precursor cells, we generated a **fate-map** and compared it with patterns of gene expression in the region of the chick olfactory placode. To this end, small populations of cells in Hamburger-Hamilton (HH) stage 6 to stage 10 chick embryos were labeled with DiI and DiO and their derivatives were analyzed two days later. At head-fold stages, olfactory placode precursor cells are spread out over a broad domain and intermingle with lens, epidermal and neural precursors. As the neural folds close, the precursors appear to converge anteriorly within the ectoderm. The lens and nasal precursors sort out from each other around HH stage 8, at which time, *Pax-6* is differentially upregulated in the region fated to form the lens while *Dlx-5* expression is enhanced

in the anterior area where the nasal precursors accumulate. To further study the **cell movements** that lead to the eventual formation of the olfactory placode, I performed confocal time-lapse analysis. The cell rearrangements that I observed are consistent with two possible outcomes: 1.**specified** lens and nasal precursors have differential adhesive properties and hence sort out or 2.**unspecified** placodal precursors differentiate according to the environment in which they are positioned by stochastic movements. To distinguish between these possibilities and to clarify whether the precursors are multipotent before they segregate, I have undertaken **single cell lineage analysis**. Surprisingly, I find no evidence for a shared olfactory and lens placode lineage from single precursors even at early neurula stages, prior to their sorting out from each other in order to contribute to one or the other placode. This raises an interesting question: does the fate of these cells motivate their migration to a certain region of the embryo?

In the next part of my thesis, I have sought to answer a fundamental question in developmental biology, which is how are organs generated in precise and reproducible locations within the body. I have attempted to answer this question in the context of the olfactory sensory system. To understand how and when the nasal structure is first induced, I decided to delineate the tissue that is competent to form the olfactory placode and to determine the spatiotemporal localization of the inducing signals. In general, either one of these two parameters is strictly delimited such that the induced structure arises only in a distinct position. In order to define the extent of **competence** within the ectoderm to form the nasal placode, I have grafted quail ectoderm from different axial levels to the chick anterior neural fold at stage 8. Cranial and trunk level ectoderm are capable of responding to the inducing

signals; they express PAX6 and subsequently form the olfactory placode. However, hindbrain and trunk level ectoderm lose this competence rapidly; by stage 10 neither tissue can express PAX6. This suggests that either the inducing signals are localized anteriorly at early stages or that later signals further refine the olfactory placode-forming region. The presumptive olfactory placode ectoderm is defined by co-expression of several markers. Therefore, I have also analyzed these grafts for DLX3 expression and find a similar trend in loss of competence as seen with PAX6. A prerequisite for studying the induction of a particular fate in a tissue is determining the time at which it is still unspecified i.e. the tissue does **not** express markers exclusive to its fate when removed from its original context in the embryo and placed in a neutral environment in vitro. I examined the **specification** of the presumptive olfactory placode ectoderm to express PAX6 and DLX3 and form neurons by culturing this tissue at various stages in three-dimensional collagen gel matrices. Presumptive olfactory placode ectoderm is specified to express PAX6 and DLX3 between stages 8-10. Neuronal specification as assayed by expression of the post-mitotic neuronal marker, Hu, begins around stage 14. This implies that the ectoderm has seen signals that will direct its fate even before it is morphologically visible as a placode. I have also determined the time at which the presumptive olfactory placode ectoderm is irreversibly **committed** to its fate by grafting this tissue at different stages to the lateral plate ectoderm at the level of the most recently formed somites in the stage 8/9 chick embryo. This occurs by stage 14 as assayed by expression of PAX6 and DLX3, concomitant with a visible thickening of the placode. The next step is to determine the molecular nature of the inducing signals. Such embryological manipulations in combination with fate-mapping and lineage studies

will hopefully afford us some insight into the basic principles by which sensory systems are assembled during development.

Table of Contents

Chapter 1. Hierarchy of regulatory events in sensory placode development..... 1

1.1 Introduction 2

1.2 Neural induction: a prequel to the formation of the embryonic nervous system 3

1.3 Induction of the neural plate border region 6

1.4 Neural crest and placodes: embryonic precursors of the PNS 7

1.5 Placode induction 8

1.5A. Diverse cell types arise from the sensory and neurogenic placodes 8

1.5B. One, to many: the multiple phases of placode induction 9

1.6 Genetic networks that operate during placode induction 12

1.6A. Upstream regulators of lens-specific Pax6 expression 13

1.6B. Downstream targets of Pax6 in the lens 14

1.6C. Negative regulators of lens formation 16

1.7 Conclusions 17

Chapter 2. Segregation of lens and olfactory precursors from a common territory: cell sorting and reciprocity of Dlx5 and Pax6 expression 23

2.1 Introduction 25

2.2 Materials and methods 27

2.2A. Embryo techniques 27

2.2B. Standardization of the position of labeled cells 28

2.2C. Video time-lapse filming 29

2.2D. Whole mount in-situ hybridization, immunohostochemistry and histology 29

2.2E. Expression constructs and in ovo electroporation 30

2.3 Results… 31

2.3A. Lens and olfactory precursors arise from a common domain 32

2.3B. Extensive cell movements lead to the segregation of lens and nasal precursors 33
2.3C. Early co-localization of Pax6 and Dlx5 mRNA defines a common nasal-lens territory, later separation of the PAX6 and DLX proteins correlates with acquisition of placodal identitity 34
2.3D. Persistent expression of Dlx5 regulates cell sorting 36
2.4 Discussion 38
2.4A. A common territory for lens and olfactory precursors 38
2.4B. Specification of the lens and olfactory precursors parallels the formation of the eye-antennal imaginal disc of Drosophila 40
2.4C. Do Pax6 and Dlx5 regulate cell sorting at placode stages? 41
2.4D. Extensive cell movements as a general feature of placode development 41
2.5 Acknowledgements 43

Chapter 3: Single cell lineage analysis of olfactory and lens placode precursors……. 53
3.1 Introduction 54
3.2 Materials and Methods 54
3.2A. Single cell injections 54
3.2B. Histology 56
3.2C. Immunocytochemistry 56
3.3 Results and discussion 57
3.3A. Single cells injected in the common lens-olfactory domain from stages 6-8 give rise to either olfactory epithelial cells or lens cells but not both 58
3.3B. Distribution of mitotic figures between HH stages 6-10C 59

Chapter 4: Spatiotemporal competence and commitment of ectoderm during the induction of the olfactory placode 66

4.1 Introduction 67

4.2 Materials and methods 70

4.2A. Quail-chick grafts 70

4.2B. Collagen gel explant cultures 71

4.2C. Immunocytochemistry 72

4.2D. Antibody generation 74

4.2E. Western blotting 74

4.2F. In situ hybridization 75

4.3 Results… 75

4.3A. Molecular markers of the olfactory placode 75

4.3B. Dlx3 *and* Pax6 *proteins are co-expressed in the olfactory placode* 77

4.3C. Neuronal markers of the olfactory epithelium 78

4.3D. Competence of embryonic ectoderm at different axial levels to express Dlx3 *and* Pax6 *and form the olfactory placode* 79

4.3E. Specification of presumptive olfactory placodal ectoderm to express Dlx3 *and* Pax6 *and form neurons* 81

4.3F. Presumptive olfactory placode ectoderm is committed to express Pax6 *and* Dlx3 *by HH stage 15* 82

4.4 Discussion 83

4.4A. Molecular markers of the developing olfactory placode 83

4.4B. Spatiotemporal distribution of competence to form the olfactory placode 84

4.4C. Timing of inductive events that lead to the formation of the olfactory placode 86

Chapter 5: Summary and future directions 103

5.1 Summary…. 104

5.2 Questions that remain and future directions 108

5.2A. What is the implication of the early lineage restriction and specification of the olfactory and lens placode precursor cells? 108

5.2B. What is the molecular nature of the signal or cohort of signals that sequentially induce placode precursor cells to differentiate into the olfactory epithelium? 110

5.2C. Identifying placode-activated enhancers: a crucial step towards building networks 112

Appendix: Cited Literature 115

List of figures:

Figure 1.1 The spatial organization of the cranial sensory and neurogenic placodes at progressive stages of chick development 19
Figure 1.2 The placode-derived cranial nerves 20
Figure 1.3 An outline of the gene regulatory network involved in lens formation 22

Figure 2.1 Diagram showing the standardization of the injection sites relative to other landmarks 44
Figure 2.2 Examples of DiI and DiO labeled embryos 46
Figure 2.3 Fate map of lens and olfactory precursors between stages HH6 and 10 47
Figure 2.4 Lens and olfactory precursors show directional movement to their final target positions 48
Figure 2.5 Individual cell populations split into streams of cells moving toward different targets 49
Figure 2.6 Changes in *Dlx5* and *Pax6* expression reflect the spatial arrangement of nasal and lens precursors 50
Figure 2.7 Dlx and Pax6 proteins are differentially expressed at the time of placode formation 51
Figure 2.8 Lens cells that continue to express Dlx5 lose lens character and are excluded from the lens 52

Figure 3.1 Experimental set-up for single cell injections 62
Figure 3.2 Single cell injections in the common lens and olfactory precursor region at stage 6 contribute to either the olfactory or the lens placode 63
Figure 3.3 Injecting single cells at stage 8 produce clones of cells that contribute exclusively to the olfactory epithelium or the lens 64
Figure 3.4 Mitotic figures in chick embryos, from stages 5-10 as revealed by phospho-histone H3 staining 65

Figure 4.1 Molecular markers of the nascent olfactory placode 89

Figure 4.2 *Pax3*, *Pax6*, *Dlx3* and *Dlx5* are expressed in the mature olfactory placode 90
Figure 4.3 Purification of the GST-Dlx3 (C-terminal) fusion protein 92
Figure 4.4 Western blot analysis and immunohistochemistry using the polyclonal antibody raised against the C-terminal of Dlx3 93
Figure 4.5 Dlx3 and Pax6 proteins are expressed in the developing olfactory placode 94
Figure 4.6 Neuronal markers of the olfactory epithelium 95
Figure 4.7 Isotopic grafts and grafts of the lateral epiblast to the anterior neural fold result in Dlx3 and Pax6 expression in the transplanted tissue 96
Figure 4.8 Midbrain level ectoderm is competent to express Dlx3 and Pax6 upto HH stage 12 97
Figure 4.9 Hindbrain level ectoderm is competent to express Pax6 upto HH stage 8+ and Dlx3 upto HH stage 12 98
Figure 4.10 Trunk level ectoderm is competent to express Dlx3 upto HH stage 9 when grafted to the anterior neural folds 99
Figure 4.11 Grafts of midbrain and hindbrain level ectoderm express Pax6 in the lens and cornea 100
Figure 4.12 Specification of presumptive olfactory placode ectoderm to express Dlx and Pax6 proteins and form neurons 101
Figure 4.13 Time course for commitment of presumptive olfactory placode ectoderm to express Pax6 and Dlx3 102

Chapter 1: Introduction

Hierarchy of regulatory events in sensory placode development

Sujata Bhattacharyya and Marianne Bronner-Fraser, 2004

Portions of this chapter were published as a review in *Current Opinion in Genetics and Development.*

1.1 Introduction

Obtaining a reproducible pattern of differentiated cell types within the forming embryo has been the focus of much scientific inquiry in the field of developmental biology. This question was first examined more than a century ago by experimental embryologists in diverse organisms. More recently, the tools of molecular biology and the development of 'genetic' model organisms have provided mechanistic insight into the phenomenology of cell division, growth and the acquisition of a mature form. The externally developing chick embryo which has a systematic classification of its development (Hamburger and Hamilton, 1951) is an excellent system for embryological manipulations. Recent advances in molecular techniques and genomic tools now permit the synthesis of embryological and molecular information to answer fundamental questions such as tissue interactions that lead to unique cell fate identity, cell movements which are responsible in part for dynamic gene expression patterns and extrinsic and intrinsic molecular cues that guide the differentiation of cells. In the last decade alone, enormous progress has been made in unraveling the molecular cues that pattern the developing embryo: from the fertilized egg to the formation of the three germ layers, within the ectoderm to form the central and peripheral nervous systems and finally in the generation of subdivisions within the nervous system.

My interest has been to understand the regional specification of the peripheral nervous system; more simply put, how are sensory organs induced at discrete and reproducible locations in the embryo. I have studied this question in the context of the nasal structure, which always arises as a sensory system anterior to

the eye. However, a prerequisite for studying this structure is determining where the cells fated to contribute to this sensory organ arise. I have generated a fate-map of precursors for both the olfactory and lens placodes and carried out single cell lineage analysis to unequivocally determine their spatial origin in the embryo. I have also analyzed how cell movements result in the segregation of these precursors and how the dynamic expression patterns of some genes are functionally relevant for this segregation. Finally, I have followed spatiotemporal changes in competence to respond to olfactory placode inducing signals and the irreversible commitment of progenitors to an olfactory fate.

In order to provide a framework for my thesis project, I will first present a basic background to the formation of the nervous system in general and placode induction in particular.

1.2 Neural induction: a prequel to the formation of the embryonic nervous system

Prior to neurulation, the process of gastrulation subdivides the embryo into three germ layers: the ectoderm, mesoderm and endoderm. The traditional view has been that ectoderm is induced to form neural tissue as a consequence of its interaction with mesoderm that is ingressing through the primitive streak during gastrulation in the chick embryo. The initial recognition of this interaction as critical to the process of neural induction was achieved in a landmark experiment by Spemann and Mangold. They identified the dorsal blastopore lip (which contains the involuting dorsal mesoderm cells) as the 'organizer' in late gastrula stage amphibian embryos (Spemann and Mangold, 1924). A secondary host-derived neural axis was obtained when they transplanted this region into the ventral portion (prospective epidermis) of another embryo. This suggested that the dorsal

blastopore lip is capable of patterning (or organizing) the tissue that it is in contact with it and hence its name. Additionally, it can induce ectoderm overlying it towards a neural fate. Equivalent structures or 'organizers' have been found in other organisms as well: Hensen's node in the chick embryo, the embryonic shield in zebrafish and the node (and **A**nterior **V**isceral **E**ndoderm) in the mouse are capable of inducing a secondary neural axis. While the phenotypic effect of transplanting organizers of various species is universal, the specific molecular nature and/or possibly timing of neural induction do not appear to be conserved. In the early 1990s, using expression cloning and other techniques, multiple secreted molecules, all expressed by the organizer in Xenopus, were identified in quick succession: noggin, chordin, follistatin and Cerberus (Lamb et al, 1993; Sasai et al, 1994; reviewed in Harland, 1997, 2000). Interestingly, they shared a common molecular mechanism for inducing neural tissue; they could all bind members of the BMP (**B**one **M**orphogenetic **P**rotein) family with varying affinities and antagonize their epidermalizing action. This led to the much- heralded and rather simplistic view of neural induction wherein BMP family members are initially expressed throughout the dorsal epidermis and later, through the creation of a gradient of BMP antagonizing activity starting from the organizer, cells closest to the organizer down-regulate their expression of BMP and become neural. In fact, when explants of animal caps are dissociated they express markers of neural tissue possibly because they are released from intercellular BMP signaling. However, in chick embryos the story is much more complex. It appears that the spatiotemporal expression patterns of various BMP family members (mainly-2, -4 and –7) and their antagonists- noggin, chordin and follistatin- are not in keeping with the Xenopus model of neural induction (Streit and Stern, 1999). Misexpression of the antagonists in prospective

epidermal tissue is not sufficient to cause them to become neural and conversely, misexpression of BMPs in the neural plate does not epidermalize it (Wilson and Edlund, 2001). However, pre-exposure of the area opaca of the epiblast to Hensen's node for 5 hours sensitizes it to respond to the overexpression of chordin (Streit et al., 1998). This suggests that node-derived signals other than BMP inhibitors are operative in neural induction in amniotes at least. Additionally, neural tissue is still generated in mice that lack noggin, chordin and follistatin (Bachiller et al., 2000).

In fact, the time at which neural induction occurs (at least in the chick embryo) has been pushed back by experiments done in embryos prior to egg-laying. In a rather dexterous experiment, the entire area of the stage XII chick embryo was dissected into a hundred equal sized pieces and their specification was tested (Wilson et al., 2000). Surprisingly, even as early as this, some of these regions have already received signals that will drive the expression of neural markers such as Sox2 and Sox3. At this stage, various FGF (**F**ibroblast **G**rowth **F**actor) family members are expressed at high levels in medial epiblast cells (Wilson et al, 2000; Streit et al., 2000; Wilson and Edlund, 2001). Interestingly, signaling through this pathway causes a down-regulation of Bmp expression in these cells and an acquisition of neural characteristics (Wilson et al., 2000; Wilson, 2001). Concurrently, Wnt signaling in lateral epiblast cells specifies an epidermal cell fate by inhibiting FGF signaling (Wilson et al., 2001). This leads to the unexpected conclusion that neural induction in the chick embryo is complete prior to the formation of mesoderm. By late gastrula stages, neural commitment has taken place. One obvious caveat to this experiment is that at such early stages, even a relatively small region will contain cells of diverse fates, so it cannot be ruled out that ongoing signaling between these cells contributes to the expression of these markers. A recent study in

chick suggests that signals other than Fgf, Wnt (**W**ingless/I**nt**) activation/inhibition and Bmp inhibition is/are required for de novo neural induction in competent tissue (Linker and Stern, 2004).

1.3 Induction of the neural plate border region

Fate-mapping data (Rosenquist, 1981; Fernandez-Garre et al, 2002) and the expression of solely neural (Sox2, Sox3) and epidermal (keratin, Gata2, Gata3) markers have helped demarcate the neural plate border region that will ultimately give rise to neural crest and placodes (McLarren et al., 2003; Schlosser and Ahrens, 2004). However, this data does not allow for an unambiguous designation of 'border' territory as gene expression patterns and fate-map data do not agree in their allocation of cells as belonging to the border. Other genes that are expressed in this somewhat ill-defined region of the embryo include Msx1, Bmp4, Slug, Six4, Eya2 and Dlx5 in the chick (McLarren et al., 2003) and Msx1, Dlx3, Six1, FoxD3 and Slug in Xenopus (Schlosser and Ahrens, 2004). Of these, Dlx5, Dlx3, Msx1 (in Xenopus), and Six4 and Eya2 (in chick) have extended domains of expression in the adjacent non-neural ectoderm. Overexpression of the Dlx genes in the neural plate of chick and Xenopus embryos leads to the upregulation of border markers such as Msx1 and Dlx5, but is not sufficient to cause the ectopic generation of neural crest or placodes (McLarren et al., 2003; Woda et al., 2003). In a dominant-negative analysis, the loss of Dlx function in the border region resulted in its repositioning to a more lateral region in the ectoderm (Woda et al., 2003). It has been hypothesized that bidirectional signaling between neural and non-neural ectoderm results in the differential specification of neural crest and placode territory; while neural cells

respond to ectodermal signals to form neural crest, placodes are induced in the ectoderm by signals from neural tissue (Schlosser and Ahrens, 2004).

1.4 Neural crest and placodes: embryonic precursors of the PNS

Ectodermal placodes and neural crest cells are morphological inventions unique to vertebrates. Cranial placodes have been empirically defined as transient embryonic thickenings of columnar epithelium that contribute extensively to the peripheral nervous system of the vertebrate head. In contrast, neural crest cells delaminate from the dorsal neural tube at all axial levels except the most anterior region, at the level of the future telencephalon. They share some similarities including their induction at the border between the prospective neural plate and epidermis as mentioned above (Knouff, 1935; Rosenquist, 1981; Fernandez-Garre et al, 2002). Both populations also undergo an epithelial to mesenchymal transition, and give rise to some of the same derivatives such as sensory neurons, glia and neuroendocrine cells (Baker and Bronner-Fraser, 1997). However, neural crest cells generate a wider range of derivatives including melanocytes, autonomic neurons, bone and cartilage.

The generation of neural crest by the apposition of neural and non-neural ectoderm (Dickinson et al., 1995; Selleck and Bronner-Fraser, 1995), the participation of BMPs (Basler et al, 1993; Liem et al, 1995) and Wnts (LaBonne and Bronner-Fraser, 1998; Garcia-Castro et al.,2002) in this process, the stereotypic migration of these cells and the molecular cues that cause their differentiation into various lineages: sensory neurons, sympathetic neurons, glial cells and smooth muscle cells (Shah et al., 1994; Shah et al., 1996; Shah et al., 1997; Greenwood et al., 1999) have been the focus of much research. Much less is known about placode induction and

differentiation at a molecular level inspite of their substantial contributions to the nervous system. Historically, placode development has been examined from an embryological perspective and these studies in a diversity of organisms have revealed tissue interactions that are crucial for the morphological formation of the different placodes. In recent times, there has been a renewed interest in understanding the molecular mechanisms that drive the generation of a varied array of cell types from these deceptively simple ectodermal regions.

1.5 Placode induction

1.5A Diverse cell types arise from the cranial sensory and neurogenic placodes

The cranial sensory placodes (the olfactory, lens and otic placodes) differentiate into a variety of cell types. For example, the olfactory placode gives rise to the regenerating **o**lfactory **s**ensory **n**eurons (OSNs) responsible for odorant detection, the **p**heromone **r**eceptor **n**eurons (PRNs) in the vomeronasal organ and the **g**onadotropi**n**-**r**eleasing **h**ormone (GnRH) neurons (for a contrary view see, (Whitlock et al., 2003) that regulate reproductive cycles. Non-neuronal derivatives originating in the olfactory epithelium include the olfactory ensheathing glial cells, the stem cell-like basal cells and support cells. The axons of the OSNs project to the olfactory bulb forming the Ist cranial nerve, the olfactory nerve (Fig. 2), and the GnRH neurons migrate alongside these axons ultimately penetrating the forebrain to localize in the basal hypothalamus (reviewed in Parhar, 2002; Wray, 2002). Conversely, the lens placode is entirely non-neurogenic; the posterior portion of the lens vesicle differentiates into lens fiber cells of the eye, which produce various crystallin proteins that endow the lens with its characteristic transparency. The otic placode gives rise to the labyrinthine structure of the inner ear: the cilia of the hair

cells in the cochlea transduce auditory signals whereas the cilia in the sensory epithelia of the three semicircular canals respond to angular acceleration of the endolymphatic fluid thereby providing a sense of balance. Furthermore, like the olfactory epithelium, structural components of the inner ear also contain support cells, which are likely required for the regeneration and maintenance of hair cells in non-mammalian organisms. The cochleovestibular ganglion arises primarily from the anteroventral aspect of the otic vesicle and is associated with the VIIIth (vestibulocochlear) cranial nerve (Figs. 1 and 2) (Riley and Phillips, 2003).

In contrast to the cranial sensory placodes, the trigeminal and epibranchial placodes are solely neurogenic. The former contributes cutaneous sensory neurons to the distal portion of the trigeminal ganglion (the Vth cranial nerve) (Fig. 2) that relays touch, pain and temperature information from the face and jaws. On the other hand, the epibranchial placodes give rise to visceral sensory neurons that innervate taste buds and transmit vital information about heart rate, blood pressure and visceral distension. The epibranchial (geniculate, petrosal and nodose) placodes arise in a rostrocaudal sequence in the vicinity of the otic vesicle, dorsal to the branchial clefts and form the distal portions of the facial (VIIth) (Fig.2), glossopharyngeal (IXth) and vagal (Xth) ganglia, respectively (Fig. 1). The proximal portions of all cranial ganglia have an alternate origin in the neural crest. Therefore, the entire cranial peripheral nervous system is generated from two multipotent cell populations, the neural crest and the placodes.

1.5B One, to many: the multiple phases of placode induction

At the very least, placode induction is a two-step process. Morphological evidence suggests that there is a thickened “pre-placodal” domain at the border of

the neural plate and ectoderm, at the early neurula stage in some species. This domain is further identifiable by a distinct combinatorial code of *Six*, *Eya* and *Dach* gene expression (for reviews see Baker and Bronner-Fraser, 2001; Streit, 2004). Additionally, fate-maps in the chick and zebrafish position the precursors for the olfactory, lens, otic and epibranchial placodes in overlapping patterns within this region (Figure 1a) (Bhattacharyya et al., 2004; Streit, 2002; Whitlock and Westerfield, 2000). An important and still outstanding question is how this domain is defined: is it a domain where every cell is fated to become or biased towards a distinct placodal fate or is it a domain where every cell has the potential or is competent to acquire properties of any of the placodes? These are not mutually exclusive options. Whereas lineage studies and gene expression patterns have provided evidence for the former option (Schlosser and Ahrens, 2004), the plasticity of open neural plate-stage ectoderm to form the appropriate placodes when rotated (Jacobson, 1963) suggests that a window of competence is present in the pre-placodal region (for further discussion, see Streit, 2004; Schlosser and Ahrens, 2004; Begbie and Graham, 2001). However, the developmental potential of a single cell in this domain has yet to be addressed. Furthermore, it has been hypothesized that specific placodes are secondarily induced from this shared territory. The temporally asynchronous acquisition of distinct placodal identities and the diversity of signaling molecules required argues against the induction of individual placodes being a simple two-step process; rather, it suggests that a coordinated series of interactions cumulatively leads to a unique cell fate. In addition to a requirement for different signaling sources over time, the placodal precursor cells undergo extensive cell movements prior to reaching their ultimate location in the head: a morphological entity is only seen after the coalescence of the initially scattered placode precursor cells

(Bhattacharyya et al., 2004; Streit, 2002; Whitlock and Westerfield, 2000). Whether this movement is directed by the prospective fate of the cells or whether this process is a stochastic one whereby precursors attain a bias towards a particular cell fate once they have reached their final destination is a question that remains closely tied to the determination of their state in the pre-placodal domain.

The Bmp, Fgf, Shh (**S**onic **h**edge**h**og) and Wnt signaling pathways have been implicated in different aspects of the inductive process, from the initial formation of the pan-placodal primordium at the border of the neural plate and ectoderm to the final steps in the differentiation of the various placodes (Baker and Bronner-Fraser, 2001; Streit, 2004). An important component of these signaling modules are transcription factors that function cell autonomously to confer placodal identity. Loss-of-function analyses have revealed the seminal role of certain transcription factors in the ectoderm to placode transition. One such example is that of Pax6, a key gene involved in the development of the lens and nasal placodes. These placodes do not form in *Small Eye (Sey)* mutant mice, which carry a semi-dominant, homozygous lethal mutation in the Pax6 coding region (Grindley et al., 1995; Hogan et al., 1986). The specific inactivation of Pax6 in the presumptive lens ectoderm also abrogates lens placode formation (Ashery-Padan et al., 2000). In addition, chimeric analyses of *Sey* and wild-type mice have shown the exclusion of Pax6-/- cells from the developing lens and nasal epithelium (Collinson et al., 2000; Collinson et al., 2003). Co-culture experiments in which ectoderm lacking Pax6 was combined with wild type optic vesicle (one of the sources for lens fate promoting signals) resulted in a lack of lens formation; conversely, wild type ectoderm was capable of forming a functional lens in response to signals from a Pax6 deficient optic vesicle (Fujiwara et al., 1994). Analogous co-culture studies with nasal epithelium and the underlying

nasal mesenchyme gave similar results (LaMantia et al., 2000). Taken together, these experiments suggest that Pax6 expression is crucial within the presumptive lens and nasal placode ectodermal cells.

Conversely, gain-of-function studies have identified some transcription factors that endow ectodermal cells with placodal characteristics. In fact, the overexpression of Sox3 (a transcription factor of the SRY gene family) in the chick and medaka causes the appearance of ectopic placode-like structures that express Pax6 and Eya1 (a marker of the nasal and otic placodes) (Koster et al., 2000); however, in the chick this only occurs in head ectoderm adjacent to the endogenous placodes (Abu-Elmagd et al., 2001). This may reflect the early loss of competence of trunk level ectoderm to respond to placode inducing signals (Groves and Bronner-Fraser, 2000, Baker et al., 1999). Surprisingly, in the medaka, otic vesicle-like structures are also found in the trunk ectoderm, an ectodermal region ordinarily devoid of placodes (Koster et al., 2000). This suggests that Sox3 could act in a permissive capacity in the ectoderm, bestowing it with the ability to respond to placode-inducing signals. Possibly, as yet unknown factors could provide such competence to non-placode forming ectodermal regions in other vertebrates.

1.6 Genetic networks that operate during placode induction

Since the hierarchy of molecular players involved in olfactory placode induction remains elusive, I will use data obtained in the study of lens induction to highlight how one can approach a network analysis of placode induction. Lens induction and differentiation have historically been studied using embryological manipulations. In this context, the genetic and biochemical dissection of a molecular pathway involved in lens formation provides a holistic view of its development. The

pivotal role of Pax6 in eye development was brought to light by the formation of ectopic eyes in a gain-of-function analysis in Drosophila (Halder et al., 1995). Its importance in lens placode induction is underscored by the study of the *Sey* mouse (Grindley et al., 1995; Hogan et al., 1986) and rat (Matsuo et al., 1993) mutants. The regulation of this gene has been extensively studied and a basic network has been defined (Chow and Lang, 2001). Since then, additional data has highlighted the complexity of this pathway (Fig. 3).

1.6A Upstream regulators of lens-specific Pax6 expression

The identification of a head ectoderm specific enhancer in the 5' upstream region of Pax6 has been the starting point of numerous inquiries into the nature of Pax6 regulation and the search for its lens-specific downstream targets. This highly conserved 341 bp enhancer (EE) approximately 4 kb upstream of the most proximal promoter (P0) of the Pax6 gene was shown to be both necessary and sufficient to control its spatio-temporal expression in the developing lens (Williams et al., 1998; Kammandel et al., 1999). The targeted deletion of this enhancer caused multiple lens defects, partly through a loss of Foxe3 expression (Dimanlig et al., 2001; Blixt et al., 2000). A significant, though not complete loss of Pax6 expression in these mutants suggests that at the very least two cis-elements are required for the full range of Pax6 expression in the lens (Fig. 3) (Dimanlig et al., 2001). Detailed biochemical analysis has identified two **t**hree **a**mino-acid **l**oop **e**xtension (TALE) homeoproteins, Meis1 and Meis2 that function as direct regulators of lens-specific Pax6 expression (Zhang et al., 2002). Additionally, the persistent expression of the Meis genes in a Pax6 null background, genetic epistasis analysis and the repression of Pax6 expression in the lens ectoderm on electroporation of a Meis dominant negative

construct, lend further support to a model wherein the Meis genes function upstream of Pax6 (Fig. 3). In addition, the hypothesized second lens-activated enhancer could likely be a "SIMO" element that has 5 Meis consensus sites (Figure 3) (Zhang et al., 2002 and references therein). It will be illuminating to determine the phenotype of Meis 1 and 2 knockout mice, especially with regard to the level of Pax6 expression and the extent of defects seen in the formation of the lens.

1.6B Downstream targets of Pax6 in the lens

The Sox B1 group genes, Sox1, 2 and 3 have also been implicated in lens formation (Kamachi et al., 1998). Sox2 expression is up -regulated in the presumptive lens ectoderm shortly after the ectoderm and optic vesicle have made contact with each other, following the initiation of Pax6 expression (Furuta and Hogan, 1998; Kamachi et al., 1998; Schlosser and Ahrens, 2004). In *Sey* mutants, Sox2 is not up regulated in the lens placode placing Sox2 downstream of Pax6 expression in the presumptive lens placode ectoderm, at least in the mouse (Fig. 3) (Furuta and Hogan, 1998). Importantly, it has been shown that the co-expression of Pax6 and Sox2 in the lens placode has functional relevance: Pax6 and Sox2 interact directly with each other (Kamachi et al., 2001), can synergistically regulate Pax6 expression via the minimal enhancer mentioned above (Figure 3) (Aota et al., 2003) and cooperatively bind DC5, a 30 bp minimal enhancer in the intronic region of δ-crystallin (Fig. 3) (Kamachi et al., 2001) to which Pax6 on its own binds poorly. However, Pax6 and Sox2 are co-expressed in other portions of the nervous system, such as the spinal cord, nasal placode and Rathke's pouch and interestingly, some of these embryonic regions have a low -level of endogenous δ-crystallin expression

(Kamachi et al., 1998). Clearly, these cells do not go on to differentiate as lens fiber cells, which implies that additional non-lens cell specific repressors and/or lens-specific activators must be present to impart a unique differentiation potential to the lens cells. This could account for the ectopic expression of L-Maf (a basic leucine zipper domain transcription factor; reviewed in (Reza and Yasuda, 2004) and δ-crystallin only in the region adjacent to the endogenous lens on co-electroporation of Pax6 and Sox2 (Kamachi et al., 2001; Reza et al.,2002). Sox2, L-Maf and Prox1 (the vertebrate homolog of Prospero) when overexpressed on their own are also incapable of inducing ∂-crystallin outside the region adjacent to lens (Kamachi et al., 2001; Reza et al., 2002; Shimada et al., 2003). Strikingly however, the co-electroporation of L-Maf and Sox2 causes the ectopic expression of δ-crystallin anywhere in the head ectoderm both cell autonomously and non-cell autonomously (Shimada et al., 2003). Possibly, this indicates that L-Maf in conjunction with Sox2 functions as a key molecular determinant of lens-forming ability.

Surprisingly, the expression of a dominant negative Pax6 construct down-regulates the expression of Prox1, L-Maf and δ-crystallin, but not of Sox2 and Six3 (Reza et al., 2002). The fact that Six3 and Sox2 expression are not down-regulated is in contrast to experiments where Six3 expression was lost when Pax6 was conditionally inactivated in the presumptive lens placode ectoderm (Ashery-Padan et al., 2000) and both Six3 and Sox2 expression were abolished in the Sey mutants (Fig. 3) (Lagutin et al., 2001; Furuta and Hogan, 1998). This may be connected to the difference in time at which Pax6 activity is lost in the two cases; alternatively, in the dominant negative situation, the activation domain of Pax6 may still be able to function in the presence of the Engrailed (En) repressor domain in some chromatin

environments. Interestingly, these cells were not excluded from the lens. The co-expression of L-Maf in conjunction with the dominant-negative Pax6 construct rescued the phenotype, thus putting L-Maf downstream of Pax6 in the lens-specific gene regulatory hierarchy (Fig. 3) (Reza et al., 2002).

1.6C Negative regulators of lens formation

All the transcription factors mentioned above function as transcriptional activators in the lens. However, repression is equally crucial to a pathway by virtue of providing negative feedback and preventing runaway activation. The vertebrate homologues of the Drosophila *sine oculis* gene, Six3 and Six6 function as negative regulators of eye development (Chow and Lang, 2001). The lack of Six3 expression in the presumptive lens placode ectoderm in *Sey* mutants suggests that Pax6 controls its expression directly or indirectly (Fig. 3); however, Six3 expression in the optic vesicle of these mutants is unaffected (Lagutin et al., 2001). Six3 overexpression either by itself or in combination with Grg5 (a mouse counterpart of Groucho, a transcriptional co-repressor) prevents the invagination of the lens placode and the expression of δ-crystallin in a majority of the overexpressing cells (Fig. 3) (Zhu et al., 2002).

Using epistasis analysis to build similar genetic networks that function in the development of the other sensory and neurogenic placodes will enable a deeper understanding of these placodes and will lead to new and testable hypotheses.

1.7 Conclusions

Our current model is that placode development is a multi-step process that initiates with partitioning of a general placode domain from which individual placodes are specified by inductive interactions from surrounding tissues. All placodes appear to have regulatory "cassettes" involving Six, Eya and Dach genes, with individual transcription factors activated in a placode-selective fashion. Activation of particular sets of genes appears to occur by integration of multiple signals with a unique read-out for each placode. The recent identification of "placode-specific" enhancers will greatly aid in dissection of these complex gene regulatory networks. However, such analysis will be meaningful only when viewed in conjunction with detailed embryological studies. Together, they will help unravel the intricate process of creating a relatively simple focal ectodermal region and will provide insight into how a considerable portion of our cranial nervous system arises.

The goal of my thesis has been to understand the step-wise progression of differentiation in placode precursor cells. In the next chapter, I discuss data regarding the spatial localization of progenitors that will contribute both to the olfactory epithelium as well as to the lens of the eye. These precursors appear to intermingle at early stages, with their eventual separation being coordinated by at least partially directed cell movements. The expression of certain genes mirrors this process and moreover, we show that maintaining expression of olfactory genes in the precursors prevents them from contributing to the lens. Using single cell lineage analysis, in chapter 3, I show that even at early stages in development when olfactory and lens precursor coexist in a common territory, single cells are already

fated to give rise to progeny that will contribute to either one or the other placode. In chapter 4, I discuss the extent to which ectoderm is competent to give rise to the olfactory placode and test the specification and commitment of presumptive placode cells. The ability to form the olfactory placode is only retained in more anterior ectoderm (forebrain and midbrain level ectoderm) beyond HH 10. While presumptive olfactory placode cells are specified early on (prior to complete segregation of the lens and olfactory fields), their commitment is delayed. This suggests a greater inherent plasticity in these cells as opposed to other placodal populations that have been similarly tested. In chapter 5, I summarize my findings, and define questions that remain in my model of olfactory placode induction.

.

Figure 1: The spatial organization of the cranial sensory and neurogenic placodes at progressive stages of chick development

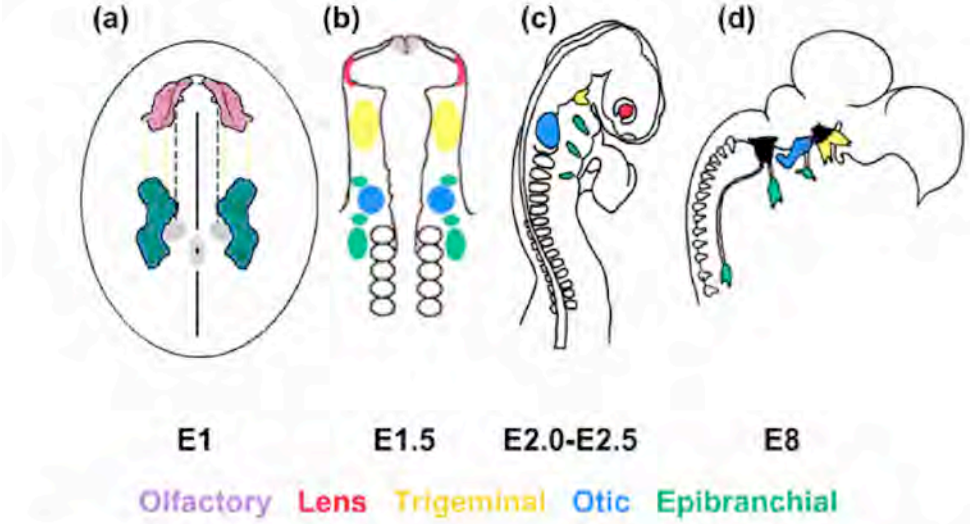

(a) At embryonic day (E) 1 of development (neurula stage), lens (shown in red) and olfactory (shown in lavender) placode precursors coexist in a common territory at the border of the anterior neural plate, while the otic (in blue) and epibranchial (in green) placode precursors arise more posteriorly, both rostral and caudal to the first somite. The dashed lines in yellow indicate where the prospective trigeminal placode precursors are likely to lie based on the continuity of the pre-placodal domain and the presence of the other placode precursors. **(b)** Approximately 12 hours later, (10-somite stage) the presumptive placode precursors occupy distinct locations within the embryo. The olfactory placode precursors are present at the rostral tip of the embryo, the lens precursors overlie the lateral portions of the diencephalon (the future optic vesicles), the trigeminal placode forms in the ectoderm adjacent to the midbrain, the otic placode forms in the ectoderm at the level of rhombomere 4/5 while the epibrancial placode precursors surround the otic placode. **(c)** By E2.5, the placodal derivatives are clearly visible and differentiation is well underway in most of the placodes. **(d)** At E8, the trigeminal, cochleovestibular (derived from the otic placode) and the epibranchial placode-derived ganglia of the glossopharyngeal, facial and vagal cranial nerves are mature structures as are the lens and the nasal epithelium (enclosed by the nasal capsule).

Figure 2: The placode-derived cranial nerves

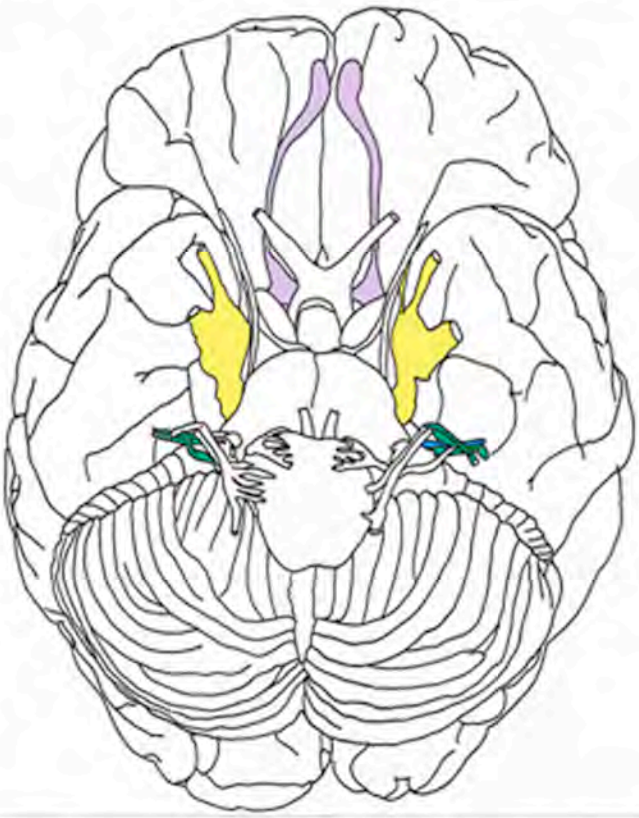

The cranial nerves that derive from placodes are shown in colour. The olfactory nerve or the first cranial nerve is shown in lavender. The ophthalmic, maxillary and mandibular nerves that arise from the trigeminal ganglion (Vth) are shown in yellow. In blue is shown the vestibulocochlear nerve (VIIIth) and in green, the facial nerve, which is the VII cranial nerve.

<u>Figure 3:</u> An outline of the gene regulatory network involved in lens formation. Schematic diagrams on the far left (**A**) illustrate the morphological development of the lens at times corresponding to gene deployment on the right **(B)**. **(a)** Presumptive lens placode ectoderm shown in white overlies and abuts the optic vesicle. **(b)** The ectoderm thickens to form the lens placode and is in direct contact with the optic vesicle. **(c)** The lens placode invaginates to form a pit, and finally **(d)** the mature lens vesicle buds off and is covered by a sheet of corneal epithelium. The lens is housed within the cup-shaped structure of the retina. **(B)** The thick solid black arrows represent direct interactions known to be mediated by binding of the indicated transcription factor to a cis-regulatory element. Enhancers are depicted as rectangular boxes with smooth edges, whereas transcription factors are shown in simple rectangular boxes. Dashed lines indicate interactions between various transcription factors inferred from epistasis experiments. Hexagons indicate growth factors that signal during lens development. Thin black solid arrows indicate the positive regulation of Pax6 and Sox2 by these growth factors. The diagram is based on published data highlighted in the text and/or described below.

Both FGF and BMP7 signaling are required to maintain placodal expression of Pax6 (Faber et al., 2001); initial expression of Pax6 is unaffected in Bmp7 -/- mice (Wawersik et al., 1999) suggesting that it is required for the later placodal stages of Pax6 expression. On the other hand, BMP4 and other optic vesicle (ov) derived signals act upstream of Sox2 expression as Sox2 expression is abolished in a BMP4 null mutant (Furuta and Hogan, 1998). Pax6 expression is not affected in this mutant (ibid).

Meis, Pax6 and Sox2 all bind to the ectoderm enhancer (EE) present upstream of the Pax6 gene. Likely, the output of both the EE and the second hypothesized cis-element ("SIMO"?) governs the lens expression of Pax6. The loss of Six3, Sox2 and FoxE3 (Brownell et al., 2000) expression in the *Sey* mutant suggests that Pax6 expression in the presumptive lens placode ectoderm is upstream of Sox2, Six3 and FoxE3 in the gene regulatory cascade. Six3 acts as a transcriptional repressor down-regulating both its own expression as well as that of δ-crystallin, one of the characteristic proteins produced in differentiating lens fiber cells. Pax6 and Sox2 cooperate to induce L-Maf and δ-crystallin expression. Pax6, Sox2 and L-Maf all bind the enhancer region of the δ-crystallin gene (Muta et al., 2002). A dominant-negative form of L-Maf eliminates Prox-1 expression in the lens implying that L-Maf may function upstream of Prox-1 (Shimada et al., 2003). Prox1 and c-Maf (not shown here) directly bind multiple cis-regulatory elements upstream of the βB1-crystallin gene (Cui et al., 2004). In another branch of the lens development pathway, Pax6 controls FoxE3 expression possibly via Mab2l1 (Dimanlig et al., 2001; Yamada et al., 2003). Defects in the FoxE3 mutant mice (*dysgenetic lens)* suggest that FoxE3 plays a role in lens vesicle closure, separation of this vesicle from the corneal epithelium and proliferation (Blixt et al., 2000). Additionally, an upregulation of Prox1 in these mutants suggests that under normal physiological conditions, FoxE3 functions to repress or contain Prox1 expression (Blixt et al., 2000; Brownell et al., 2000).

Figure 3: An outline of the gene regulatory network involved in lens formation

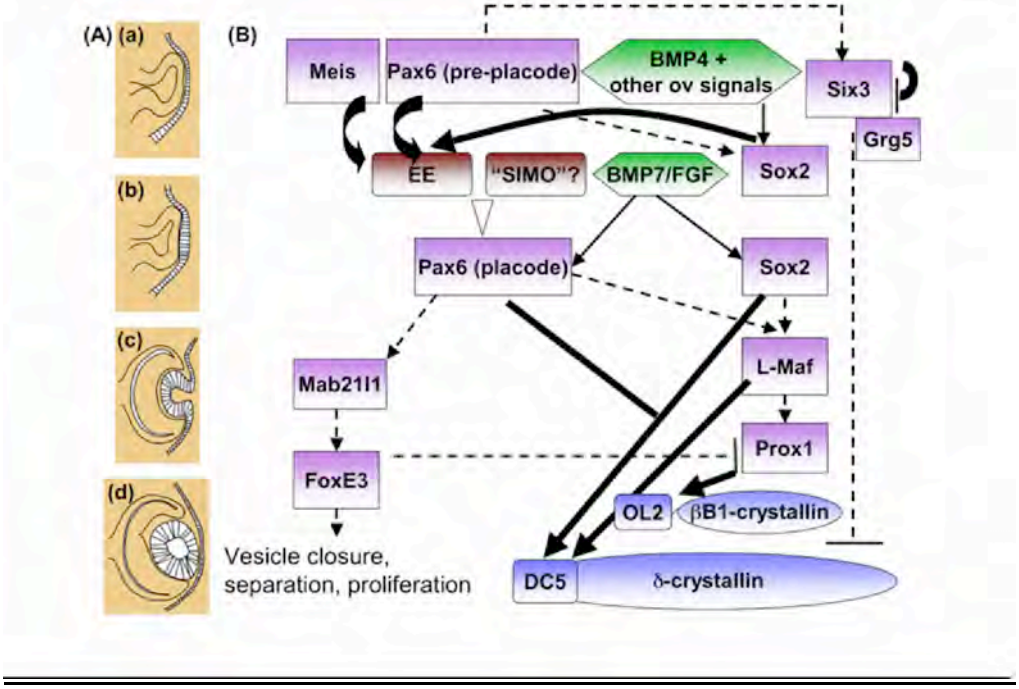

Chapter 2

Segregation of lens and olfactory precursors from a common territory: cell sorting and reciprocity of Dlx5 and Pax6 expression

Sujata Bhattacharyya, Andrew Bailey, Marianne Bronner-Fraser and Andrea Streit, 2004.

This chapter was published in *Developmental Biology*.

Abstract

Cranial placodes are focal regions of columnar epithelium next to the neural tube that contribute to sensory ganglia and organs in the vertebrate head, including the olfactory epithelium and the crystalline lens of the eye. Using focal dye labeling within the presumptive placode domain, we show that lens and nasal precursors arise from a common territory surrounding the anterior neural plate. They then segregate over time and converge to their final positions in discrete placodes by apparently directed movements. Since these events closely parallel the separation of eye and antennal primordia (containing olfactory sensory cells) from a common imaginal disc in Drosophila, we investigated whether the vertebrate homologues of Distalless and Eyeless, which determine antennal and eye identity in the fly, play a role in segregation of lens and nasal precursors in the chick. Dlx5 and Pax6 are initially co-expressed by future lens and olfactory cells. As soon as presumptive lens cells acquire columnar morphology all Dlx family members are down-regulated in the placode, while Pax6 is lost in the olfactory region. Lens precursor cells that express ectopic Dlx5 never acquire lens specific gene expression and are excluded from the lens placode to cluster in the head ectoderm. These results suggest that the loss of Dlx5 is required for cells to adopt a lens fate and that the balance of Pax6 and Dlx expression regulates cell sorting into appropriate placodal domains.

2.1 Introduction

In the vertebrate head, critical parts of the peripheral sensory nervous system arise from transient ectodermal thickenings, the cranial placodes, which develop at unique positions next to the neural tube (Baker and Bronner-Fraser, 2001). The olfactory placode gives rise to the nasal epithelium, the lens placode to the crystalline lens of the eye and the otic placode forms the inner ear. The trigeminal and the three epibranchial placodes, together with neural crest cells, form the cranial ganglia.

In the chick embryo, cells that will contribute to different placodes (like future otic and epibranchial cells) are initially intermingled and only later segregate to form separate placodes (Streit, 2002). Like otic precursors in the chick, olfactory cells in zebrafish are recruited from a large, but defined region of the head ectoderm and converge to their final position through cell rearrangements and movements (Whitlock and Westerfield, 2000). These observations raise the possibility that an initial step in placode formation is the establishment of a pre-placodal domain containing precursors for multiple placodes and that unique regional identities are imparted as a later step. In agreement with this notion, classical embryological experiments indicate that common tissue interactions and probably common signals are required for the initial induction of different placodes (Jacobson, 1963b; Jacobson, 1963c; Jacobson, 1963d). Moreover, the paired-domain transcription factor *Pax6* (Walther and Gruss, 1991) as well as members of the Six (Bovolenta et al., 1998; Esteve and Bovolenta, 1999; Oliver et al., 1995; Pandur and Moody, 2000) and Eya (Mishima and Tomarev, 1998; Sahly et al., 1999; Xu et al., 1997) families are

expressed in both nasal and lens placodes, and loss of Pax6 function results in the failure of both of these placodes to form (Grindley et al., 1995; Quinn et al., 1996; van Heyningen and Williamson, 2002; Wawersik et al., 2000).

The idea that olfactory and visual cells may share a common origin is surprisingly reminiscent of the development of sensory organs in holometabolous insects: the antenna, an odour-detecting organ, and the eye arise from a common imaginal disc, the eye-antenna disc. During larval development these territories separate and acquire distinct identities to give rise to the adult antenna and compound eye. This process is partially dependent on the action of two transcription factors that seem to regulate each other (Kurata et al., 2000): the Dlx gene Distalless (Dll) is required to confer antennal identity (Cohen et al., 1989; Dong et al., 2000; Panganiban and Rubenstein, 2002; Sunkel and Whittle, 1987), while the Pax6 homologue Eyeless (Ey) is essential for eye specification (Halder et al., 1995; Quiring et al., 1994); for review: (Gehring, 1996; Kumar and Moses, 2001c).

This raises the intriguing question of whether a similar principle may hold true for vertebrate nasal and lens placode formation. Here, we show in the chick that precursors for these two placodes arise from a common territory next to the anterior neural plate and segregate over time by apparently directional movements. As in the fly, *Dlx5* and *Pax6* are initially co-expressed in the common nasal-lens domain. As streams of cells destined to the lens and to olfactory regions segregate, expression of these two transcripts separates accordingly, suggesting that cell migration and regulation of these genes are coordinately regulated. However, the proteins they encode only become differentially expressed as the placodes begin to form: Dlx5 expression is lost from the lens and Pax6 expression is transiently down-regulated in

nasal precursors. Loss of Dlx5 is required for cells to acquire a lens identity: no cells that continued to express Dlx5 were found in the lens. This points to a remarkable and hitherto unnoticed similarity in the developmental processes that generate olfactory and visual organs in vertebrates and arthropods.

2.2 Materials and methods

2.2A Embryo techniques

Fertile hens' eggs (Winter Farm, Hertfordshire, UK; Spafas, Charles River Laboratories, Roanoke, IL, USA) were incubated at 38ºC for 24-45 hours to obtain embryos at stages 6-10 (Hamburger and Hamilton, 1951). For fate mapping, small groups of epiblast cells were labeled using the fluorescent dyes DiI and/or DiO as described previously (Ruiz i Altaba et al., 1993). Briefly, stocks of 0.5% DiI or of 0.25% DiO in absolute alcohol or DMSO were diluted 1:10 in 0.3M sucrose at 50ºC and injected by air pressure using a micropipette made from 50 μl borosilicate glass capillaries. The labeled position was measured in relation to other landmarks (see below) and the embryos then cultured *in ovo* until the lens and olfactory placodes could be identified by morphological criteria (stage 15-19). The position of labeled cells was assessed in whole mounts or after cryosectioning.

For video time-lapse analysis, embryos were labeled as described above, incubated for 1-2 hours in ovo and then explanted dorsal side down on fibronectin (20 μg/ml) coated Millicell inserts (Millipore) and cultured in Neurobasal medium containing B27 supplement as previously described (Krull and Kulesa, 1998).

2.2B Standardization of the position of labelled cells

The antero-posterior and medio-lateral positions of DiI and/or DiO labelled cells were measured using an eyepiece graticule immediately after injection. In stage 6-7 embryos, the distances from the centre of Hensen's node (primitive pit) to the tip of the prechordal plate (pp-hn = 100%; Fig. 1A.) and to the labelled cells, respectively, were measured and the position of the label was calculated as a percentage of the total length pp-hn. To standardize the medio-lateral position, the distance between the midline and the labelled cells was expressed as % of the distance between the midline and the edge of the neural plate at the level just anterior to the node (ml-np = 100%; Fig. 1A).

In embryos with 2-5 somites or more, distances were measured from the anterior edge of the first somite to the anterior neural ridge (anr-som = 100%; see Fig. 1B) and to the labelled cells. The position of the label was calculated as percentage of the total distance anr-som. The medio-lateral position of the labelled cells was determined in relation to the width of half the neural plate at the level just anterior to the first somite (ml-np = 100%; see above and Fig. 1B).

In embryos older than 5 somites, the distances from the first somite to the neuropore (np-som = 100%; Fig 1C) and to the labelled cells, respectively, was measured and the position of the label expressed as percentage of the total length np-som. To standardize the medio-lateral position, the distance from the midline to the labelled cells was expressed as percentage of the distance between the midline and the lateral edge of the optic vesicles (ml-ov = 100%).

Note that using this system, these measurements are relative such that the 100% value differs considerably between the medio-lateral and antero-posterior axes, as well as between different stages.

2.2C Video time-lapse filming

Four different positions of the epiblast on each side of stage 7-8 embryos were labelled with DiI as described above. The embryos were cultured in a heated chamber placed around an inverted Zeiss 410 laser scanning confocal microscope. For some movies, 3D stacks of pictures were taken every 10-15 minutes. These stacks were of 70 μm in thickness, with individual sections 14 μm apart. In other cases, the pinhole was opened up completely and a single thick section was imaged at an interval of 5-7 minutes. All movies were filmed at 5x or 10x magnification. Cell migration was visualised using Quick Time and groups of cells were tracked using Image J. To determine the trajectories taken by the labelled cells in an unbiased manner, all the time frames for each movie were collapsed into a single image. Single channel information at successive time-points was opened as an image sequence in Image J and a Z projection, at maximum intensity, of the resulting stack was created.

2.2D Whole mount in situ hybridisation, immunohistochemistry and histology

cDNAs for Dlx-5 (Ferrari et al., 1995) and Pax6 (Goulding et al., 1993) were kindly provided by R.A. Kosher and A. Bang. Whole mount in situ hybridisation using DIG-labelled antisense RNA-probes was performed as previously described (Streit et al., 1997; Thery and Stern, 1996). The colour reaction was developed using NBT/BCIP as a substrate. After post-fixing the embryos were embedded in

ovalbumin/agar for vibratome sectioning. DiI and DiO labelled embryos were embedded in gelatin and 10 μm cryo-sections were cut.

Mouse monoclonal antibody against Pax6 was obtained from Developmental Studies Hybridoma Bank (Department of Pharmacology and Molecular Sciences, The Johns Hopkins University School of Medicine, Baltimore, MD 21205 and Department of Biological Sciences, University of Iowa, Iowa City 52242 under contract N01-HD-2-3144 from NICHD); polyclonal antibodies recognising all Dlx proteins were a kind gift from Jhumku Kohtz, Northwestern University; polyclonal antibodies against chick δ-crystallin were generously provided by Joram Piatigorski, National Eye Institute. Rabbit anti-GFP antibodies were purchased from Molecular Probes. For immunohistochemistry, embryos were fixed in 4% paraformaldehyde in phosphate buffered saline (PBS) at 4˚C for 1 hr and embedded in gelatin for cyrosectioning. Immunostaining was performed as described previously (Stern, 1993) using anti rabbit, mouse or sheep secondary antibodies coupled to Alexa fluor 488 and 594 (Molecular Probes). Nuclei were visualised with DAPI (Molecular Probes).

2.2E Expression constructs and in ovo electroporation

The coding sequence of chick Dlx5 was cloned into pCAB-IRES-eGFP as previously described (McLarren et al., 2003) to generate a bicistronic expression construct under the control of the ubiquitous chick β-actin promoter. pCAB-IRES-eGFP without insert was used as control.

Exogenous DNA (2-5 μg/μl) was injected in ovo under the vitelline membrane overlying the presumptive nasal-lens ectoderm of embryos between

stage HH 8-10. DNA transfer into the ectoderm was achieved by electropration using one broad silver (cathode) and one pointed tungsten (anode) electrode to apply 4 pulses of 20V, 50ms at 1000ms intervals. Eggs were then sealed and incubated for 1-2 days until the embryos had reached HH13-20. Specimens were recovered in PBS, photographed and processed for cryosections and immunohistochemistry.

2.3 Results

In the chick, the lens and olfactory placodes are first visible as patches of thickened epithelium at the 12-14 (HH11) and 21-23-somite stage (HH 14) respectively (Bancroft and Bellairs, 1977; Romanoff, 1960). To investigate whether precursors for both placodes arise from a common territory, we constructed fate maps at different developmental stages. Small cell populations in the epiblast of chick embryos from head fold (HH6) to the 12-somite stage (HH11) were labelled with the fluorescent dyes DiI and DiO. Their position in relation to other landmarks was measured immediately after labelling (Fig. 1; Fig. 2A''- F''). One dye injection on average labelled 10-30 cells. Embryos were allowed to develop until stage HH15-18, when both placodes are morphologically visible, and the position of the labelled cells was determined in whole mounts (Fig. 2A-F). Some of the embryos were then sectioned to confirm the location of labelled cells (Fig. 2A'-F'). In total, 429 embryos were labelled; of the 325 survivors most had received one DiI and one DiO injection on each side of the embryo.

2.3A Lens and olfactory precursors arise from a common domain

At stage HH6-7, olfactory and lens precursors reside in the anterior ectoderm next to the neural plate where they are intermingled with future epidermal cells (Fig. 3). In addition, precursors for all three cell populations are found amongst prospective neural cells in the lateral edge of the neural plate (width: 10-15% ml-np). Nasal precursors spread from the most anterior tip of the neural plate to approximately one third of its length (0-28% pp-hn), while future lens cells are found slightly more posterior (8-36% pp-hn). Precursors for both placodes reach out into the lateral epiblast as far as 50% of the width of half the neural plate (50% ml-np).

At the 2-3-somite stage ($HH7^{+}/8^{-}$), the anterior neural folds contain precursors for all four tissues: nasal and lens placode, neural tube and epidermis (Fig. 3). Nasal and lens precursors are found from the most anterior tip (0% anr-som) to about one third of the distance between the first somite and the anterior neural ridge (30% anr-som). The adjacent ectoderm contains a mixture of future olfactory, lens and epidermal cells. While many cell groups contributed progeny to more than one tissue (51/121; nasal and lens, nasal and epidermal, lens and epidermal or all three), very few injections led to labelled cells in both the brain and the olfactory placode (6/51) and none simultaneously contributed labelled cells to the lens and the central nervous system.

Thus, precursors for both the olfactory and lens placode overlap in a large region of the epiblast next to the anterior neural plate at head fold stages and continue to do so in the anterior neural folds and the adjacent ectoderm until early somite stages. Cells just inside the neural folds occasionally contribute to olfactory placodes, but the majority contributes to the neural tube only.

From stage HH 8 onwards, prospective nasal cells begin to accumulate in the anterior neural folds and adjacent ectoderm, while lens precursors concentrate in the lateral ectoderm that will come to overlie the optic vesicle. At this stage, very few dye injections contributed cells to both placodes. Over the next few stages the separation of lens and nasal precursors continues until it is complete at the 10-somite stage (HH 10): prospective lens cells are located in the ectoderm adjacent and dorsal to the optic vesicles and presumptive nasal cells have converged to the most anterior ectoderm surrounding the open neuropore.

2.3B Extensive cell movements lead to the segregation of lens and nasal precursors

Our fate map analysis shows that lens and olfactory precursors originally arise from a common domain shared by other ectodermal derivates. This raises the intriguing question of how these cells become segregated over time. One possibility is that cells divide and move randomly with no predisposition to a particular ectodermal fate; those that end up close to the anterior neural tube receive signals instructing them to differentiate into olfactory placode, while those that localise next to the optic vesicle are induced to become lens. Alternatively, the two sets of precursors may already differ before they start to migrate, and then move in a directed manner to their appropriate locations in the presumptive olfactory and lens domains.

To begin to distinguish between these possibilities, we performed a time-lapse analysis of embryos from stage 7 or 8, which were then filmed for 12-14 hours until they reached stages 10-11. We analysed 28 embryos, each with multiple DiI injections on the left and right side within the common olfactory-lens precursor domain as well as more caudally to facilitate comparison between different regions.

In all cases, DiI-labelled cells moved extensively. Most cells tended to move from lateral to medial towards the midline as the neural folds closed (Fig. 4A: t=300 min and t=375 min; white arrowheads; Fig. 4B: t=140 min; red arrowhead). However, some labelled cells subsequently underwent extensive lateral movements, generally directed towards the future lens territory at about stage HH $8^{+}/9$ (Fig.4A, B green arrowheads). Analysis of the trajectories of cell groups (Fig. 4B and Fig. 5) showed that after initially following a common track individual cell populations often split such that one group moved more medially and the other laterally away from the midline.

Those cells that remained medially often turned, at times abruptly, and began moving rostrally towards the presumptive olfactory placode (Fig. 4B red dots and arrowheads). Even from quite disparate injection sites at several different rostrocaudal levels, we observed cells merging at the anterior tip of the embryo. This suggests that at least some cells may move in a directional fashion towards the presumptive olfactory placode, while others move towards the future lens. However, other cells (e.g. those derived from the most rostral injections) underwent little cell movement before becoming localised in the olfactory territory (Fig. 4B white arrowheads).

2.3C Early co-localisation of Pax6 and Dlx5 mRNA defines a common nasal-lens territory, later separation of the PAX6 and DLX proteins correlates with acquisition of placodal identity

In Drosophila, the homeobox transcription factor Dll and the paired domain protein Ey are initially co-expressed in the eye-antennal disc; during the second larval instar, however, a negative feedback loop acts to restrict Dll to the antennal

and Ey to the eye primordium and establishes disc identity (Cohen et al., 1989; Dong et al., 2000; Halder et al., 1995b; Kurata et al., 2000; Panganiban and Rubenstein, 2002; Quiring et al., 1994; Sunkel and Whittle, 1987). To test whether a similar molecular mechanism might regulate the segregation behaviour of lens and olfactory precursors observed in the time-lapse analysis, we investigated the expression of *Dlx5* and *Pax6* transcripts and of the proteins they encode in relation to the separation of future lens and nasal cells.

The mRNAs of both genes overlap at the 1-2-somite stage (HH7) in the anterior ectoderm (Fig. 6A, A', D, D'), although expression appears to be mosaic with some cells expressing high and others low levels of transcripts (Fig. 6A', D' insets). Like the lens and olfactory precursors, the *Pax6* domain surrounds the neural plate from its most anterior tip to about 35% of its length, while *Dlx5* expression continues more posteriorly, to the level of Hensen's node. Both transcripts extend mediolaterally from the edge of the neural plate into the ectoderm for about 50% of the width of half the neural plate. From stage HH8 onwards, the two expression domains begin to separate: while *Dlx5* transcripts concentrate in the most anterior neural folds and ectoderm, *Pax6* remains expressed strongly in the neural folds and the more posterior surface ectoderm (Fig. 6B, E). By stage 10, *Dlx5* expression is confined to the most anterior tip of the surface ectoderm (Fig. 6F, F'), where *Pax6* is absent (Fig. 6C, C'). Thus, the region where *Dlx5* and *Pax6* mRNAs are coexpressed matches precisely the position where lens and nasal precursors reside at early stages, and the expression domains separate as cells begin to segregate, suggesting that the mechanisms that regulate differential transcription of these genes are initially deployed as the two streams of cells separate.

However, a slightly different result is obtained when examining the distribution of Pax6 and Dlx proteins. At HH 7 the level of expression of both proteins is extremely low (not shown) becoming robust at HH 8, when all cells in the nasal-lens territory show high levels of Dlx and Pax6 (Fig. 7A-C). Unlike the mRNA, Dlx protein is maintained in presumptive lens cells until stage HH12/13 to disappear from lens cells as soon as placode morphology is established. The lens only contains $Pax6^+/Dlx^-$ cells (Fig. 7G-H). Cornea precursors overlying the lens are mainly $Pax6^+/Dlx^-$ except for few double labelled cells in the periphery. In contrast, the anterior ectoderm containing olfactory precursors retains Dlx protein, while losing Pax6 around stage HH 10 (not shown) and is clearly $Pax6^-$ once the placode is formed (Fig.7H). Thus, rather than reflecting the separation of olfactory and lens precursors (like the mRNA) the differential expression of Dlx and Pax6 proteins correlates with the acquisition of a particular fate (e.g. lens) and placodal morphology.

2.3D Persistent expression of Dlx5 regulates cell sorting

In the fly, Dll and Ey have been suggested to negatively regulate each other to determine antennal versus eye disc identity (Kurata et al., 2000). To test whether their vertebrate homologues have similar functions during nasal and lens placode development, we maintained expression of Dlx5 in lens precursors beyond the time when they have normally lost it and investigated the effect on their differentiation, localization or fate. If vertebrate placode development uses a molecular mechanism akin to the one that operates in Drosophila imaginal disc formation, this would predict that $Dlx5^+$ future lens cells should lose their lens character and lens-specific gene expression.

The ectoderm containing lens precursors of HH 8-10 chick embryos was transfected by electroporation with GFP control (pCAB-IRES-GFP) or Dlx5 vector (pCAB-Dlx5-IRES-GFP). To investigate the behaviour of cells during the entire process of lens formation embryos were grown for different times to reach early lens placode or later lens vesicle stages (HH12-20). The location of electroporated cells was monitored in whole mounts by their GFP expression. Numerous GFP^+ cells were found within the lens of all control electroporated embryos (16/16; Fig. 8A, C, D). In contrast, while $Dlx5^+/GFP^+$ cells were abundant in the ectoderm overlying the lens (future cornea), head epidermis and olfactory placodes, no $Dlx5^+/GFP^+$ cells contributed to the lens itself in Dlx5 electroporated embryos (2/23; Fig. 8E, G, H). Most of the experimental embryos (22/23) showed either extremely small or deformed lenses whereas controls looked normal. In addition, control electroporated cells were well dispersed within the lens and head ectoderm, whereas Dlx5 expressing cells were always found in clusters indicating that they display different adhesive properties than their neighbours (compare insets in Fig. 8A and E).

To investigate the phenotype with better cellular resolution, all embryos were sectioned and immunostained for GFP and the lens specific protein δ-crystallin. While both proteins are coexpressed in control electroporated embryos (Fig. 8B, D), none of the $Dlx5^+/GFP^+$ cells in experimental embryos expressed δ-crystallin (Fig. 8F, H). Occasionally, a single isolated $Dlx5^+/GFP^+$ cell was present in the lens; however, these cells have lost lens morphology as well as δ-crystallin expression (not shown). Sections of embryos at stage HH12/13 revealed that $Dlx5^+/GFP^+$ cells are excluded from the lens placode as soon as the cells develop the typical columnar morphology (not shown). The sections also confirmed that lenses in Dlx5

electroporated embryos display abnormal morphology and are generally much smaller than lenses in control embryos or on the contralateral side. Consequently, optic vesicle formation was often severely disrupted (Fig. 8F, G). Thus, Dlx5 expressing cells are never incorporated into the lens placode but are excluded from it as soon as it forms, suggesting that down-regulation of Dlx5 is an important prerequisite for cells to adopt a lens fate. Furthermore, these results indicate that by the time the proteins are differentially expressed, the transcription factors Dlx5 and Pax6 may regulate cell sorting events to ensure that cells with the incorrect expression profile do not end up in inappropriate placodes.

2.4 Discussion

2.4A A common territory for lens and olfactory precursors

In a 3-day-old chick embryo, the olfactory and lens placodes are clearly separate entities adjacent to the ventral forebrain and the optic vesicle, respectively. Here, we report that at earlier stages precursors for both structures are extensively mixed and occupy a common domain surrounding the anterior neural plate at head fold stages and only begin to separate at early somite stages. Therefore, this finding differs from earlier fate and specification maps (Carpenter, 1937; Kozlowski et al., 1997; Röhlich, 1931; Rudnick, 1944) from amphibians, fish and amniotes reporting an early segregation of lens and nasal cells into distinct domains. In zebrafish, in agreement with our findings, future olfactory cells converge from a large field towards their final position in the placode (Whitlock and Westerfield, 2000). Although their co-localisation with lens precursors has not been reported, the possibility that there is considerable overlap at earlier stages is not excluded.

It has been suggested that olfactory precursors arise from the neural territory either from isolated cell groups that migrate away from the neural plate (Farbman, 1992; Verwoerd and van Oostrom, 1979) or from a large territory surrounding the future telencephalon (Whitlock and Westerfield, 2000). Similarly, an earlier fate map using chick-quail chimaeras localised the presumptive olfactory placode to a very small domain within the neural folds at the 3-4 somite stage (Couly and Le Douarin, 1985; Couly and Le Douarin, 1987). In contrast, our data show that the majority of nasal precursors arise from the non-neural ectoderm in close association with future lens cells. In fact, while single injections into the neural folds at early somite stages often contribute to the olfactory and lens placode or to these placodes and surface ectoderm, only a negligible number of labelled cell groups give rise to progeny in both the neural tube and the nasal placode. Even at earlier stages, there is only limited mixing of future neural, lens and olfactory cells. Therefore, the segregation of neural from olfactory and lens progenitors is almost complete by early somite stages.

Genetic evidence suggests that not only do nasal and lens precursors share a common origin, but they also may use similar molecular pathways for their initial specification (Grindley et al., 1995; Quinn et al., 1996; van Heyningen and Williamson, 2002; Walther and Gruss, 1991; Wawersik et al., 2000; Xu et al., 1997). *Pax6* expression clearly matches the nasal-lens territory at head fold stages. Mice lacking Pax6 function never form nasal or lens placodes (Grindley et al., 1995), suggesting that Pax6 is required at early stages of their development, perhaps at the time when the common territory is specified. Afterwards, the molecular events that control differentiation of each placode seem to diverge. While the lens maintains

Pax6 expression throughout development, olfactory precursors lose *Pax6* at intermediate stages before re-acquiring it at late placode stages.

2.4B Specification of lens and olfactory precursors parallels the formation of the eye-antennal imaginal disc of Drosophila

Like the nasal epithelium in vertebrates, the insect antenna contains olfactory receptor cells responsible for odour discrimination. The Dlx-protein Dll and the Pax6 homologue Ey are initially co-expressed in the eye-antenna disc; however, by the time the eye and antennal primordia become distinct, Ey expression is restricted to the eye, while Dll is only found in the antennal anlage (Kumar and Moses, 2001a; Kumar and Moses, 2001b). Indeed, these transcription factors negatively regulate each other (Kurata et al., 2000) and are required to establish eye and antennal identity, respectively (Cohen et al., 1989; Dong et al., 2000; Halder et al., 1995; Panganiban and Rubenstein, 2002; Quiring et al., 1994; Sunkel and Whittle, 1987); for review: (Gehring, 1996; Kumar and Moses, 2001c). In the chick the situation is comparable: the co-expression of *Dlx5* and *Pax6* transcripts precisely matches the common lens-olfactory territory. Their expression domains separate just as lens and nasal precursors segregate, with *Dlx5* concentrating nasally and *Pax6* accumulating in the lens.

Based on these observations, an intriguing possibility is that these two factors control the process of segregation as well as the directional movements observed in films. However, analysis of Dlx and Pax6 proteins reveals that both factors remain co-expressed for much longer and Dlx is only lost from lens cells when the placode is established as a morphological entity, suggesting that these factors are unlikely to confer placodal identity until the time of placode formation. In agreement with this,

maintenance of Dlx5 protein in future lens cells results in the loss of lens morphology and lens specific gene expression, and the cells themselves fail to incorporate in the forming lens. Interestingly, in a complementary experiment $Pax6^{-/-}$ cells in mouse chimaeras sort out from neighbouring wild-type lens cells (Collinson et al, 2000). Together these observations suggest that the loss of Dlx protein is essential for lens cells to acquire lens identity, reminiscent of how eye and antennal disc identity is conferred in the fly.

2.4C Do Pax6 and Dlx5 regulate cell sorting at placode stages?

The observations that lens cells that are forced to maintain Dlx5 expression (this study), as well as $Pax6^{-/-}$ cells in mouse chimaeras (Collinson et al, 2000) are expelled from the developing lens indicate that at the time of placode formation Pax6 and Dlx transcription factors regulate a cell sorting event to ensure that only cells with appropriate fates are included in the lens. Indeed, Pax6 is known to regulate cell adhesive properties (Chalepakis et al., 1994; Davis et al., 2003; Stoykova et al., 1997; Tyas et al., 2003). Similarly, in the leg imaginal disc in Drosophila, $Dll^{-/-}$ clones segregate from their Dll-positive neighbours (Gorfinkiel et al., 1997; Panganiban and Rubenstein, 2002; Wu and Cohen, 1999). Thus, it is likely that the control of adhesive properties by these transcription factors is important for placode formation.

2.4D Extensive cell movements as a general feature of placode development

Our findings reveal that extensive cell movements accompany the formation of both the lens and olfactory placode in the chick embryo. In addition, individual cells or cell groups constantly change their neighbours until a homogeneous domain

of presumptive lens or olfactory cells is formed. Similar movements and cell rearrangements have recently been described during the formation of the chick otic (Streit, 2002) and of the zebrafish olfactory placode (Whitlock and Westerfield, 2000), raising the possibility that this is a general feature of placode formation.

From within a large pre-placodal domain next to the anterior neural plate, precursors for specific placodes converge to their final position while undergoing constant cell rearrangements. How do these cells segregate? One possibility is that cell movements are random and that only cells that happen to encounter appropriate inducing signals are directed towards a specific fate. An alternative is that cells move directionally to their final destination and/or sort out from their neighbours due to differential properties. The findings that some cells like lens (this study) and otic precursors (Streit, 2002) seem to move against the mainstream (laterally away from the neural tube and midline) suggests that directional cues may govern their behaviour.

As discussed above, Pax6 and Dlx5 appear to act late, perhaps in connection with the acquisition of specific fates, rather than early to control the segregation behaviour of lens and nasal precursors. On the other hand, in situ hybridisation reveals mosaic expression and more importantly an early bias of mRNA distribution for both factors at the time when streams of future lens and olfactory cells start to diverge, suggesting that the upstream regulatory mechanisms that govern both migration and the differential expression of these factors are deployed very early. Taken together, our study suggests that cells within the common placodal territory may have an early bias towards a specific placodal fate, which is subsequently reinforced by a combination of two mechanisms: local signals to control gene expression, including which factor wins over the other in a tug-of-war (as in the fly),

and cell sorting mechanisms, which leads to incorporation into appropriate placodal territories.

2.5 Acknowledgments

We thank Drs. A. Bang and D. Kosher for cDNA clones, Jhumku Kohtz and Joram Piatigorski for antibodies and Heide Olsen for excellent technical assistance. We also thank Dan Darcy, Carole Lu, Ying Gong and Seth Ruffins for invaluable advice on confocal time-lapse movies and their analysis. We are grateful to Dr. C.D. Stern for critical reading of the manuscript. This work was supported by BBSRC 29/G13701 and a Royal Society grant to AS and by NS41070 to MBF. S.B. is supported by a Howard Hughes Predoctoral Fellowship and A.B. is supported by a Fight for Sight Studentship.

Figure 1: Diagram showing the standardisation of the injection sites relative to other landmarks

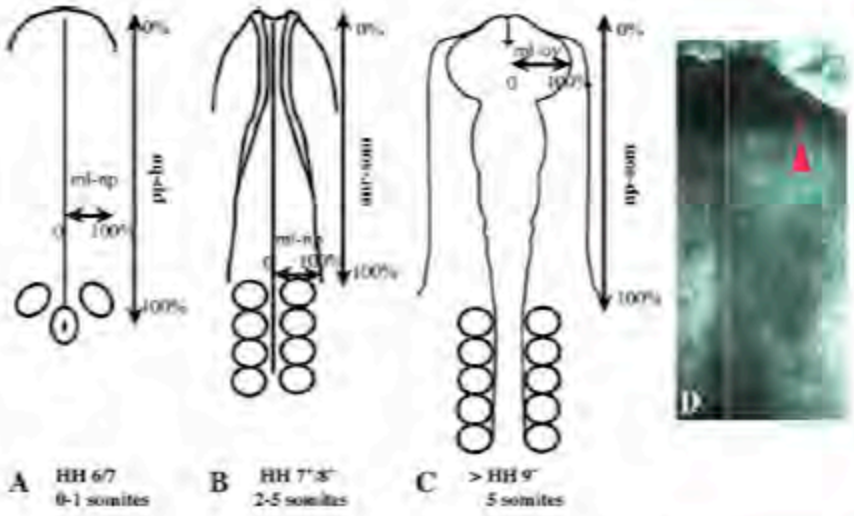

A. In stage HH 6/7 embryos (0-1 somite), the distance between the centre of Hensen's node and the anterior tip of the prechordal mesoderm (pp-hn; 0-100%) was measured and set to 100%. The position of labelled cells along the anteroposterior axis was expressed as % pp-hn. The mediolateral position was expressed as % of the distance between the midline (0%) and the lateral edge of the neural plate (100%; ml-np; half the width of the neural plate). **B.** In embryos with 2-5 somites (HH 7 *-8*) the mediolateral position of the labelled cells was determined as described in A. The distance from the anterior neural ridge to the anterior border of the first somite was set to 100% (anr-som) and the anteroposterior position of the labelled cells was expressed as % anr-som. **C.** In embryos with more than 5 somites (>HH 9) the anteroposterior position of labelled cells was measured as described in B. Their mediolateral position was determined as % of the distance between the midline and the most lateral edge of the optic vesicle (ml-ov). **D.** Example of an embryo labelled with a single DiI injection at HH7 (one somite stage).

Figure 2: Examples of DiI and DiO labelled embryos.
Small cell populations in the ectoderm of embryos at different developmental stages were labelled with DiI and DiO in the positions indicated in the diagrams (**A''**- **F''**). The embryos were grown until stage 15-18 when both the nasal and lens placode can be identified by their morphology. **A**, **A'**, **A''** a cell population labelled at stage 7 just outside the neural plate (**A''**) gave rise to progeny in both the lens and the nasal placode (**A**, **A'**). **B**, **B'**, **B''** two cell populations in a 2-somite embryo were labeled at the same anteroposterior level, but in different mediolateral positions (**B''**). Both labels contributed to the olfactory placode (**B**, **B'**) and surface ectoderm, while only DiI labelled cells (red) gave rise to lens cells. **C**, **C'**, **C''** groups of cells in a 5-somite embryo were labelled at different anteroposterior levels (**C''**). Both DiI (red) and DiO (green) labelled cells populated the lens (red; **C**, **C'**) as well as the nasal placode; DiO labelled cells are also found in surface ectoderm. **D**, **D'**, **D''** two cell populations were labelled at the 7-somite stage (**D''**). DiI labelled cells gave rise to the lens and surface ectoderm (Red; **D**, **D'**), while DiO labelled cells contributed to the nasal placode and the adjacent ectoderm (green; **D**). Note: DiO label in the eye is confined to optic vesicle derived cells and are due to accidental labeling of the vesicle underlying the surface ectoderm. **E**, **E'**, **E''** when labelled at the 9-somite stage cells in the anterior ectoderm give rise to the olfactory placode and surrounding ectoderm (**E**, **E''**). **F**, **F'**, **F''** show an embryo labelled in the ventral ectoderm at the 11-somite stage (ventral view in **F''**). DiO labelled cells close to the anterior neuropore contributed to the olfactory placode (**F**, **F'**), while DiI labelled cells further away populated the ectoderm of the 1st branchial arch (**F**). **A'**, **B'**, **E'** and **F'** show sections through the nasal placode of the embryos shown in **A**, **B**, **E** and **F**, respectively; **C'**, **D'** represent sections through the lens of the embryos shown in **C** and **D**, respectively.

Figure 2: Examples of DiI and DiO labelled embryos

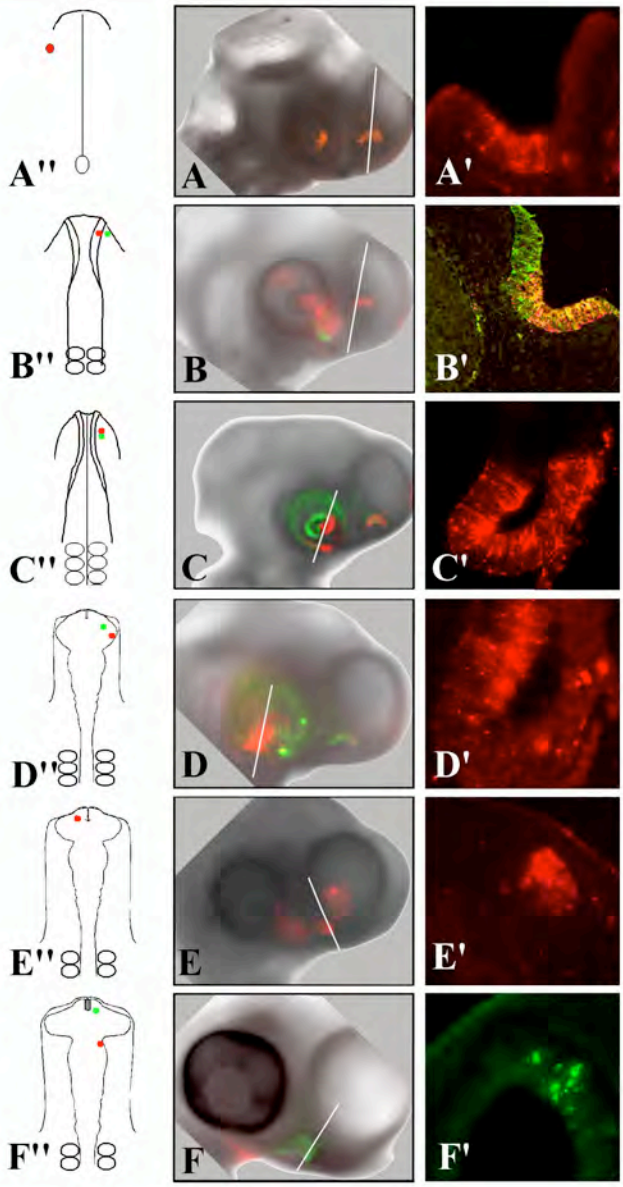

Figure 3: Fate map of lens and olfactory precursors between stages HH6 and 10

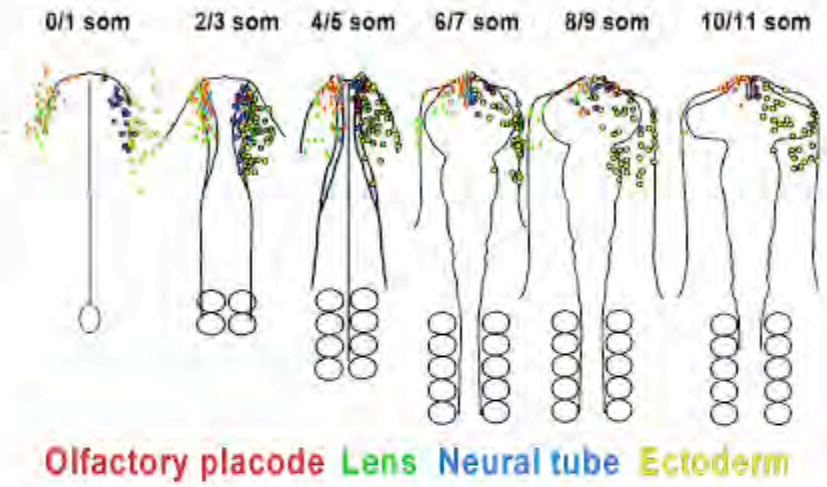

Small cell populations in the epiblast were labelled with DiI and DiO at stages HH 6-10: embryos were grown until the nasal and lens placodes were morphologically visible. Each circle (right) or square (left) represents one dye injection; each injection contributed to one (circle) or more tissues (squares) that are colour coded; red: olfactory placode, green: lens placode, blue: neural tube, yellow: surface ectoderm (including corneal ectoderm and ectoderm of the branchial arches). At stage HH 6/7 (0-1 somites) lens and nasal placode precursors are intermingled with each other and future epidermis cells; there is some overlap with neural precursors in the outer edge of the neural plate. At the 2-3-somite stage (HH 7^{+}/8^{-}) precursors for both placodes localise to the anterior neural folds and the adjacent ectoderm and are still mixed. From the 4-5-somite stage onwards (HH 8/8^{+}), future lens and nasal cells begin to separate until by the 10-somite stage (HH 10) no overlap between both cell groups is observed. At this stage, single injections still contribute progeny to the nasal placode and epidermis or to the lens and epidermis.

Figure 4: Lens and olfactory precursors show directional movement to their final target position

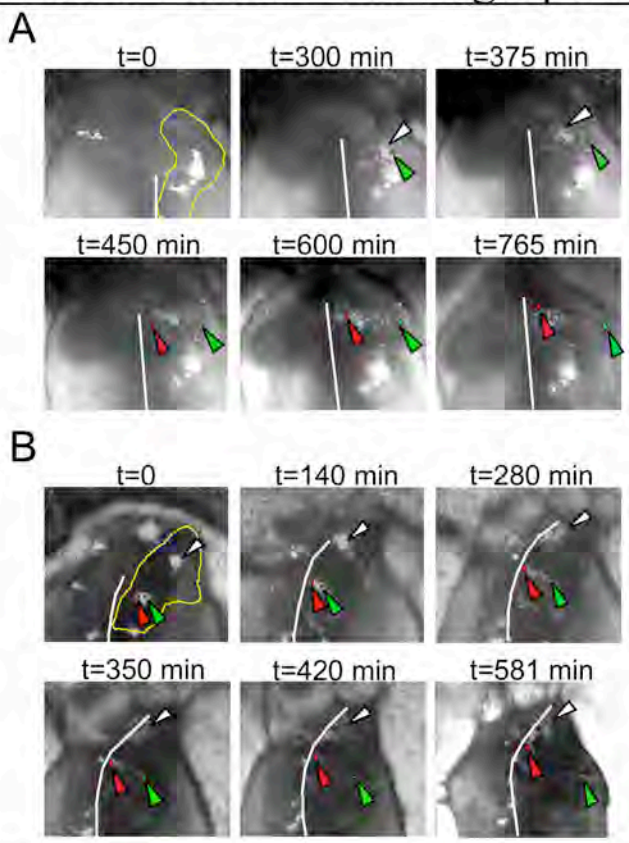

Single frames from time-lapse movies illustrate that extensive movements occur within the placode domain, leading to the segregation of olfactory and lens precursors. Times are indicated above each frame in minutes and the white line indicates the embryonic midline. **A.** An embryo that received multiple DiI injections within the placode domain (indicated by yellow outline) at stage HH 8 -. The green cell group (green arrowhead) underwent lateral movement towards the lens whereas the adjacent cells (white arrowhead) moved rostromedially towards the olfactory placode. The group indicated in red (red arrowhead) first came into the plane of focus near the midline at t = 450 min. From this location, this cell population moved rostrally to the olfactory placode. **B.** An embryo labelled at stage HH 8, with three injection sites within the placode domain (yellow outline). The green cell group (green arrowhead) moved laterally towards the lens. The immediately adjacent red population (red arrowhead) moved medially in the direction of the olfactory placode. The most rostral injection (white circle and arrowhead) underwent little apparent cell movement and cells became localised to the anterior neural folds within the olfactory placode domain.

Figure 5: Individual cell populations split into streams of cells moving towards different targets

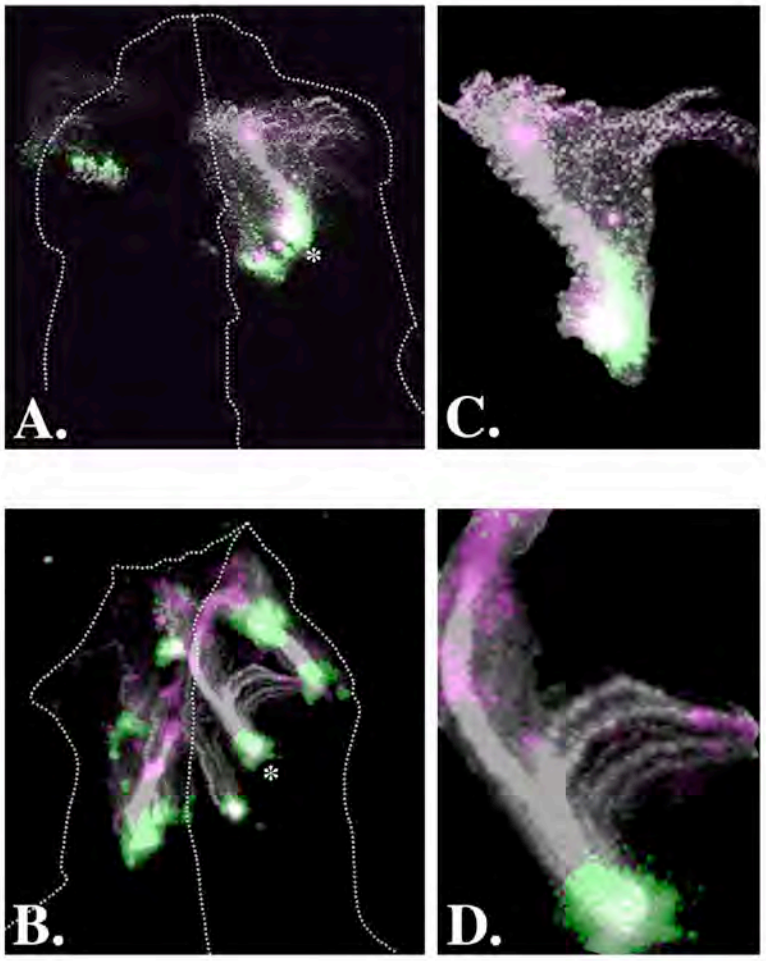

A and B: Trajectories of cell groups shown in Fig. 4A and B, respectively, obtained by collapsing all time frames for each movie into a single image. The first frame is indicated in green and the last in magenta to indicate the start and final position of the label. The outline and midline of the embryo in the last frame are depicted by the dotted lines. **C and D** show high magnification views of individual groups (white asterisks in A and B, respectively). Approximately 40 cells were labelled in C and about 20 cells in D.

Figure 6: Changes in *Dlx5* and *Pax6* expression reflect the spatial arrangement of nasal and lens precursors

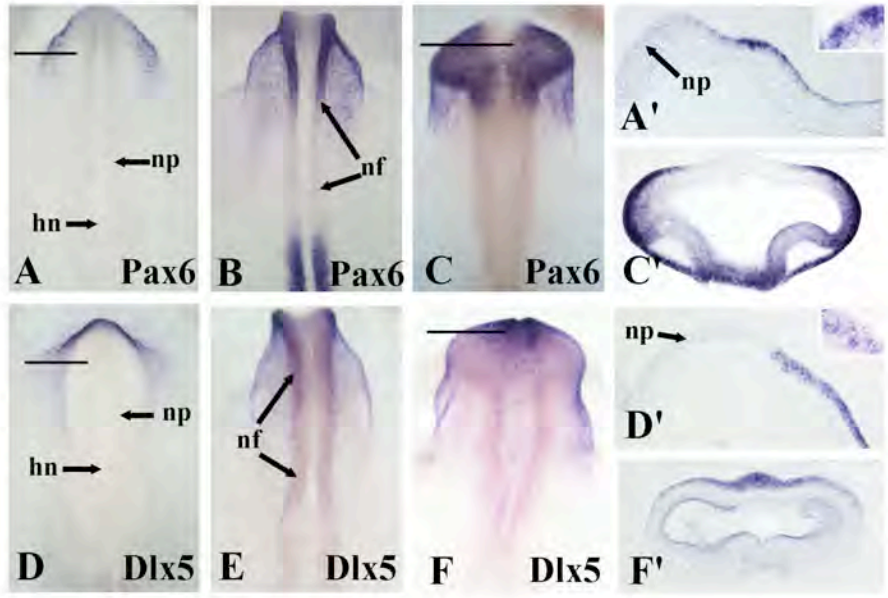

Whole mount in situ hybridisation showing the expression of *Pax6* (**A-C**; **A', C'**), *Dlx5* (**D-F**; **D', F'**), at stages 7 (**A, D**), 8 (**B, E**), 10 (**C, F**). *Pax6* and *Dlx5* are co-expressed at the border of the neural plate at stage 7 (**A, A', D**, **D'**) although expression seems to be mosaic (insets in A', D'); while *Dlx5* begins to concentrate in the most anterior ectoderm and neural folds (**E**; stage 8), *Pax6* remains expressed in the folds and the ectoderm lateral to the diencephalic region (**B**; stage 8). By stage 10, *Pax6* (**C; C'**) and *Dlx5* (**F; F'**) expression domains are mutually exclusive. **A', C', D', F'** show sections through the embryos in A, C, D and F respectively, at the level indicated by black lines. hn: Hensen's node, nf: neural folds, np: neural plate.

Figure 7: Dlx and Pax6 proteins are differentially expressed at the time of placode formation

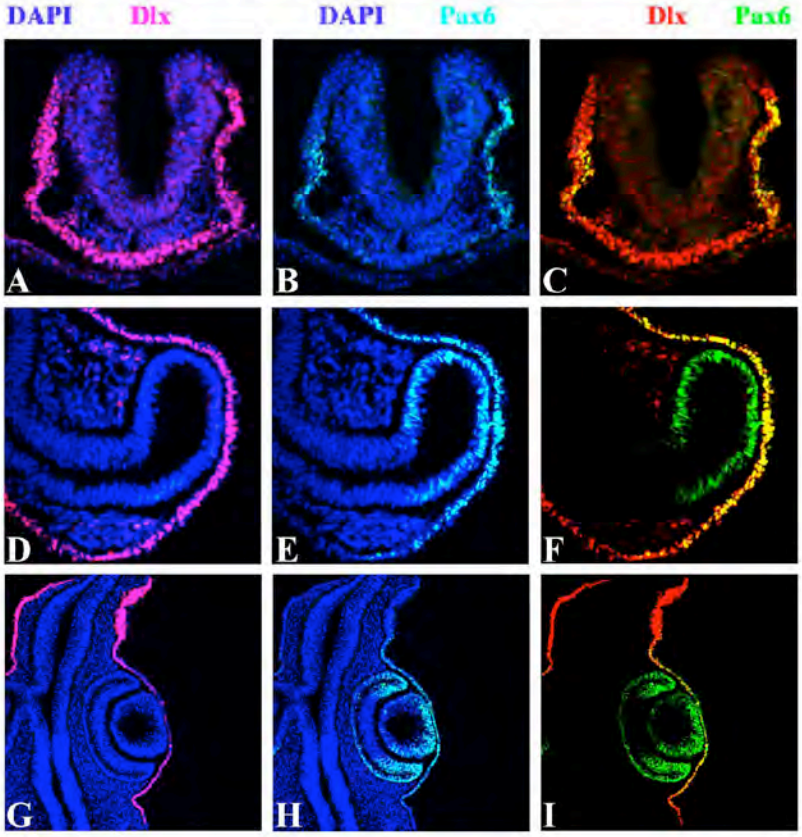

Immunohistochemistry was performed on frozen sections of stage HH 8 (**A-C**), 12 (**D-F**) and 15 (**G-I**) embryos using a pan-Dlx (red; **A, D, G, C, F, I**) and a Pax6 specific antibody (green; **B, F, H, C, F, I**). To visualise nuclei sections were stained with DAPI (blue). **C, F** and **I** show overlay of Dlx and Pax6 staining. At stage 8, Dlx (**A**) and Pax6 (**B**) are coexpressed in the lateral ectoderm next to the anterior neural plate (**C**, yellow) and continue to do so in the presumptive lens ectoderm until stage 12, just before the lens placode forms (**D-F**). Note: optic vesicle is Pax6^{+} (green). The mature lens placode (**G-I**) has lost Dlx expression (**G, I**), but retained Pax6 (**H, I**); likewise, the future cornea gradually loses Dlx protein. In contrast, the olfactory placode is strongly Dlx positive, but does not show any Pax6 expression. c: future cornea, l: lens, nt: neural tube, op: olfactory placode, ov: optic vesicle, ple: presumptive lens ectoderm.

Figure 8: Lens cells that continue to express Dlx5 lose lens character and are excluded from the lens

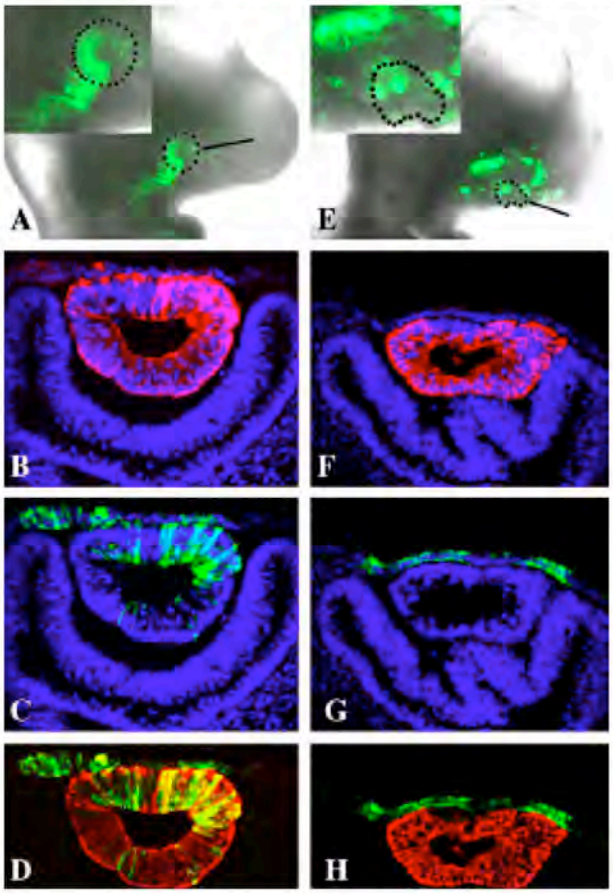

The lens-olfactory territory was electroporated with pCAB-IRES-GFP (control; **A-D**) or pCAB-Dlx5-IRES-GFP (**E-H**) at stage HH 8-9. The distribution of GFP positive cells was evaluated in whole mounts (**A, E**) and cryosections (**C, D, G, H**). Control electroporated cells are found in the lens as well as widespread in the head ectoderm (**A, C, D**, inset in **A**), while Dlx5 containing cells never occupy the lens and cluster (**E, G, H**, inset in **E**). Cryosections were stained using antibodies against GFP (**B, C, G, H**; green) and the lens specific δ-crystallin (**B, D, F, H**; red) and DAPI to visualise nuclei (blue). **D** and **H** show overlays of GFP and δ-crystallin expression. In control embryos, lens morphology is normal and GFP and δ-crystallin are coexpressed in the lens (**B-C**; yellow in **C**). In contrast, in Dlx5 electroporated embryos the lens is smaller and malformed and no Dlx5 expressing cells (green, **G, H**) are found in the δ-crystallin positive lens (**F, H**).

Chapter 3

Single cell lineage analysis of olfactory and lens placode precursors

3.1 Introduction

The lens of the eye and the olfactory epithelium of the nose are both derivatives of sensory placodes. The nasal placode develops anterior to the eye and in fairly close proximity to it. Not only do lens and nasal placode precursor cells arise from a common population of cells, they also share the expression of certain molecular markers, such as Pax6 and Dlx5 before they form morphologically distinct placodes. To determine whether single cells at early neurula stages could give rise to both cell types, we decided to follow the lineage of individual cells in the shared lens-olfactory territory. We achieved this goal using the most direct method, by intracellularly injecting a cell with high molecular weight rhodamine dextran (Fraser, 1996, Stern and Fraser, 2001). This technique has been used with much success in the analysis of neural crest lineages (Bronner-Fraser and Fraser, 1988, Bronner-Fraser and Fraser, 1989), in determining the multipotency of retinal cells (Wetts and Fraser, 1989), and in following the segmentation of the somatic mesoderm (Stern et al, 1988).

Our results suggest that individual cells in the common lens and olfactory region are restricted in their cell fate decisions at HH stage 6: they either contribute to the olfactory epithelium or to the lens, never to both.

3.2 Materials and methods

3.2A Single cell injections

Injecting electrodes were made from heat pulled aluminosilicate glass microcapillaries (A-M systems) using a horizontal Sutter electrode puller.

Aluminosilicate glass is preferred over borosilicate for this purpose as it is harder, has improved chemical durability, reduced electrical conductivity and a lower coefficient of thermal expansion. Also, aluminosilicate glass can be drawn to produce very fine tips. To allow for a wide bore but very fine tip, the electrodes were pulled in two steps: first high heat was applied for a short time and then lower heat was applied and the needle pulled apart. The electrodes were back-filled with 1μl of 10 kDa rhodamine dextran. High molecular weight rhodamine dextran does not pass through gap junctions and leak into neighbouring cells; hence, it is required for unambiguously labeling a single cell. Just prior to injecting, the rhodamine dextran in the electrode was overlaid with 1.2M LiCl. The electrode is then placed in the electrode holder reservoir and the reservoir is similarly filled with 1.2M LiCl to complete the circuit.

Once the electrode is prepared, the egg is opened and India ink diluted 1:20 is injected in the sub-blastodermal cavity to visualize the embryo. A ground electrode is placed in the egg white via a small hole in the shell. The position of the crosshairs in the eyepiece of the microscope is adjusted such that it is on the site to be injected. The embryo is lowered such that it is out of focus. The electrode is then brought in and the very tip of the electrode is focused at the centre of the cross–hairs. The embryo is then focused upon using the fine focus and the electrode is lowered using the coarse controls. Once the electrode is in the Ringer's solution bathing the embryo, a trace on the oscilloscope is evident. The resistance of the electrode is measured. A tip resistance on the order of 20-30 MΩ is indicative of a sharp electrode and can be used to penetrate the cell membrane of a single cell. The electrode is then slowly lowered towards the embryo using fine controls. An increase in noise is noted as the electrode approaches the embryo. The electrode is

"rung" by very quickly turning the capacitance knob. If the electrode enters a cell, a drop in the voltage, ranging from 10-40 mV is noted. The dye is then released into the cell by injecting 4nA of current for 5 seconds. The electrode is then quickly removed from the cell and the oscilloscope trace should return to its ground value. The success of the injection is then verified using epifluorescence. If fluorescence was clearly visible, the eggs were sealed using Scotch tape. Signals were amplified using an intracellular amplifier and electrical activity was observed on an oscilloscope. The experimental set-up is shown in Figure 1A. Embryos were harvested 24- 48 hours later and fixed in 4% paraformaldehyde overnight at 4°C. Approximately 90% of the embryos survived 24 hours later (96 out of 131 embryos injected).

3.2B Histology

Fixed embryos were washed several times in PBS and then scored for labeled cells in the head region using an upright Zeiss Axiophot fluorescence microscope. Labeled embryos were photographed using an Axiocam digital camera attached to the fluorescence microscope. Some of these embryos were then processed for cryosectioning. The embryos were equilibrated in PBS containing 5% and 15% sucrose before being embedded in 7.5% gelatin (300 bloom, Sigma) and 15% sucrose. The embryos were sectioned at 10 μm and the slides stored at 4°C.

3.2C Immunocytochemistry

Chick embryos from HH stages 5-10 were collected and the vitelline membrane removed. The embryos were fixed in 4% paraformaldehyde overnight at

4°C. After fixation, the embryos were rinsed and washed several times in PBS. Whole mount immunocytochemistry was begun by blocking the embryos in 10% donkey serum in PBS containing 0.1% BSA and 0.1% Triton-X-100 for 2 hours at room temperature. The primary antibody, a rabbit polyclonal antibody against phosphohistone H3 was used at a dilution of 1:5000 in the blocking solution and was applied overnight at 4°C. Secondary antibody (goat anti-rabbit Alexa 568) was used at a dilution of 1:1000 in blocking solution. Extensive washes with PBS were carried out after each antibody application. Embryos were mounted in PBS and photographed on an upright Zeiss Axiophot fluorescent microscope.

Slides with sections through embryos were degelatinised by soaking in PBS warmed to 42°C for 5-10 minutes. Neurofilament (1:250) and βIII-tubulin were diluted in blocking buffer as the primary antibodies with a goat anti-mouse IgG Alexa 488 used as the secondary antibody to detect both primary antibodies. Several washes with PBS containing 0.1% Tween were carried out after each application of antibody. Slides were finally rinsed in distilled water before being mounted in Permount containing 10μg/ml DAPI, a nuclear stain.

3.3 Results and discussion

The previous chapter details the generation of a fate-map of the chick olfactory and lens placodes from HH stage 6-10 by DiI and DiO labeling small populations of cells. This fate-map reveals the origin of olfactory and lens placode precursor cells from a shared territory at the border of the anterior neural plate at HH stages 6-8. A single injection (on average comprising 10-30 cells) at these stages can contribute to both olfactory and lens placodes in addition to epidermal cell

types. Does this reflect the potency of cells at the single cell level or is it simply that each labeled cell population is made up of single cells that are already fated to contribute to one particular tissue type? To address this question, we chose to inject single cells in the common olfactory-lens region from stages 6-8.

3.3A Single cells injected in the common lens-olfactory domain from stages 6-8 give rise to either olfactory epithelial cells or lens cells but not both

Single cell injections were first attempted in the dorsal neural tube in order to learn the technique (Fig. 1B). A clone of neural crest cells derived from one such injection is documented in Fig. 1B. We next attempted labeling single cells in the shared olfactory-lens region. An electrode of high resistance (20-30 MΩ) is crucial for efficient penetration of the cell without going through the epiblast or ectoderm to the layer of cells below. Of the 96 surviving embryos, only 22 had detectable label when analyzed in whole mount under a fluorescent microscope. Embryos injected at stage 6 produced clones that spanned multiple tissue types. More medial injections (closer to the midline of the embryo) gave rise to cells in the forming olfactory placode (Fig. 2A) and in the forebrain (seen in sections through this region, data not shown). Slightly more lateral injections produced cells in the lens and neighbouring ectoderm (Fig. 2B).

By HH stage 8, clones derived from single cells contribute exclusively to the olfactory epithelium or the lens (Fig. 3A, E). In sections through the olfactory epithelium, rhodamine dextran can be seen in olfactory sensory neurons, which are visualized through their expression of neurofilament and βIII-tubulin (Fig. 3B-D). While an accurate estimation of clone size has not been undertaken, an

approximation suggests that cells at the border of the anterior neural plate at stages 6-8 undergo cell division at the rate of 1 every 4-6 hours. This is considerably faster than a previous estimate of 10 hours per round of cell division in the ectoderm (Smith and Schoenwolf, 1987), though cell death has not been taken into account in this calculation. Interestingly, clones of cells derived from a single cell do not disperse throughout the area but rather form compact streams of cells inspite several rounds of cell division and fairly vigorous morphogenetic movements taking place.

3.3B Distribution of mitotic figures between HH stages 6-10

To determine if there is a differential distribution of cells undergoing mitosis between stages 6-10, the developmental stages at which the fate-map was constructed, we immunostained embryos in whole mount preparations. Counting cells in a given area of the anterior of the embryo versus the posterior did not suggest a significant difference in the number of cells undergoing mitosis (Fig. 4). However, this technique does not allow a determination of cells in S-phase; hence it is possible that the total number of cells entering the cell cycle may be higher in the anterior of the embryo. The immense morphogenetic movements occurring in the region of the head might be due to a higher density of cells in the head as compared to the trunk and/or it may be a result of the intrinsic property of cells in these disparate regions.

Our fate map study of the chick olfactory and lens placodes suggested that the precursors for these embryonic cell populations arise from a common territory at

the border of the anterior neural plate between HH stages 6-8. To determine whether individual cells at these stages are already fated to contribute to a single sensory structure, we injected single cells at these stages and analyzed the resultant clones. Our data indicate that single cells at HH stage 6 are pluripotent and can contribute to neuroepithelial and olfactory cells or to epidermal and lens cells. We found no evidence for cells giving rise to progeny both in the lens and the olfactory epithelium. By HH stage 8, clones derived from single cells contributed exclusively to the olfactory epithelium or to the lens. One obvious caveat in this study is the small number of embryos analyzed. While 131 embryos were injected, only 22 were found to found to have detectable label most likely as a consequence of death of the cells that were injected. Given that the area encompassed by the common lens-olfactory domain likely contains hundreds of cells, a large number of embryos would need to be analyzed to definitively rule out the possibility of common lens and olfactory progenitor cells. Additionally, unlike in *C. elegans*, cells in the chick embryo do not occupy an invariant position and consequently do not have an invariant lineage.

When single cells in zebrafish were labeled at slightly older stages (equivalent to chick HH stage 8+), mixed clones containing both telencephalic and olfactory placode cells were never found in contrast to our findings, although a few clones did give rise to both the olfactory organ and the anterior pituitary (Whitlock and Westerfield, 2000). More recently, it has been found that single precursor cells at bud stage in zebrafish (equivalent to chick HH stage 7) are destined to contribute to either olfactory, lens or pituitary placode (Dutta et al., 2005). Possibly, cells in this most anterior region of the embryo are lineage-restricted early in development. Interestingly, inspite of this high degree of specification seen at a single cell level

very early in development, these precursors are found to intermingle in a shared area (Dutta et al., 2005, Bhattacharyya et al., 2004, Whitlock and Westerfield, 2000).

Figure 1: Experimental set-up for single cell injections

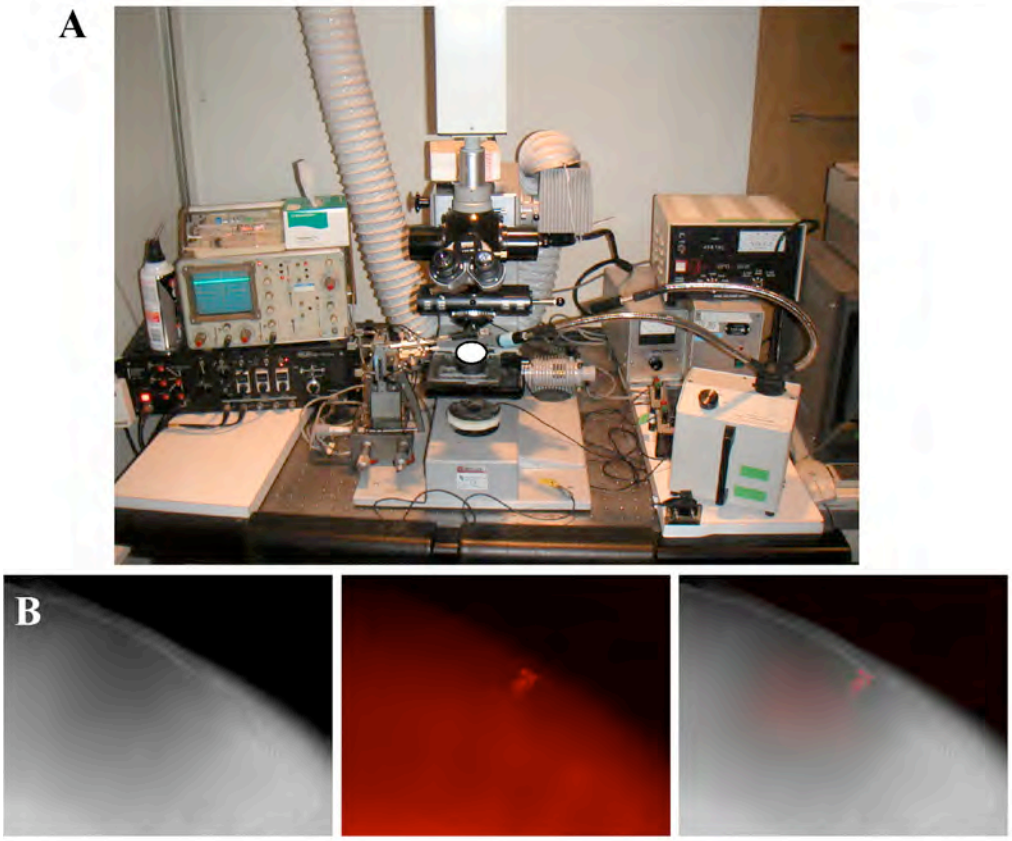

A. Experimental set-up for single cell injections. **B**. Example of an embryo in which a single dorsal neural tube was injected at HH stage 10 and harvested 24 hours later. The clone of cells derived from this one cell is seen in the fluorescent panel. An overlay of the brightfield and fluorescence images is shown in the third panel for a better appreciation of the location of the clone.

Figure 2: Single cell injections in the common lens and olfactory precursor region at stage 6 contribute to either the olfactory or the lens placode

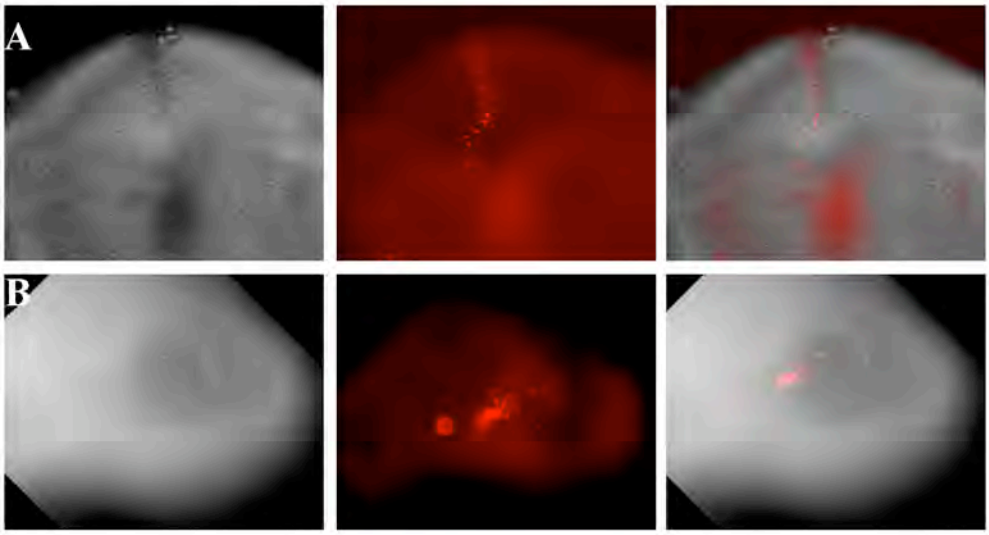

A. Example of an embryo in which a cell was injected at HH stage 6 in the common lens-olfactory domain and harvested a few hours later at HH stage 10. Labeled cells are clearly noted in the forming olfactory placode region on the ventral surface of the ectoderm. Some labeled cells also contributed to the forebrain (seen in section, data not shown here). **B**. Another example of an embryo injected between HH stages 6-7 and harvested 28 hours later. Labeled cells are clearly visible in the lens and adjacent ectoderm.

Figure 3: Injecting single cells at stage 8 produces clones of cells that contribute exclusively to the olfactory epithelium or the lens

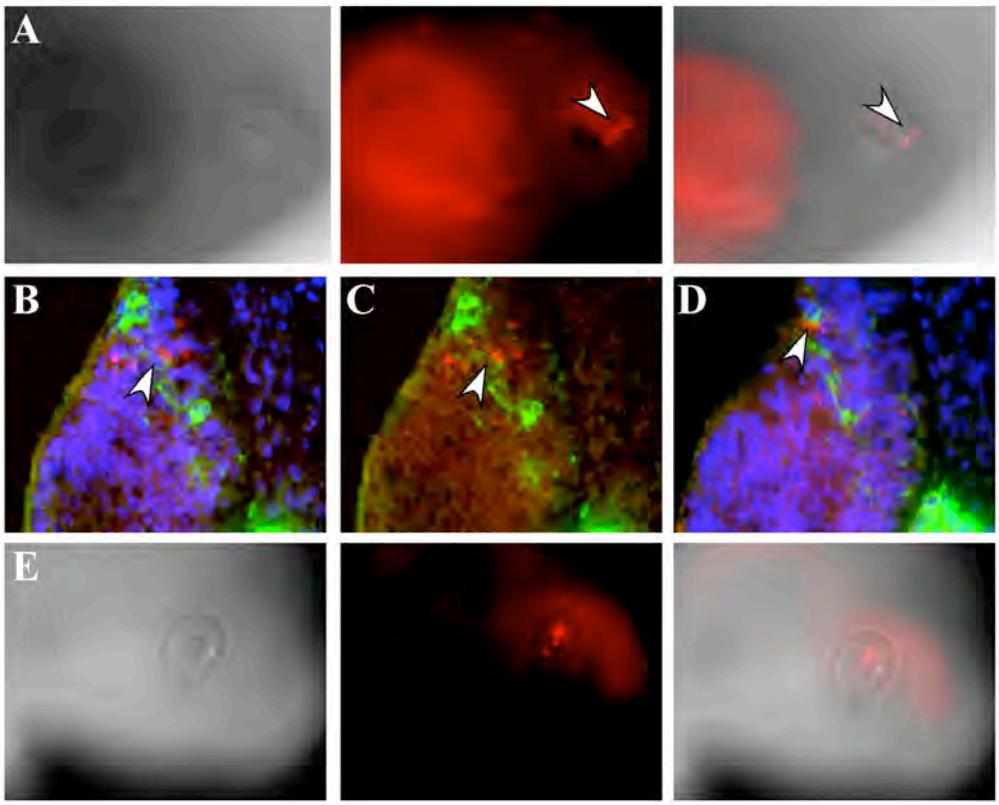

A. Example of an embryo in which a cell at the edge of the anterior neural fold was injected at HH stage 8 and harvested 48 hours later. The arrowheads point to the stream of labeled cells seen in the olfactory epithelium. Staining in the eye is not as a result of dye injection. **B, C**: A section through the embryo shown in **A**. In **B**, DAPI staining is shown in blue and neurofilament staining in green. Rhodamine dextran is seen in red. **C** shows the same figure without the DAPI staining. The arrowheads in both panels point to a cell that has rhodamine dextran in its cytoplasm and neurofilament staining emanates from it suggesting that it is an olfactory sensory neuron. **D**. Another section through the same embryo showing the close apposition of rhodamine dextran with neurofilament staining (arrowhead). **E**. Another embryo injected at HH stage 8 in the ectoderm lateral to the anterior neural fold. Progeny of this cell are found exclusively in the lens of the eye.

Figure 4: Mitotic figures in chick embryos, from stages 5-10 as revealed by phospho-histone H3 staining

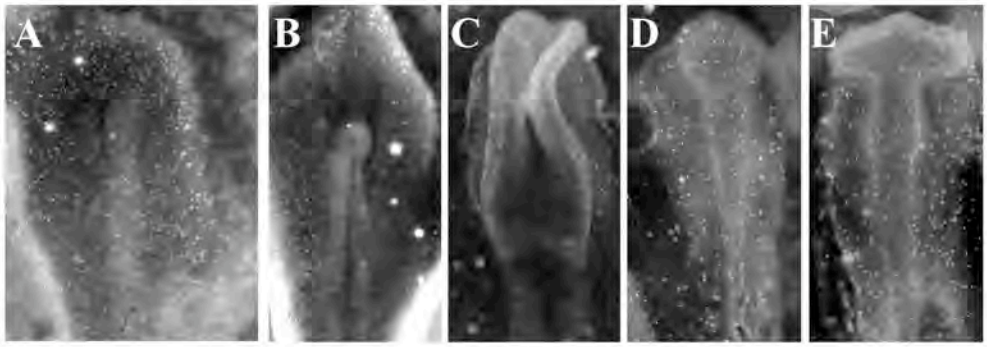

Whole mount immunostaining with the phosphohistone H3 antibody at different developmental stages. **A**. HH stage 5. **B**. HH stage 6. **C**. HH stage 8. **D**. HH stage 9. **E**. HH stage 10. No appreciable difference in the number of cells undergoing mitosis is noticeable when comparing the presumptive olfactory placode territory with the rest of the embryo.

Chapter 4

Spatiotemporal competence and commitment of ectoderm during the induction of the olfactory placode

4.1 Introduction

Cranial placodes were first observed over a century ago and since then have been empirically defined as localized regions of thickened columnar epithelium that give rise to the paired sense organs of the nose, the lens and the inner ear in addition to contributing to various cranial ganglia (van Wighe, 1883; Baker and Bronner-Fraser, 2001; Schlosser and Northcutt, 2000; Graham and Begbie, 2000). Of the three sensory placodes —the olfactory, the lens and the otic— the study of the lens placode has the longest tradition, starting with the characterization of lens induction from an embryological standpoint. In fact, lens induction has often been exemplified as a paradigm for embryonic induction (Grainger, 1992). Both lens and otic placode induction have received much attention as these structures form morphologically distinguishable landmarks relatively early (within the first two days of development in avians) in the embryo. Recently, with the advent of molecular tools, genetic networks operational in both lens and otic placode induction have begun to be characterized. The olfactory sensory system on the other hand has been examined at substantially later time points. The olfactory epithelium makes an attractive model system for studying neurogenesis as the olfactory sensory neurons are regenerated for the duration of the lifetime of an organism (Farbman, 1992; Farbman, 1994). In addition to giving rise to the olfactory sensory neurons that are responsible for our perception of smell, the olfactory epithelium also gives rise to specialized neuroendocrine cells, known as the gonadotropin-releasing hormone (GnRH) neurons (Wray, 2002; Parhar, 2002) and pheromone receptor neurons in the vomeronasal organ (Dulac, 1997). The role of various extracellular growth factors and intracellular transcription factors has been defined in the differentiation of the olfactory epithelium, particularly along the olfactory sensory lineage (Gordon et al.,

1995; DeHamer et al., 1994; Calof et al., 1996; Calof et al., 1998; Guillemot et al., 1993; Guillemot, 1995; Cau et al., 1997, Cau et al., 2000; Cau et al., 2002). The molecular mechanism by which these neurons project to the olfactory bulb has also been elucidated in much detail in many elegant studies (Vassar et al., 1994, Mombaerts et al., 1996; Wang et al., 1998). However, the investigation of the initial creation of this complex structure has largely been ignored.

This has been due in part to the more intangible development of the olfactory placode. The placode, though it is present as a thickening at HH stage 14 (by which time, the other sensory placodes have begun to differentiate), it is still not easily distinguishable until 8 hours later. Till recently the only fate-map available for this placode was at HH stage 8 (3-4ss) (Couly and Le Douarin, 1985) at which time point, the precursors are found to straddle the lateral edge of the anterior neural folds and the adjacent ectoderm. In the intervening stages of development (stage 8+-14), the exact location of these precursor cells was unclear. This in turn impeded the identification of molecular markers of these cells at stages prior to its morphological identification. With the generation of a more complete fate-map (Bhattacharyya et al., 2004), it has now been possible to compare it with gene expression patterns to identify potential molecular markers of the olfactory placode. We show here that at different stages, Pax3, Pax6, Dlx3 and Dlx5 can serve as molecular guideposts of olfactory placode precursor cells.

We further wished to understand how and when the nasal structure is first induced. To investigate these issues, we examined the **competence** of embryonic ectoderm to form the olfactory placode and the time at which this placode was determined as regards its cells' fates. The terms of competence and determination are operationally defined and hence our experimental approach has been dictated

by these definitions. Competence has been described as "the total of all pathways of development of a cell or tissue region which can be achieved by exposure to environments present within the embryo" (Slack, 1991). Competence to form the olfactory placode was addressed by grafting ectoderm from different axial levels to the anterior neural fold at stage 8. Cranial and trunk level ectoderm are capable of responding to olfactory placode inducing signals by expressing Dlx3 and Pax6 and subsequently contributing to the olfactory epithelium. However, hindbrain and trunk level ectoderm lose the ability to express Dlx3 and Pax6 between stages 9-10. **Determination** is sometimes divided into two phases: a more labile phase of **specification** and an irreversible one of **commitment.** Specification has been experimentally defined as "commitment of a cell or tissue region which is manifested on culture in a neutral medium but may still be reversible" whereas commitment is the "aspect of the intrinsic character of a cell or tissue region which causes it to follow a particular pathway of development or fate" (Slack, 1991). We, therefore, examined the specification of the presumptive olfactory placode ectoderm to express Pax6 and Dlx3 and form neurons by culturing this tissue from various stages in three-dimensional collagen gel matrices, in order to determined the time by which induction had occurred. We observed that presumptive olfactory placode ectoderm is specified to express Pax6 and Dlx3 between stages 10-12 whereas neuronal specification occurs shortly thereafter. Thus, induction is complete even before the placode becomes morphologically visible. Finally, we determined the time at which the presumptive olfactory placode ectoderm is irreversibly **committed** to its fate by grafting this tissue at different stages to the trunk lateral plate ectoderm at stage 8/9. Commitment to an olfactory placode fate takes place by stage 15 as assayed by expression of Dlx3 and Pax6. These results show that development of the

olfactory placode is a step-wise process whereby signals from adjacent tissues (the forebrain and the prechordal mesoderm have been suggested as sources) induce the placode at or before stage 10 when the olfactory precursors have segregated from their neighbours to form a homogenous population of cells. While an initially broad region of ectoderm has the ability to form the olfactory placode, this ability is restricted as a function of time to allow for the positioning of the nasal cavity specifically at the very anterior end of the embryo.

4.2 Materials and methods

4.2A Quail-chick grafts

Fertilized chick (*Gallus gallus domesticus*, White Leghorn and Rhode Island Red) and quail (*Coturnix coturnix japonica*) eggs were obtained from a local commercial supplier (AA Labs, Westminster, CA, USA). Fertilized Spafas eggs were obtained from Charles River Laboratories, Roanoke, IL, USA. The eggs were incubated at 38° C in a humidified atmosphere until the desired stage was reached as per the Hamburger-Hamilton table. Donor and host embryos were visualized by cutting a window in the shell and injecting India ink diluted 1:20 or blue vegetable dye diluted 1:10 with Ringer's solution or Hank's buffered saline solution, under the blastoderm. To expose the region to be dissected in both, host and donor embryos, the overlying vitelline membrane was removed using a finely sharpened tungsten needle. Most stage 10 or older embryos were explanted and enzymatically treated to remove contaminating tissues: in the case of the cranial level ectoderm, the accompanying neural crest cells and in the case of the presumptive olfactory placode ectoderm, the subjacent mesenchyme and forebrain tissues. For the clean removal of the presumptive olfactory placode ectoderm, the embryos were treated with

1mg/ml dispase in DMEM (Boehringer Mannheim) (30 minutes on ice, 10 minutes at 37°C) or a combination of 1mg/ml dispase and 0.25% trypsin (30 minutes on ice, 10 minutes at 37°C) or 0.2 %-0.25% collagenase (Worthington) dissolved in Dulbecco's PBS (Gibco-BRL) (20 minutes at 37°C). Of these, 0.2% collagenase worked best. Cranial level ectoderm was dissected from explanted quail embryos that were treated with 1 mg/ml dispase. All embryos were washed in Ringer's solution to remove any traces of the enzyme and then allowed to recover in PB1 medium on ice for at least 30 minutes. After recovery, the embryos were placed in Ringer's solution and the ectoderm dissected out using a pulled glass needle. In younger embryos, the ectoderm of interest was simply dissected in ovo using a pulled glass needle. The dissected or explanted ectoderm was immediately grafted into a host embryo in which the graft site was already prepared. The graft was transferred from the donor to host embryo with a glass mouth pipette. While rostrocaudal or mediolateral orientation of the grafts was not preserved, all grafts were positioned in the correct inside-outside orientation. After grafting, the host eggs were sealed with Scotch tape and returned to the incubator for 48-72 hours. The surviving embryos, a total of 309 (on average **60**% of the embryos) were collected in Ringer's solution and fixed in 4% paraformaldehyde for 2 hours at room temperature or 4°C.

4.2B Collagen gel explant cultures

Quail embryos from Hamburger-Hamilton (HH) stages 6-21 were collected in Ringer's solution and stored on ice. Small pieces of HH 6-8 anterior neural fold and HH 9-21 presumptive olfactory placode ectoderm or olfactory epithelium were

dissected free of surrounding tissue. For older embryos (HH 9-21), the heads were treated with 0.25% trypsin in DMEM or 0.2% collagenase in Dulbecco's PBS for 20 minutes at 37°C to ensure adequate removal of adherent mesenchymal and forebrain tissue. Additionally, 1 mg/ml dispase was included in the Ringer's solution for the dissection of older embryos. After enzymatic treatment, the ectodermal explants were rinsed thoroughly in Ringer's solution and PB1 and the explants were stored in PB1 medium on ice while the remaining embryos were being dissected. Collagen gels were prepared by combining 90 μl of collagen (Collaborative Research) with 10 μl of 10X DMEM in the presence of 0.375% sodium bicarbonate. The collagen was allowed to solidify for 20 minutes at room temperature as 10 μL gels in 4-well tissue culture plates. Once the gels had set, the tissue pieces were transferred to the surface of these gels and overlaid with 5 μL of collagen. Following uniform solidification, the gels were submerged in 0.5 ml of F12-N2 medium and incubated at 37°C in the presence of 5% carbon dioxide for 24-48 hours. The collagen gels were then fixed in 4% paraformaldehyde overnight at 4°C for immunostaining.

4.2C Immunocytochemistry

Fixed embryos and collagen gels were equilibrated in PBS containing 5% and then 15% sucrose before being embedded in 7.5% gelatin (300 bloom, Sigma) and 15% sucrose. 10 μm sections were mounted on Superfrost® Plus glass slides (Fisher) and stored at -20°C. Sections were degelatinised in PBS at 42°C for 5-10 minutes prior to being blocked with PBS containing 0.1% BSA, 0.1% Triton-X-100 and 10% heat inactivated donkey serum. Primary antibodies were diluted in blocking

solution and applied overnight at 4°C while secondary antibody staining was performed for 2 hours at room temperature. Slides were rinsed twice and washed three times in PBS after each application of antibody. Finally, slides were rinsed several times in distilled water before being mounted in Fluromount-G (Southern Biotechnology) or in Permount containing 10μg/ml DAPI. For grafted embryos, two successive rounds of immunostaining were carried out: first to determine those in which the quail grafts had incorporated in the correct location (approximately **33**% of the surviving embryos) and subsequently, these embryos were scored for PAX6 and DLX3 expressing quail cells. The primary antibodies used in the study include:

1. QCPN IgG1 monoclonal antibody (DSHB, University of Iowa, USA) at a dilution of 1:1,
2. a rabbit polyclonal antibody to PAX6 (Covance) at 1:100,
3. a goat polyclonal antibody to DLX3 used at 1:1500 or at 1:150 if preadsorbed to chicken liver acetone powder (as described below),
4. a rabbit polyclonal antibody that recognizes all DLX family proteins (courtesy of Dr. Jhumku Kohtz, Northwestern University, USA),
5. Hu IgG2b monoclonal antibody (Molecular Probes) at 1:250,
6. a rabbit polyclonal antibody against Olf-1 (courtesy of Dr. Randall Reed) and
7. the monoclonal antibody RMO 270.3 directed against neurofilament (Lee et al, 1987, gift of Dr. Virginia Lee) used at 1:300.

Secondary fluorescent antibodies used in this study were purchased from Jackson Immunochemicals and Molecular Probes (Alexa fluorophores).

4.2D Antibody generation

The C-terminal region of the chick Dlx-3 protein (aa185-aa278) was used to raise an antibody that specifically recognizes the Dlx-3 protein. This region was amplified from pBluescript containing the entire coding sequence of cDlx3 (courtesy Dr. Andy Groves) using PCR. Appropriate restriction enzyme sites were included in the primers to allow cloning into the pGEX-KG vector (Pharmacia). The GST-DLX3 fusion protein was expressed in BL-21 cells using an IPTG inducible promoter and purified using Glutathione Sepharose beads (Pharmacia) following standard protocols outlined in *Molecular cloning*. A small-scale purification was performed to determine the optimal temperature, concentration of IPTG and length of induction time. Bacterial cultures induced with 0.25mM IPTG at 37°C or with 0.375mM IPTG at 30°C for 4 hours gave sufficient yields of protein. Based on these criteria, the Protein Expression Facility at Caltech carried out a large-scale preparation of the fusion protein. Polyclonal antibodies were generated in goat by injecting 5 mg of the fusion protein (Alpha Diagnostic Intl. Inc., San Antonio, TX). Western blots and immunostaining were performed to confirm specific staining.

4.2E Western blotting

Purified GST protein, GST-Dlx3 fusion protein and 10 d embryo extract were run out on a 12% SDS-PAGE gel for 1 hour at 140V at constant voltage. The proteins were then transferred onto nitrocellulose paper at 80 V for 2-3 hours on ice. The blot was blocked for 2 hours at room temperature in 5% milk in TBS-T buffer. The Dlx3 antibody was applied at a dilution of 1:1000 or 1:1500 overnight at 4°C. The blot was then washed extensively in TBS-T before applying the secondary antibody at a

dilution of 1:2000. The blot was again washed thoroughly before using the ECL Chemiluminescent kit to detect the proteins.

4.2F In situ hybridization

Whole mount in situ hybridization was performed according to protocols developed by Dr. David Wilkinson (In situ hybridization: a practical approach). Probes were generated from cDNAs for Dlx3 (courtesy Dr. Andy Groves), Pax3, Pax6 and Dlx5 (courtesy Dr. Michael Kessel).

4.3 Results

4.3A Molecular markers of the olfactory placode

Of the cranial sensory placodes, the nasal or olfactory placode is the last to undergo thickening to form a clearly discernible morphological structure at HH stage 14-15. The developmental progression from "naïve" epiblast to the self-evident olfactory placode encompasses approximately 52 hours since the egg is first laid. Significant changes occur in the number of cells, the position of cells with respect to each other and their molecular signatures over this time-span. To follow the presumptive olfactory placode cells, we analyzed the spatiotemporal expression patterns of a number of genes to determine those whose expression might reflect the acquisition of olfactory fate. These can be divided into two categories: genes that mark the presumptive olfactory placode cells in addition to various other head structures and genes that mark the anterior of the embryo and hence mark the olfactory placode as well (Otx2 and Six3, data not shown). We describe here the expression pattern of four genes that label presumptive olfactory placode cells.

Homeodomain transcription factors of the Dlx family (Panganiban and Rubenstein, 2002), Dlx3 (Pera and Kessel, 1999) and Dlx5 (Pera et al., 1999) , and the paired domain transcription factors, Pax3 and Pax6 are expressed in the presumptive olfactory placode. Dlx5 and Pax6 expression overlap in the common olfactory-lens domain in the anterior ectoderm proximal to the neural plate at stage 6 (Bhattacharyya et al., 2004). Their overlap is maintained until just prior to stage 10 when Dlx5 is upregulated in the presumptive olfactory precursors and Pax6 is down-regulated in these cells. Dlx3 expression while absent from the anterior neural folds and adjacent ectoderm at HH stage 8 (Fig. 1A, B), is strongly up-regulated in the olfactory placode precursors at stage 10 (Fig. 1C, D), at the same time as Dlx5. However, it is also expressed throughout the cranial ectoderm at lower levels at this stage (Fig. 1C, D). This expression is refined over time to a region in the midline of the ventral portion of the head ectoderm (Fig. 1E, F). Ultimately, in the head, Dlx3 is found exclusively in the olfactory and otic placodes and in the neural crest derived branchial arch derivatives (Fig. 2C). Like Dlx3, Dlx5 is expressed in both the olfactory and otic placodes at HH stages 19-20 (Fig. 2B).

Pax6 though initially expressed in the olfactory and lens precursor region (Fig. 1I), is interestingly down-regulated in the presumptive olfactory placode ectoderm from stage 10 onwards (Fig. 1J,K). Its expression is revived only once the olfactory placode has formed (Fig, 1L). By HH stages 19-20, Pax6 is expressed in both the lens and nasal epithelium (Fig. 2A). However, it is not expressed uniformly throughout the nasal epithelium, Instead, its expression is more pronounced in the aboral and lateral parts of the epithelium (Fig. 2A’). Unlike Pax6, Pax3 is strongly expressed in olfactory placode precursor cells from HH stage 9 onwards (Fig. 1G,H, Fig. 2D). Its expression is relegated to the aboral portion of the olfactory epithelium

(Fig. 2D'). It is also expressed in another placode-derived structure, the trigeminal ganglion (Fig. 2D). As is evident, all the genes mentioned above are not uniquely expressed in the olfactory placode; in fact, all of them are expressed in one other placode and its derivative: Pax6 in the lens, Dlx3 and Dlx5 in the otic placode and Pax3 in the trigeminal placode. However, the combined expression of these genes by HH stage 19 is a singular feature of the olfactory placode.

4.3B Dlx3 and Pax6 proteins are co-expressed in the olfactory placode

In order to better determine the colocalisation between the Pax6 and Dlx3 proteins, we generated a polyclonal antibody against the C-terminal portion of the Dlx3 protein. The C-terminal region was used, as it is the most dissimilar between the six Dlx family members. The GST fusion protein was purified using glutathione sepharose beads and standard protocols (Fig. 3B). The polyclonal antibody raised against the fusion protein was used to probe a Western blot (Fig. 4). The antiserum detected both GST as well as the fusion protein (fig. 4B). This is due to GST also raising an immune response in the animal; however, it could also be that the fusion protein was recognized solely due to the presence of GST antibodies in the antiserum. Multiple bands, including one at the right size for the native Dlx3 protein, were detected in the embryo extract (fig. 4B, lane 6). As the Western blot proved inconclusive, immunostaining of embryo sections was carried out. Using the polyclonal antibody it was possible to recapitulate the Dlx3 expression pattern. By in situ hybridization, large amounts of the Dlx3 transcript are detected in the otic placode at HH stage 10 (fig. 4C). Specific nuclear staining is observed in ectodermal cells destined to form the otic placode (fig. 4D). Taking these two lines of evidence- the Western blot data and the immunostaining- together, it suggests that an

antibody specific to Dlx3 has been raised. Additionally, only Dlx3 and one other family member are not expressed in the embryonic CNS and no CNS staining was detected in these sections. However, to prove beyond a doubt that the antibody recognizes the Dlx3 protein and none of the other family members, it is imperative to show that the antibody interacts with Dlx3 alone. Co-immunoprecipitation with the Dlx3 antibody would be one way to get around this issue. However, all Dlx family members are roughly the same size. Experiments are underway to in vitro translate the various family members and then carry out a Western blot.

At HH stage 14, when the olfactory placode first begins to thicken, Dlx3 protein is present at high levels in the ectoderm at the level of the forebrain (Fig. 5A,C). Pax6 protein is present in scattered cells within this region (Fig. 5B,C). Between HH stages 19-21, robust expression of both Dlx3 and Pax6 proteins is noticeable in the now pseudostratified epithelium (Fig. 5D, E). Significant overlap of expression is noted in cells in the cup-shaped structure of the olfactory epithelium (Fig. 5F). In fact, the combined expression of these two genes at this stage exclusively demarcates the olfactory epithelium in the embryonic nervous system. Antibodies against both proteins detected roughly similar levels of Pax6 and Dlx3 in quail cells as well (data not shown).

4.3C Neuronal markers of the olfactory epithelium

Multiple neuronal and non-neuronal cell types arise within the olfactory epithelium. Olfactory placode cells differentiate into olfactory sensory neurons, which are responsible for odour perception and the neuroendocrine gonadotropin-releasing hormone (GnRH) neurons (Schwanzel-Fukuda and Pfaff, 1989). In addition, non-neuronal derivatives of the olfactory epithelium include the olfactory

ensheathing glial cells, support cells and basal cells. Otx2, another homeodomain transcription factor, is expressed broadly in the olfactory epithelium (Mallamaci et al., 1996) (Fig. 6A, C). Its expression is maintained in the GnRH neurons where it is likely responsible for switching on expression of the gonadotropin-releasing hormone (Kelley et al., 2000). Also, Sox 10, an HMG box containing protein, which is expressed in peripheral glia and neural crest, is also expressed at low levels in the olfactory epithelium (Fig. 6B, C). Generic markers of post-mitotic neurons that are also expressed in the olfactory epithelium include the HLH transcription factor, Olf-1 (Davis and Reed, 1996) (Fig. 6D), the cytoplasmic RNA-binding protein Hu (Fornaro et al., 2001) (fig. 6E) and finally neurofilament (fig. 6F) (Drapkin and Silverman, 1999). Unlike other parts of the nervous system, Hu precedes neurofilament expression in the olfactory epithelium.

4.3D Competence of embryonic ectoderm at different axial levels to express Dlx-3 and Pax-6 and form the olfactory placode

To determine the spatiotemporal extent to which the embryonic ectoderm has the capacity to form the olfactory placode, we constructed quail-chick chimaeras, which were allowed to survive until such time as the olfactory placode was distinctly visible (usually 48-72 hours). The ages of the chick host varied between HH stage7 (0ss) to stage9 (7ss). They were then analyzed for the expression of the olfactory placode markers, Dlx3, Pax3 or Pax6 in addition to the quail specific marker, QCPN (**q**uail **c**ell **p**eri-**n**uclear antigen). There was no apparent difference in the behaviour of the transplanted tissue across these varying ages.

Based on a fate-map of HH stage 8 (3-4ss) chick embryo generated using such chimeras (Couly and Le Douarin, 1985) and our fate-map using dye labeling (Bhattacharyya et al., 2004), the olfactory placode arises from a population of cells distributed in and around the anterior neural fold. Isotopic control grafts of the quail anterior neural fold and adjacent ectoderm into a chick host at HH stage 8 (3-4ss) gave rise to quail cells in the olfactory placode that expressed Dlx3, Pax3 (data not shown) or Pax6 (n=6, Fig. 7B, C). Often times, quail cells were also found in the telencephalon (Fig. 7C) or in the lens of the eye (data not shown). This is not surprising as olfactory placode precursors are closely associated with both lens (in ectoderm) and forebrain (in the neural folds) progenitors (Bhattacharyya et al., 2004).

How early in development is ectoderm capable of responding to olfactory placode inducing signals? To answer this question, HH stage 4 (gastrula) to stage 5 (early neurula) anterior, or lateral epiblast (adjacent to the area opaca) was grafted into the anterior neural fold of HH stage 8 embryos. This most anterior or lateral epiblast does not contribute to neural tissue; instead it is specified for and gives rise to extraembryonic ectoderm (Garcia-Martinez et al, 1993; Rosenquist, 1966). Epiblast tissue is capable of expressing Pax6 and Dlx3 in the olfactory placode (n=3, Fig. 7D and data not shown). Interestingly, in one of the embryos, the grafted tissue that incorporated into one side of the endogenous olfactory placode, also underwent thickening to form another placode-like structure (Fig. 7D, arrow).

In order to define the extent of **competence** within the ectoderm to form the nasal placode, we grafted quail ectoderm from different axial levels. Midbrain level ectoderm, which is fated to give rise to the trigeminal placode (Stark et al., 1997; Baker et al., 1999) ectoderm at the level of rhombomeres 1-8, including presumptive

otic placode ectoderm (Couly and Le Douarin, 1990; Streit, 2002) and trunk level ectoderm at the level of the 7th to the 10th somite were heterotopically transplanted into the anterior neural folds of HH stage 7-9 embryos. All populations tested are competent to give rise to Dlx3+ and Pax6+ cells in the olfactory placode. Of the three, midbrain level ectoderm remains responsive to olfactory-placode inducing signals for the longest. This ectoderm shows high levels of expression of Dlx3 and Pax6 in the olfactory placode at HH stage 8 (3-4ss) (Fig. 8A, B and data not shown). This robust expression is maintained until stage 10 (10ss) (Fig. 8C) and is down-regulated by stage 11 (13ss). In fact, from 14ss onwards, no expression of Pax6 is seen if the graft localizes to the periphery of the olfactory placode, even though this ectoderm is ordinarily Pax6-positive (Fig. 8D). Weak expression in a few cells is noted only if the graft incorporates into the placode (data not shown). On the other hand, both hindbrain and trunk level ectoderm lose the capacity to respond to olfactory placode-inducing signals more rapidly with age. Hindbrain level ectoderm loses the competence to express Pax6 in the olfactory placode by HH stage 8+ (5ss) (Fig. 9B). Interestingly, however, this ectoderm can continue to express Pax6 in the lens even at HH stage 12 (Fig.11). It also maintains expression of Dlx3 in the olfactory placode upto HH stage 10 (Fig. 9A). Trunk level ectoderm cannot express Dlx3 beyond stage 9- (7ss) (Fig. 10A-C).

4.3E Specification of presumptive olfactory placodal ectoderm to express Dlx-3 and Pax-6 and form neurons

To determine when olfactory placode precursor cells become specified to express Dlx3 and Pax6, we isolated presumptive olfactory placode ectoderm from HH stage 6 to HH stage 21 and cultured it in collagen gel cultures without serum for

24 to 60 hours (Fig. 12F). From stages 6-9, the ectoderm containing the olfactory placode precursors is not a homogenous population of cells as lens precursors occupy the same territory. Inspite of this, some explants at stage 6 were found to contain a few (<10) Dlx3 positive cells (Fig. 12A). By stage 11, most explants have some Dlx3+ cells (>20), but only a few Pax6+ cells (<10) (Fig. 12B). Specification to express Pax6 robustly occurs later, only by HH 14, which is when the olfactory placode is first evident (Fig. 12C). Neuronal specification as assayed by Hu expression starts at around stage 11 and is complete by stage 14 (Fig. 12C, D) when Hu expression is first noted in the endogenous olfactory placode (Fornaro et al., 2001). The olfactory placode is specified to express neurofilament and Olf-1 a little later, by stage 19 (Fig. 12E).

4.3F Presumptive olfactory placode ectoderm is committed to express Pax6 and Dlx3 by HH stage 15

The definition of commitment is also an operational one: a tissue is said to be committed to its fate if it attains this fate even when challenged by transplantation to a novel embryonic environment. To determine the time at which the presumptive olfactory placode ectoderm is irreversibly **committed** to its fate, we grafted the presumptive olfactory placode ectoderm at different stages (from 10 to 16) to the lateral plate ectoderm at the level of the most recently formed somites in the stage 8-9 chick embryo. This location was chosen for its distance away from the neural tube and the somites, possible sources of inducing signals. At stage 10, the close apposition of the presumptive olfactory placode ectoderm with the forebrain prevents their absolute separation. When the two tissues are grafted together, the transplanted ectoderm is found to be Dlx3 and Pax6-positive (data not shown).

Heterotopic grafts of older placodal ectoderm (st.12-14) with adhering mesenchymal and/or forebrain tissue, to the ectoderm overlying the lateral plate mesoderm also results in Pax6 and Dlx3 expression in the ectodermal quail cells (Fig. 13C, D). However, when only placodal ectoderm is grafted to the lateral trunk ectoderm, no expression of Pax6 and Dlx3 is seen until HH stage 15 (compare Fig. 13B, E, F to Fig. 13 G), inspite of the transplanted ectoderm retaining the capacity for invagination (Fig. 13 E).

4.4 Discussion

4.4A Molecular markers of the developing olfactory placode

Our aim in this study has been to understand the earliest events in olfactory placode induction. The cranial sensory placodes are generated through a cumulative process of appositional induction (Slack, 1991) wherein the inducing tissue signals in a unidirectional manner to the responding tissue and alters its developmental state as a consequence. To study the development of an embryonic structure prior to its morphological appearance, molecular markers are a necessity. We have identified four transcription factors, Dlx3, Dlx5, Pax3 and Pax6 that are expressed in the developing olfactory placode and in the olfactory epithelium. An important point to note is that the expression of none of these genes is specific for the olfactory placode. Both Dlx3 and Dlx5 are expressed in the mature olfactory and otic placodes, while Pax3 is strongly expressed in the ophthalmic lobe of the trigeminal ganglion and Pax6 is a much-studied marker of the lens of the eye. However, the combinatorial expression of these genes is a distinctive feature of the olfactory placode. While Dlx3 and Dlx5 are broadly expressed in the head ectoderm initially, there is a subsequent refinement of the expression pattern of these genes. Whether this dynamic pattern of

expression is a reflection of the movement of olfactory placode precursor cells to their eventual destination or whether cells destined to give rise to other derivatives down-regulate the expression of these genes remains to be determined. The most likely possibility is that both mechanisms operate to ultimately ensure specific expression of these genes in the olfactory and otic placodes. Conversely, Pax6 expression in the presumptive olfactory placode cells is down-regulated during the intermediate stages of its development before later de novo expression in the olfactory epithelium. It is not known at this time, whether this downregulation is crucial for regulating olfactory placode formation and differentiation. Additionally, these genes play functional roles in the induction of the olfactory placode as highlighted by loss-of-function studies. The otic and olfactory placodes are not induced in a zebrafish deletion mutant, b380, which lacks the Dlx3 a, and b genes (Solomon and Fritz, 2002). The Dlx5 mouse knockout shows a severely reduced nasal epithelium and a very rudimentary vomeronasal organ in addition to having grossly impaired otic vesicle derivatives (Depew et al., 1999). Similarly, nasal placodes do not form and the nasal cavities are absent in the Small eye (Sey) mouse and rat mutants (Hogan et al., 1986; Matsuo et al., 1993; Fujiwara et al., 1994; Grindley et al., 1995).

4.4B Spatiotemporal distribution of competence to form the olfactory placode

To understand how and when the nasal structure is first induced, we decided to delineate ectoderm that is competent to form the olfactory placode. The spatiotemporal localization of the inducing signals remains to be determined. In general, either one of these two parameters is strictly delimited such that the induced structure arises only in a distinct position. The trigeminal placode arises

from midbrain level ectoderm (d'Amico-Martel and Noden, 1980; Baker et al., 1999) and expresses Pax3 (Stark et al., 1997). The current model for trigeminal placode induction is that while the inducing signal is present in the dorsal neural tube at all axial levels, competence to respond to this signal is relegated to cranial ectoderm (Baker et al., 1999) . Furthermore, inhibitory signals present at the level of rhombomeres 2 and 3 in the hindbrain might help resolve the domain of Pax3 induction to midbrain level ectoderm. However, the converse holds true in otic placode induction: Pax2 (otic placode marker) expression is induced in epiblast tissue only at the level of rhombomeres 2-7 (the otic placode normally arises at the level of rhombomeres 4-6) while both midbrain and trunk level ectoderm are competent early on to contribute to the otic vesicle and express Pax2 (Groves and Bronner-Fraser, 2000). In this study, both cranial and trunk level ectoderm are capable of forming the olfactory placode and expressing Dlx3 and Pax6. In fact, some cells in the midbrain level ectoderm are capable of sustained expression of Pax6 even past the time when the ectoderm is committed to a trigeminal placode fate (HH stage 10) (Baker et al., 1999). A possible explanation for this finding is that some cells in midbrain level ectoderm (just posterior to the eye) express low levels of Pax6 well beyond HH stage 10 (at least upto HH stage 14) and it is these cells that maintain their expression when grafted anteriorly to the olfactory placode-forming region. Detailed analysis of Dlx3 expression in these grafts at later stages will help clarify the degree to which these cells are competent to express olfactory placode markers. Hindbrain and trunk level ectoderm lose this competence rapidly; between stages 9-10 neither tissue can express Pax6 and Dlx3 respectively. Presumptive otic placode ectoderm continues to express Dlx3 at low levels beyond stage 10, as it would continue to express this marker in the otic placode itself. The loss of Pax6

expression in grafts of hindbrain level ectoderm correlates well with studies on otic placode commitment, which is complete by HH stage 10+ (Groves and Bronner-Fraser, 2000). This suggests that either olfactory placode inducing signals are localized anteriorly at early stages or that later signals further refine the olfactory placode-forming region.

4.4C Timing of inductive events that lead to the formation of the olfactory placode

A prerequisite for studying the induction of a particular fate in a tissue in vitro is determining the time at which it is still unspecified i.e. the tissue does **not** express markers exclusive to its fate when removed from its original context in the embryo and placed in a neutral environment. We examined the **specification** of the presumptive olfactory placode ectoderm to express Pax6 and Dlx3 and form neurons by culturing this tissue at various stages in three-dimensional collagen gel matrices. Presumptive olfactory placode ectoderm is specified to express Pax6 and Dlx3 between stages 12-14 and stages 10-11 respectively. Neuronal specification as assayed by expression of the post-mitotic neuronal marker, Hu, begins around stage 11. This implies that the ectoderm has seen signals that will direct its fate even before it is morphologically visible as a placode. This is similar to results obtained in trigeminal and otic placode specification (Baker et al., 1999; Groves and Bronner-Fraser, 2000). We have also determined the time at which the presumptive olfactory placode ectoderm is irreversibly **committed** to its fate by grafting this tissue at different stages to the lateral plate ectoderm at the level of the most recently formed somites in the stage 8/9 chick embryo. The choice of location has the caveat that it is not necessarily devoid of inducing signals. On the other hand, by its very virtue of containing signals (antagonistic ones as well), it might prove to be a more rigorous

test of commitment as compared to grafting to the area opaca, which is extraembryonic and hence devoid of signals. It will be worthwhile to test this hypothesis. Commitment to express Pax6 and Dlx3 is found to occur by stage 15 once the placode is a self-evident structure.

The next step is to determine the location and the molecular nature of the inducing signals. The expression of Fgf8 in the anterior neural folds and later in some regions of the olfactory epithelium is tantalizing and suggests that Fgf signaling could play a role in the ectoderm to placode transition as well as in later differentiation of the epithelium. We are currently testing this hypothesis.

Figure 1: **A-F**: Expression pattern of *Dlx3* at HH stage 8 (**A**: dorsal view, **B**: ventral view), at HH stage 10 (**C**: dorsal view, **D**: ventral view), at HH stage 13 (**E**) and at HH stage 14 (**F**). The arrows in **A** demarcate the region of the anterior neural fold that contains the precursors to the olfactory placode. This portion of the neural folds does not express *Dlx3*. The arrowheads in **C** and **D** indicate Dlx3-expressing cells surrounding the anterior neuropore both dorsally and ventrally. In **E** and **F**, the arrowheads point toward cells that are strongly expressing *Dlx3*, in two stripes just ventral to the eyes (e). **G, H:** Expression pattern of *Pax3* at HH stage 9 (**G**) and at HH stage 12 (**H**). Arrowheads show presumptive olfactory placode cells expressing *Pax3*. **I-L:** Expression pattern of *Pax6* at HH stage 8 (**I**), at HH stage 11 (**J:** dorsal view**, K:** ventral view) and at HH stage 14 (**L**). The arrows in **I** point to the anterior neural folds that are expressing *Pax6*. The arrowhead in **K** points toward a Pax6 non-expressing zone that contains the olfactory placode precursors, whereas very low level expression is seen in the placodal cells at stage 14 (arrowhead in **L**).

Figure 1: Molecular markers of the nascent olfactory placode

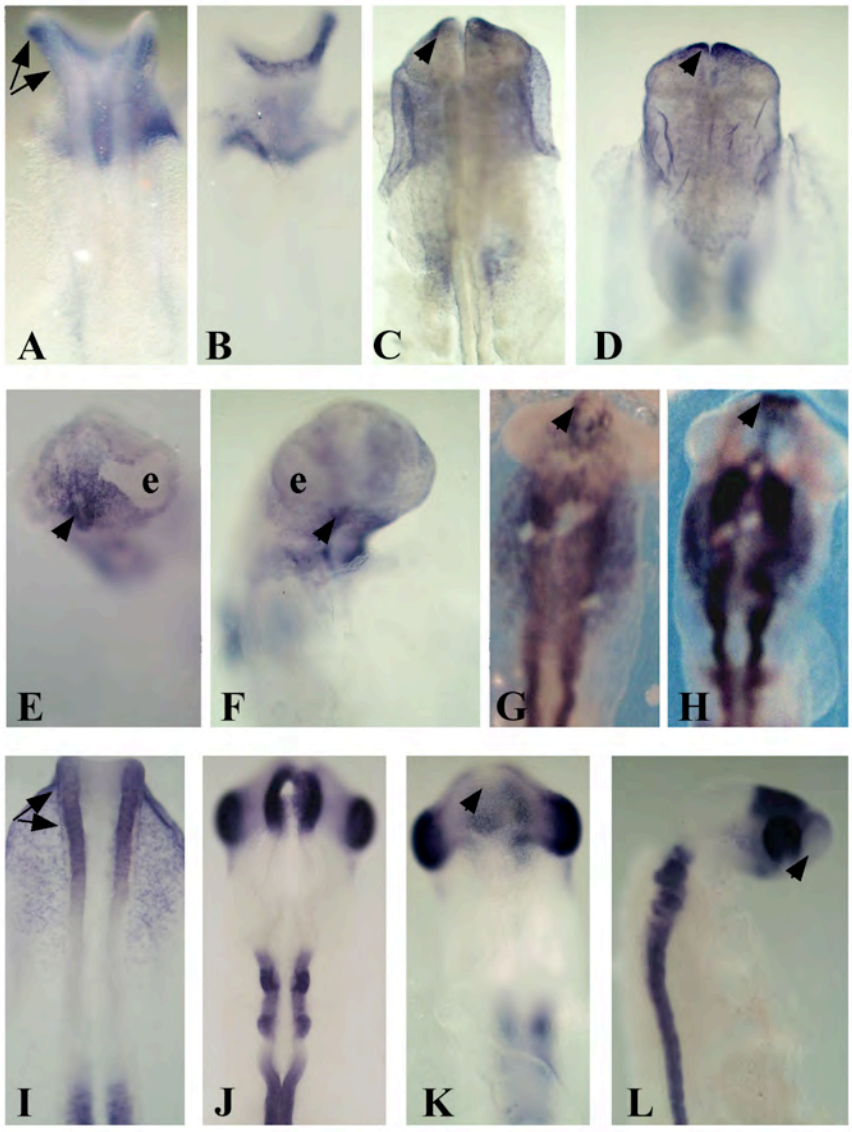

Figure 2: *Pax3*, *Pax6*, *Dlx3* and *Dlx5* are expressed in the mature olfactory placode

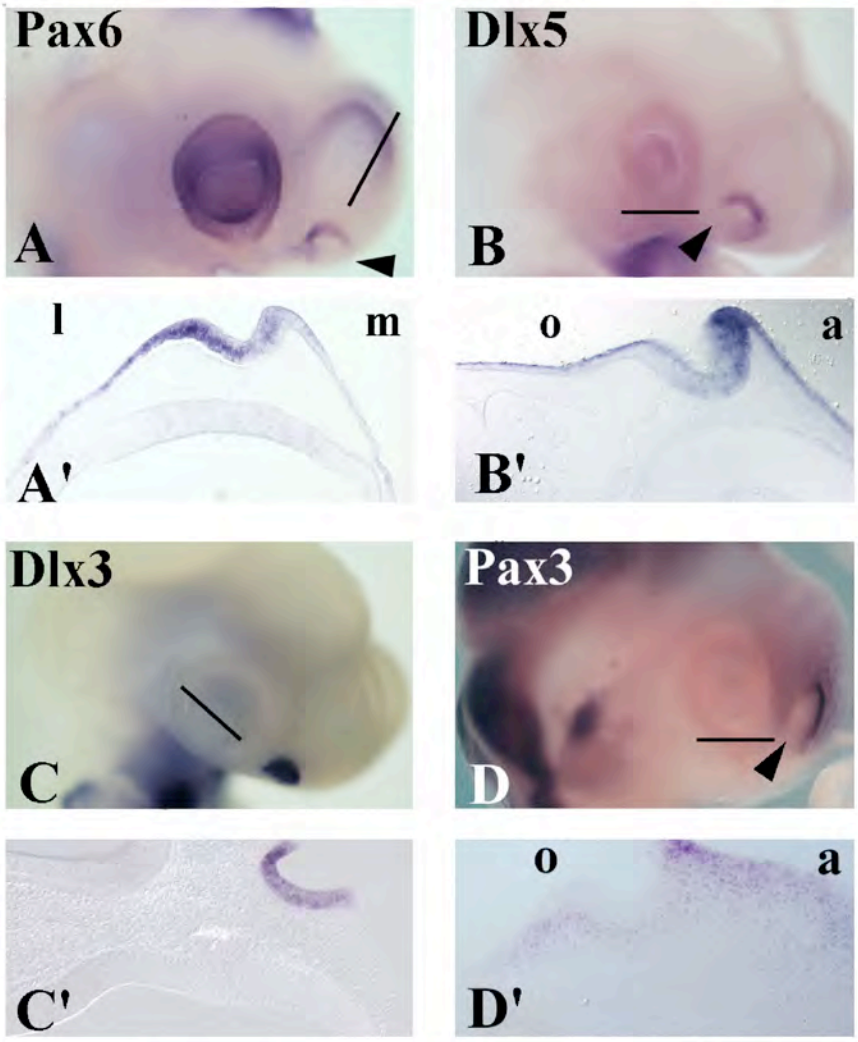

Whole mount in situ hybridization of stage 19-20 embryos shows that while *Dlx3* (C, C') is expressed throughout the nasal placode, *Pax6* is absent from the medial placode (A, A'; arrow head) and *Dlx5* and *Pax3* from its oral part (B, B'; arrow head, D, D'; arrowhead). l: lateral; m: medial; o: oral; a: aboral, e:eye, tg: trigeminal ganglion. Black lines denote the planes of section through the olfactory placode.

Figure 3: Dlx3 is a 278 amino acid protein of which 57 amino acids (128-184) constitute the homeodomain (shown in italics). The homeodomain is highly conserved across all six Dlx family members. A rabbit polyclonal antibody raised against the homeodomain of the Drosophila distalless family recognizes all vertebrate Dlx proteins. To produce an antibody that would specifically recognize the Dlx3 protein, the C-terminal portion of the protein (185-278) (shown in blue) was fused to GST (Glutathione-S-transferase). + and – in **A** and **B** indicate bacterial cultures induced with and without IPTG respectively. Uninduced bacterial cultures were treated identically as the induced ones and serve as a negative control. **A** shows the various steps in the purification of GST protein as a control while **B** documents the purification of the GST-Dlx3 fusion protein. In each part of the figure, lane 1 has the Benchmark protein ladder, the pink band indicating 61 kDa, lanes 2 and 3 are crude lysates of induced and uninduced bacterial cultures, lanes 4 and 5 are the supernatants of these lysates (induced proteins not seen in these as they are not secreted), lanes 6 and 7 contain glutathione sepharose beads bound to the protein and finally lanes 8 and 9 contain the protein eluted off the beads. The arrowhead in **A** points toward the purified 27 kDa GST protein while the arrow in **B** indicates the 37 kDa fusion protein. Some degradation of the fusion protein is seen.

Figure 3: Purification of the GST-Dlx3(C-terminal) fusion protein

1 msgsfdkkls siltdlsgsl schasskdsp tlpessvtdl gyysgqhdyy pgqsygqpva
61 hypypqfnln aigaggnysp ksdysyspsy rqyghfrdqq lpaqdavsvk eepepevrmv
121 ngkpkki ***rkp rtiyssyqla alqrrfqkaq ylalperael aaqlgltqtq vkiwfqnrrs***
181 ***kfkk*** lyknge vplehspnns dsmacnspps pavwdsathg sapgrtplpq plpyspspaf
241 leehspwyhp qslaaphqpp aamhhtspgp ppnpgavy

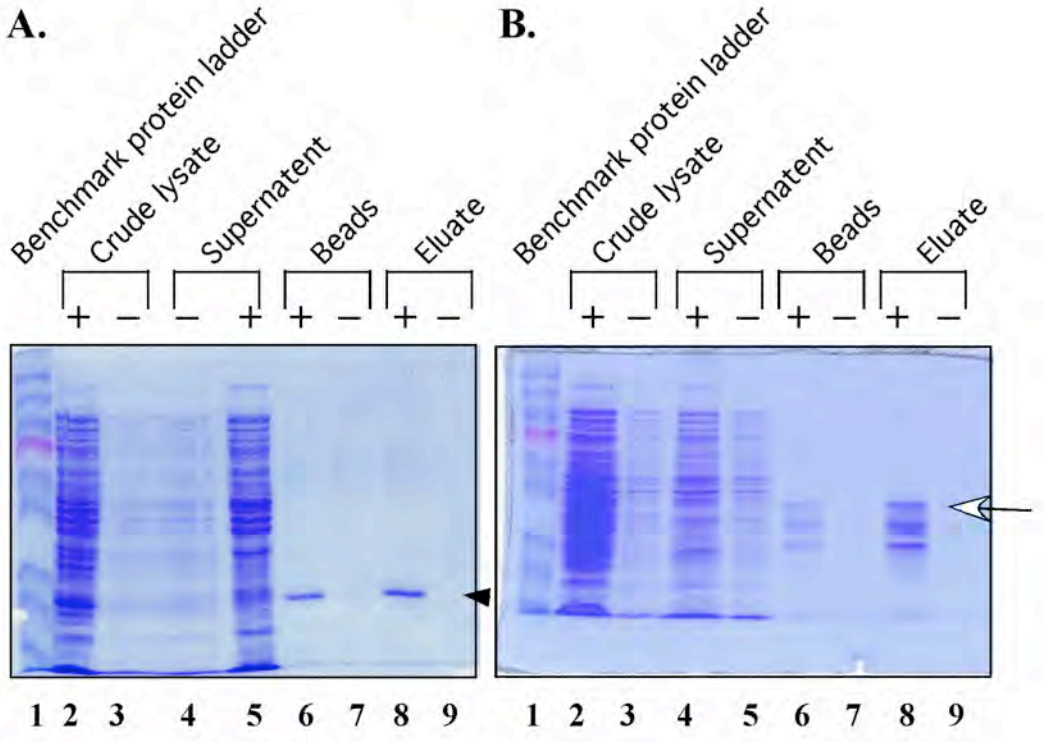

Figure 4: Western blot analysis and immunohistochemistry using the polyclonal antibody raised against the C-terminal of Dlx3

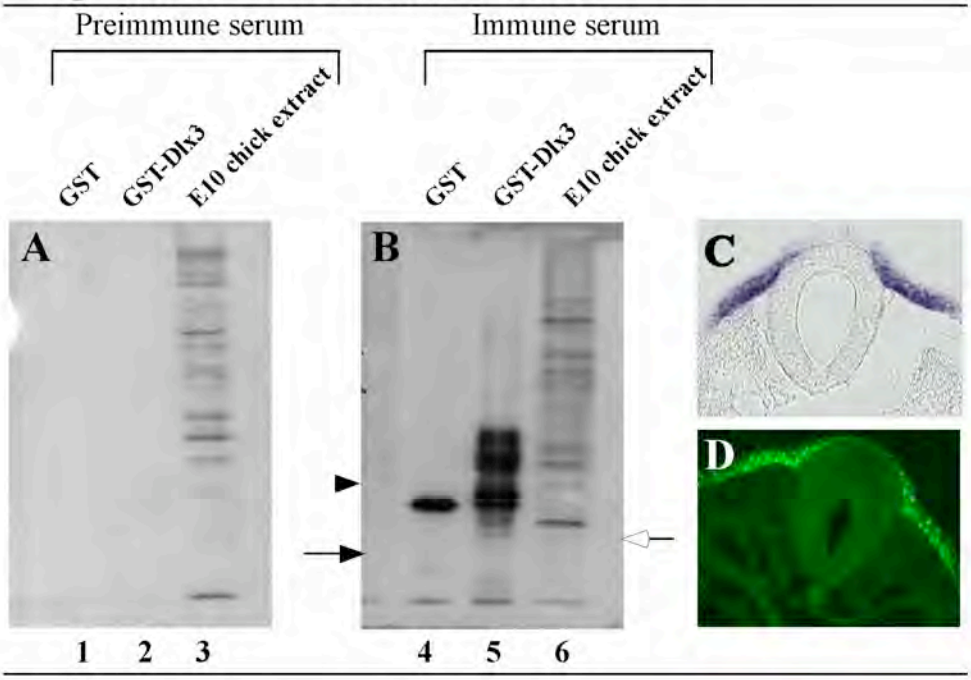

A and B. Lane 1: Purified GST protein, Lane 2: GST-Dlx3 fusion protein, Lane 3: E10 chick extract. **A.** Western blot probed with preimmune serum. **B**. Western blot probed with immune serum. The preimmune serum does not detect either GST or the fusion protein (lanes 1 and 2, Fig. **A**); however, it does detect a number of antigens in E10 chick extract. This is due to the animal's naturally present immune response. The immune serum is capable of detecting both GST and the fusion protein (arrow and arrowhead, lanes 4 and 5 respectively, **B**). The skeleton arrow to the right of **B** indicates a band of the size of the native Dlx3 protein (30 kDa) in lane 6. A smaller band of higher intensity is also noted in this lane, which is not present in the blot probed with preimmune serum. Possibly, the native protein may have undergone degradation. To determine if the polyclonal antibody can detect the native protein in tissue sections, immunostaining was performed with the preimmune and immune serum.

While the preimmune serum did not provide any appreciable signal (data not shown), the immune serum was able to recapitulate the Dlx3 expression pattern. Shown in **C**, a section through the hindbrain at the level of the otic placode. The otic placode strongly expresses Dlx3 as shown by in situ hybridization. This ectoderm in section shows clear nuclear staining when immunostained with the Dlx3 polyclonal antibody (**D**).

Figure 5: Dlx3 and Pax6 proteins are expressed in the developing olfactory placode

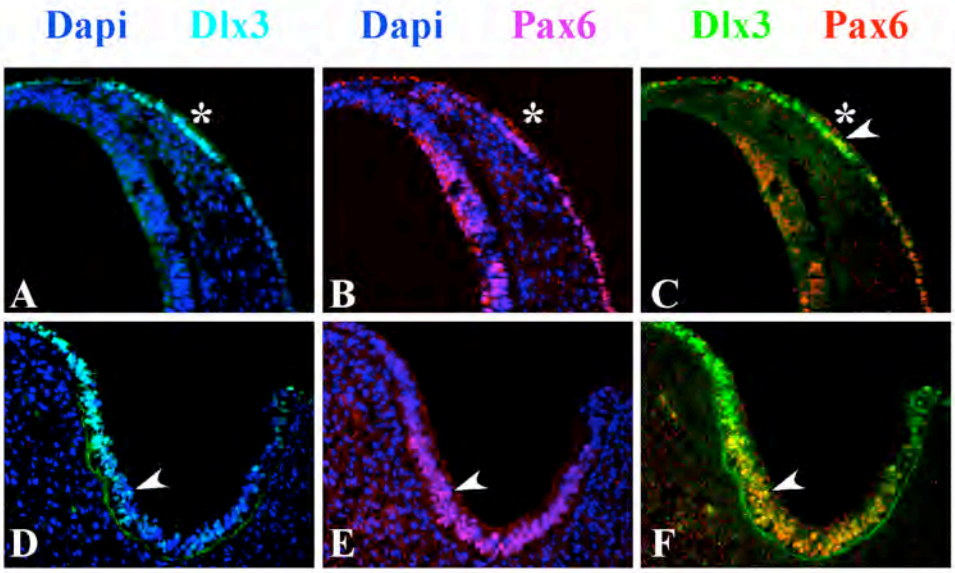

A-C: Dlx3 and Pax6 protein expression in the forming olfactory placode (denoted by an asterisk) at HH stage 14. **A**. Dlx3 (in turquoise) is expressed in ectodermal cells proximal to the forebrain. **B**. Pax6 (in purple) is expressed in a few scattered cells in this same region; however, it is much more strongly expressed in ectodermal cells present more posteriorly, in the future cornea. **C**. The overlay of Dlx3 (green) and Pax6 (red). A few cells co-express both markers (yellow). The arrowhead indicates one such cell. **D-F**: Dlx3 and Pax6 protein expression in the olfactory epithelium at HH stage 26. **D**. Dlx3 (in turquoise) is expressed throughout the epithelium, though it is present at higher levels at the margins. **E**. Pax6 (purple) is expressed in the cup-shaped structure of the olfactory epithelium. **F**. Dlx3 (green) and Pax6 (red) are coexpressed in a number of cells (yellow). The arrowheads in D-F indicate one such cell.
DAPI, a nuclear stain is seen in blue in all sections **A-F**.

Figure 6: Neuronal markers of the olfactory epithelium

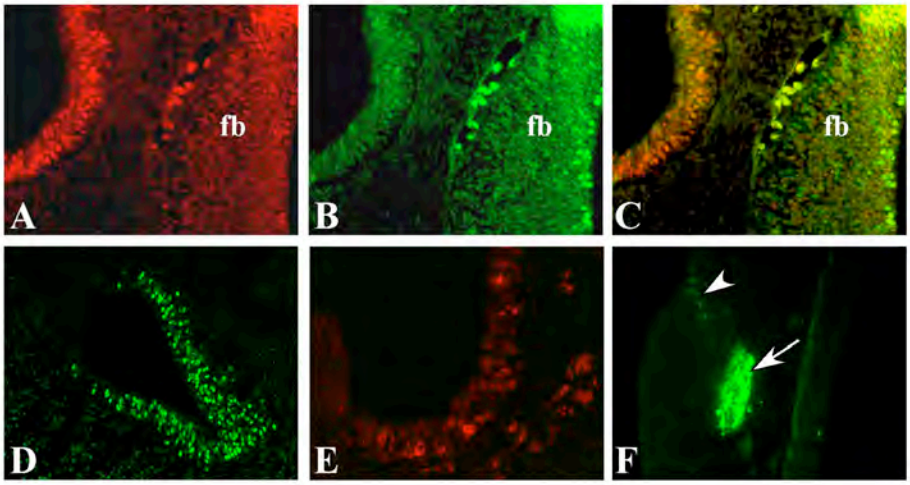

A. Otx2 expression in the olfactory epithelium and adjacent forebrain (fb) at HH stage 19. Otx2 protein is subsequently expressed in the GnRH neurons. **B**. Low levels of Sox10 are also expressed in the olfactory epithelium. **C**. Overlay of Otx2 (red) and Sox10 (green). **D**. Olf-1 expression in post-mitotic neurons of the olfactory epithelium at HH stage 22. **E**. Hu expression at HH stage 19. Hu, an RNA-binding protein, labels the cell bodies of neurons. **F**. Neurofilament expression in the olfactory epithelium (arrowhead) and in the olfactory nerve (arrow) at HH stage 19.

Figure 7: Isotopic grafts and grafts of the lateral epiblast to the anterior neural fold result in Dlx3 and Pax6 expression in the transplanted tissue

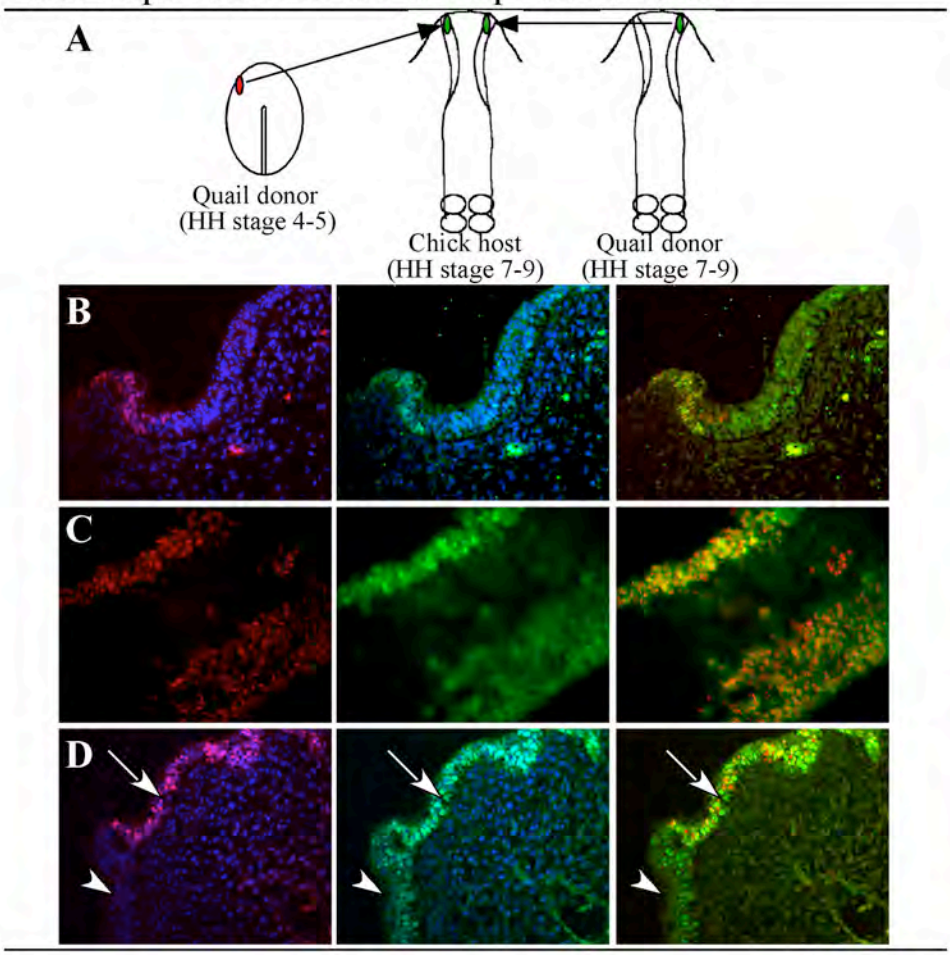

A. Chick embryos received grafts of quail lateral epiblast from stage 4-5 embryos or isotopic grafts of quail placodal ectoderm. **B**. An isotopic quail graft gives rise to a Dlx3+ olfactory placode. **C**. Another isotopic graft shows Pax6+ quail cells in the olfactory placode. The graft has also contributed to the telecephalon. **D**. Lateral epiblast grafts also express Dlx3. This particular graft has incorporated to one side of the host olfactory placode. The graft is indicated by an arrow and the endogenous placode by an arrowhead.

Figure 8: Midbrain level ectoderm is competent to express Dlx3 and Pax6 upto HH stage 12

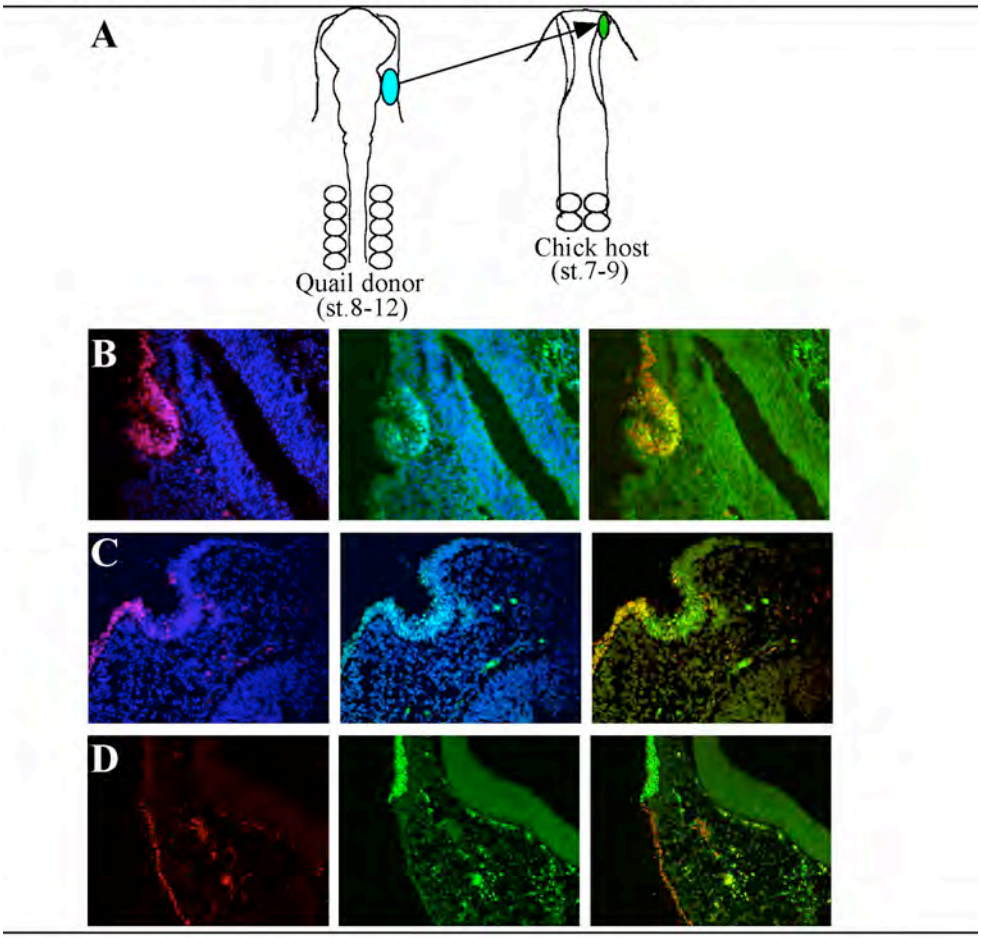

A. Schematic of grafts of midbrain level ectoderm to the anterior neural fold. **B**. HH stage 8 midbrain level ectoderm (in purple) expresses high levels of Dlx3 (turquoise). **C**. HH stage 10 ectoderm (in purple) expresses Pax6 (turquoise) even in ectoderm adjacent to the olfactory placode. **D**. HH stage 11 ectoderm (in red) can no longer express Pax6 (green) at the margin of the olfactory placode.

Figure 9: Hindbrain level ectoderm is competent to express Pax6 upto the HH stage 8+ and Dlx3 upto HH st.12

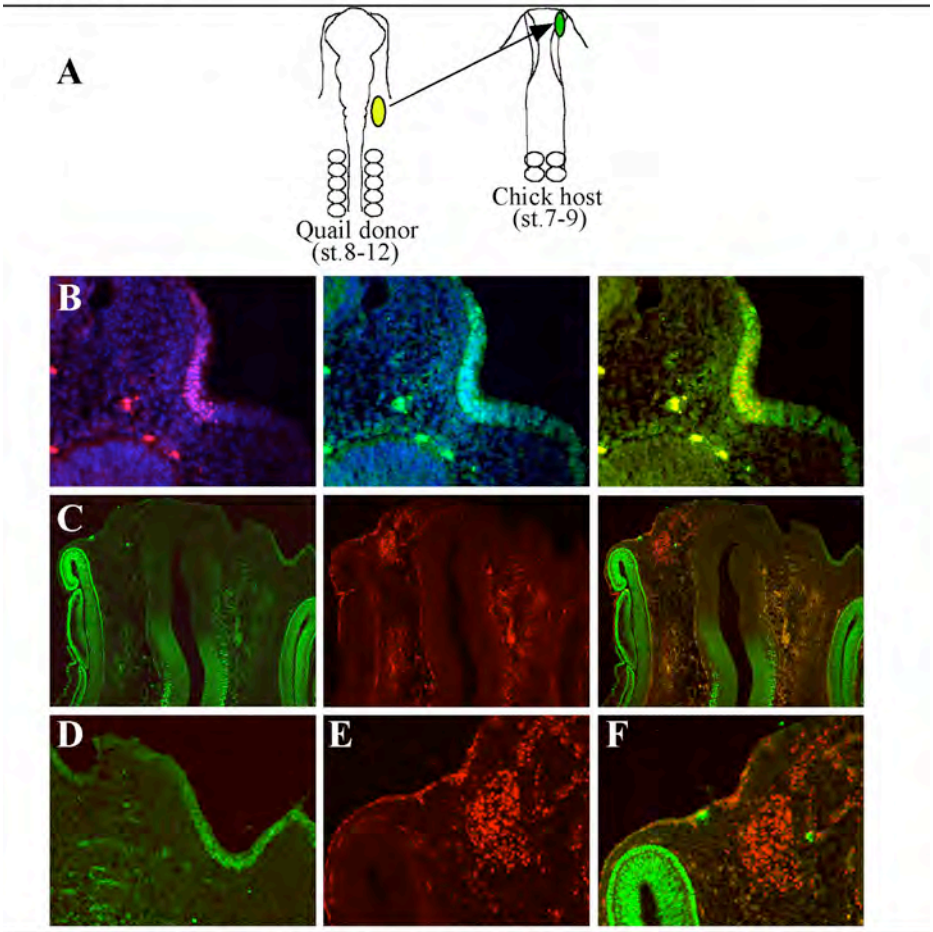

A. Schematic of grafts of hindbrain level ectoderm to the anterior neural fold. **B**. HH stage 8 quail ectoderm (purple) is Dlx3-positive (turquoise). **C**. HH stage 8+ ectoderm (red) can no longer express Pax6 (green). **D**. High magnification view of Pax6 expression in the contralateral side of the graft (non-grafted side). **E**. High magnification of ectoderm on grafted side. **F**. Overlay of Pax6 and QCPN staining showing the lack of Pax6 expression in the graft.

Figure 10: Trunk level ectoderm is competent to express Dlx3 upto HH stage 9 when grafted to the anterior neural folds

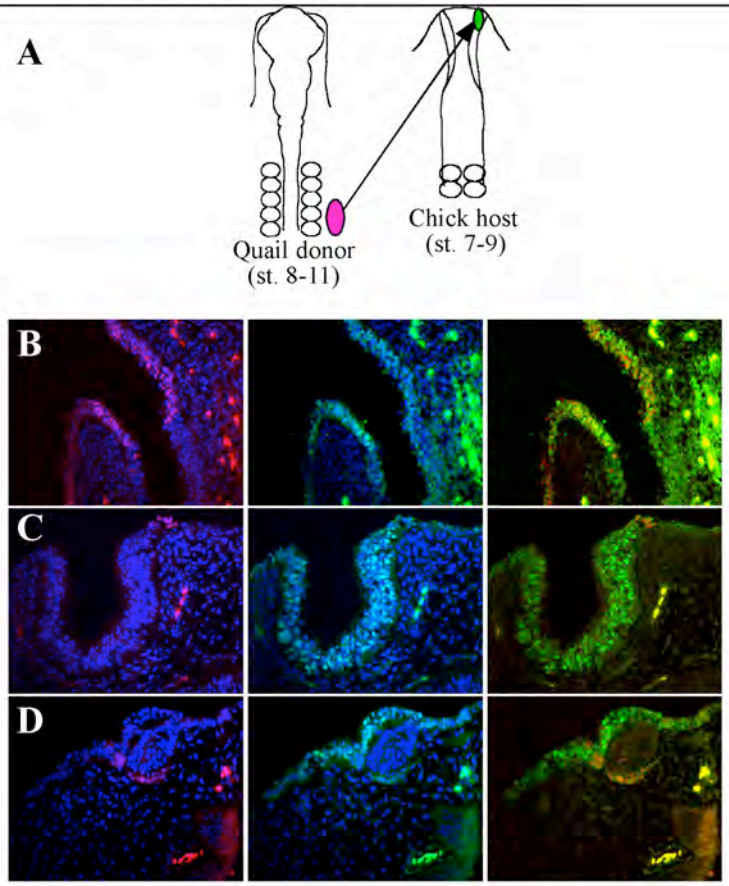

A. Schematic of grafts of trunk level ectoderm to the anterior neural fold. **B**. HH stage 8+ trunk level ectoderm (purple) is Dlx3-positive (turquoise). **C**. HH stage 10+ ectoderm (very few cells in purple) does not express Dlx3 (turquoise). **D**. HH stage 11 trunk level ectoderm (purple) is also incapable of expressing Dlx3.

Figure 11: Grafts of midbrain and hindbrain level ectoderm express Pax6 in the lens and cornea

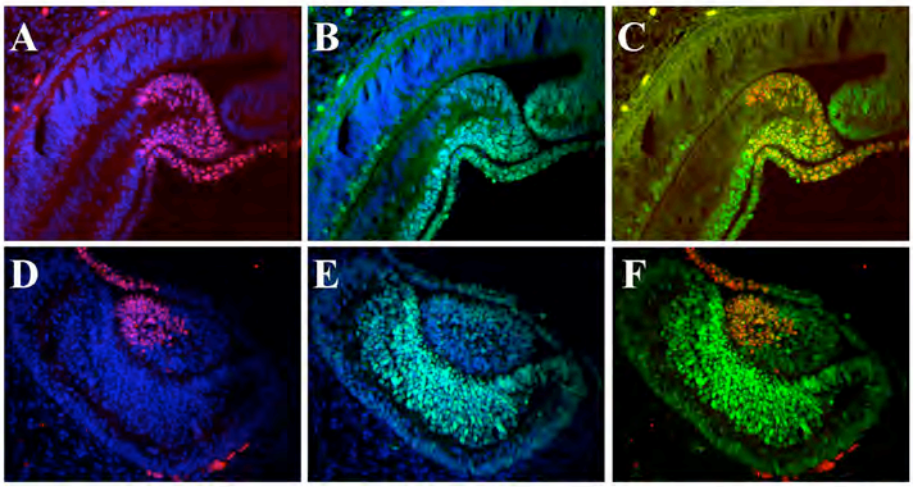

A-C Example of HH stage 8+ graft of midbrain level ectoderm (purple) that has incorporated into the cornea and lens and expresses high levels of Pax6 (turquoise). **D-F** Example of HH stage 12 graft of hindbrain level ectoderm (purple) that has incorporated into the lens and cornea and expressed moderate levels of Pax6 (turquoise) in the lens. By this stage, it can no longer express Pax6 in the olfactory placode.

Figure 12: Specification of presumptive olfactory placode ectoderm to express Dlx and Pax6 proteins and form neurons

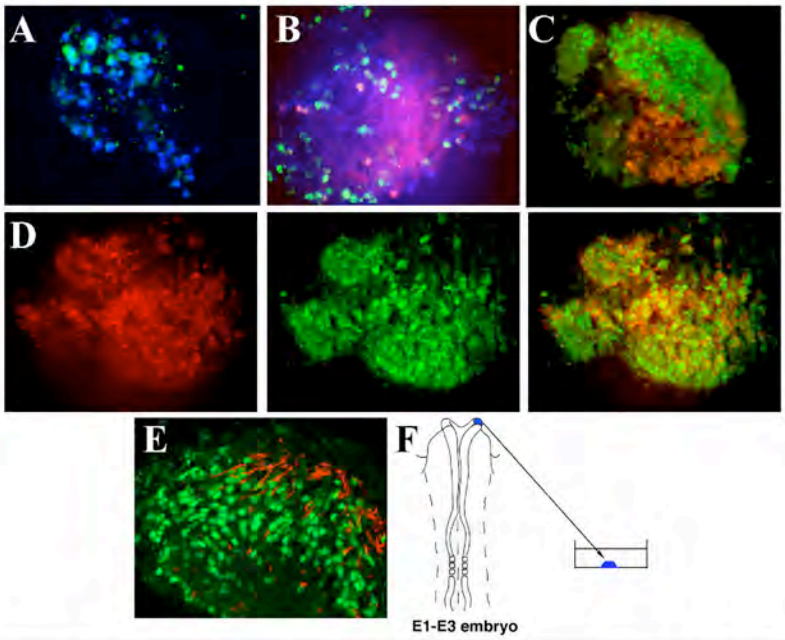

A. HH stage 6 explant; a few cells are positive for Dlx3 (turquoise). **B**. HH stage 11 explant; there are Dlx positive cells (green), a few Pax6 positive cells (red) and neurons as assayed by expression of Hu (blue). **C**. HH stage 14 explant; large number of Pax6 positive cells (green) and neurons (Hu in red). **D**. HH stage 17 explant; large number of Dlx3 positive cells (green) and neurons (Hu in red). **E**. HH stage 19 explant; almost all cells are expressing Olf-1 (green) and some nerve fibres are seen in red (neurofilament). **F**. Schematic of specification assay.

Figure 13: Time course for commitment of presumptive olfactory placode ectoderm to express Pax6 and Dlx3

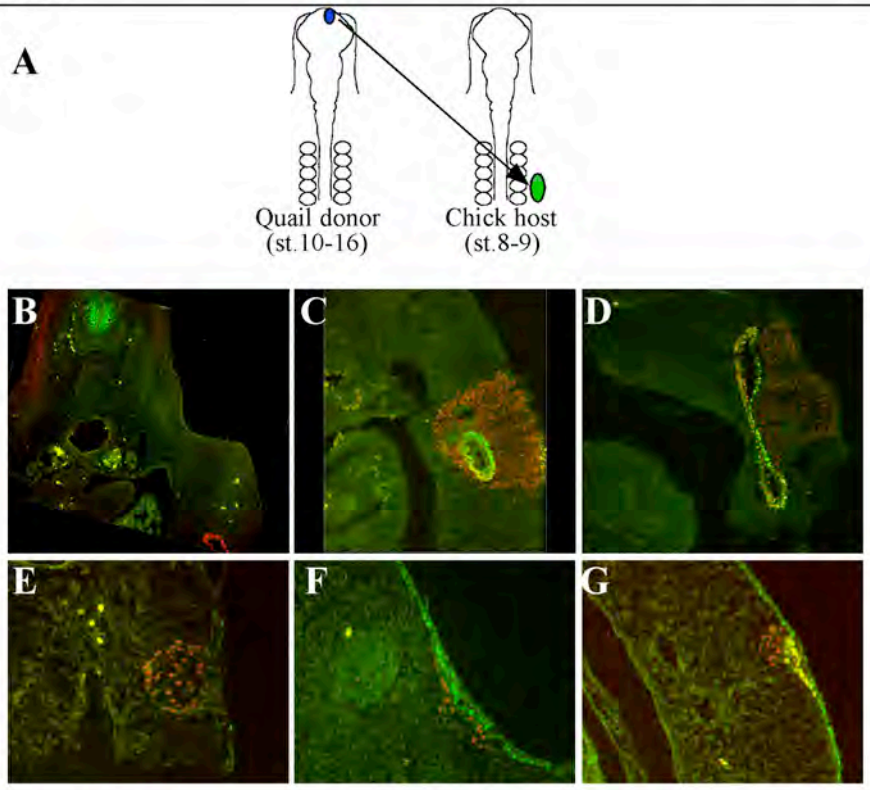

A. Schematic of commitment; quail presumptive olfactory placode is grafted over the lateral plate mesoderm. **B**. Low magnification view of graft (in red) of HH stage 12 presumptive olfactory placode ectoderm. It does not express Pax6 (green); on the other hand, the neural tube expresses Pax6 at high levels. **C. D** At slightly older stages, at HH stage 12+ and 14 respectively, the grafted ectoderm is positive for Pax6 (green, overlay in yellow). However, the grafts are large and it is likely that there is mesenchymal or forebrain tissue present as well. **E, F**. However at these same stages, i.e. stage 12+ and 14 respectively, cleaner grafts do not express either Pax6 or Dlx3. **G**. By HH stages 15-16, commitment of placodal ectoderm is evident by the robust expression of Dlx3 (overlay in yellow) in a very small graft. Some quail cells do not express Dlx3; it is unclear whether these cells are mesenchymal in origin or whether these cells have invaginated and hence lost expression of Dlx3.

Chapter 5

Summary and future directions

5.1 Summary

Cranial placodes were first observed as focal embryonic thickenings of columnar epithelium in the shark embryo more than two hundred years ago (van Wijhe, 1883). The investigation of their development is being revived today as a combination of molecular, genetic and embryological approaches are being brought to bear on the study of their induction and differentiation. Classical studies utilizing transplantation and in vitro co-culture assays have helped broadly define tissue interactions that lead to the eventual induction of the olfactory placode amongst others (Haggis, 1956; Jacobson, 1966). However, these studies relied heavily on the morphology of the responsive tissue in their assessment of successful induction. Not obvious from these studies is the fact that embryonic induction is a cumulative process that can be broken down into discrete steps (each step being defined by changes in gene expression) prior to the generation of a morphologically detectable placode. In the past decade, the explosion in our knowledge of molecular markers that correlate with the progression of differentiation in a tissue, has allowed for the careful examination of each phase of the continuum of induction. We can now ask more precisely when a tissue has been induced to express a unique combination of genes and which molecular pathways regulate each of these phases. Additionally, we are now well placed to address questions such as: what are the molecular underpinnings of developmental phenomenon such as competence, specification and commitment?

The formation of the avian olfactory placode has been the main subject of my graduate research. During the course of my study, my interest has evolved to encompass the broader question of how placode precursor cells are differentially specified to contribute to diverse sensory organs. To begin with, it was essential to

determine the origin of olfactory placode precursors across developmental stages. To address this question, I constructed a fate-map of the chick olfactory placode using lipophilic dye labeling of small populations (10-30) of cells from HH stages 6-10 in collaboration with Dr. Andrea Streit. We found that olfactory and lens placode precursor cells coexist in a common region at the border of the anterior neural plate. Using DiI labeling and confocal time-lapse analysis, I documented the segregation of these cell types over time. Interestingly, dynamic changes in the expression pattern of specific transcription factors mirrored the rearrangement of these cells in the embryo. Furthermore, when placode precursor cells in the common lens-olfactory territory were forced to maintain expression of a transcription factor that demarcates olfactory placode fate, none of these cells were able to contribute to the lens. A question that arose as a consequence of this study is whether the heterogeneity of the common lens-olfactory territory is reflected at the level of a single cell. To address this issue, I injected single cells within this territory and determined the fate of their progeny. Surprisingly, I found no evidence for a shared olfactory and lens placode lineage. Descendants of single progenitors labeled at early neurula stages (prior to placodal precursors sorting out from each other) contribute to either one or the other placode.

The parallels between placode development in vertebrates and imaginal disc development in Drosophila are striking. As mentioned previously in chapter 2, the molecular mechanisms used to differentiate olfactory from lens precursors appear to be conserved with mechanisms that operate to specify the eye and antennal lineages in the eye-antennal imaginal disc. This is, of course, a very particular example of conservation between structures that could be considered functionally homologous. However, on closer examination, placode and imaginal disc development seem to

have general features in common as well. Like placode precursors, imaginal disc primordia originate as bilaterally paired (with the exception of the lone genital disc) groups of cells in the embryonic ectoderm, some of which undergo invagination and most of which give rise to sensory structures (Garcia-Bellido and Merriam, 1969; Garcia-Bellido et al., 1976; Wieschaus and Gehring, 1976; Crick and Lawrence, 1975; Szabad et al, 1979; Bate and Martinez-Arias, 1991; Cohen et al, 1993). Furthermore, the wing, haltere and leg imaginal discs originate from a common primordium: the thoracic imaginal disc (Cohen et al, 1993). The wing and haltere progenitors reside in the dorsal aspect of the thoracic imaginal disc primordium and separate from the ventrally located leg progenitors by cell movements that cannot be accounted for by gross morphogenetic movements of the embryo alone (Cohen et al, 1993). And lastly, as ascertained by clonal analysis, imaginal disc primordia appear to be specified very early at the blastoderm stage in Drosophila embryogenesis (Wieschaus and Gehring, 1976; Steiner, 1976; Lawrence and Morata, 1977); though conflicting data derived from transplantation studies suggest that this may not be the case (Meise and Janning, 1991). Taken together these lines of evidence are reminiscent of the early lineage restriction of the olfactory and lens placode precursors, their origin from a common region and their subsequent segregation. Further, it has been shown that the intersection of the wingless (wg) and decapentaplegic (dpp) pathways specifies imaginal disc primordia in Drosophila (Cohen et al, 1993): could these signaling pathways be involved in setting aside placode precursors from embryonic ectoderm in vertebrates? Future research will undoubtedly answer this question.

I also wished to understand how the olfactory placode is induced to form specifically at a distinct position in the anterior-most ectoderm of the embryo,

adjacent to the forebrain. To determine the spatiotemporal extent of competence in embryonic ectoderm to respond to olfactory placode inducing signals, I have transplanted ectoderm from different axial levels to the anterior neural fold. I found that competence is restricted to forebrain and midbrain level ectoderm beyond HH stage 10. Possibly, by this stage, the olfactory placode inducing signals are confined to the forebrain level of the embryo such that the nose only forms within the ectoderm adjacent to the telencephalon. Inhibitory signals at the midbrain level might additionally operate to impede olfactory placode formation at this level. Using the technique of quail chick chimeras and an in vitro collagen gel assay system, I further probed the timing of induction of the olfactory placode. Specification of the presumptive olfactory placode ectoderm as assayed by co-expression of Pax6 and Dlx3 (a combinatorial signature unique to the olfactory placode) in olfactory precursors when removed from the context of the embryo, is complete by HH stage 10. This suggests that by the time olfactory placode precursors have physically segregated from other placodal progenitors, they have already received signals that will direct their fate. Commitment to an olfactory fate occurs much later by stage 15 at which point the placode is a visible entity. It is interesting that although olfactory placode precursor cells are specified early on, they continue to remain responsive to foreign environments for a long time afterwards.

5.2 Questions that remain and future directions

5.2A What is the implication of the early lineage restriction of olfactory and lens placode precursor cells?

Our fate-map has shown that olfactory placode and lens placode precursor cells initially occupy a common territory in the anterior ectoderm of the embryo. A single labeled population of cells (comprising between 10-30 cells) in early neurula stage embryos can contribute to both the olfactory and lens placodes. When the fate of individual cells within this population is explored further, it appears that each cell in this population is already destined to be a part of either the olfactory or then the lens placodes. This result, although preliminary, is in agreement with observations made in the zebrafish embryo where cells are already allocated to either the pituitary, olfactory or lens placode lineages but continue to intermingle in a shared region (Whitlock and Westerfield, 2000; Dutta et al., 2005). Could this be a means of setting aside sufficient and reproducible numbers of precursors to form each placode? Does the fate of these placode precursor cells program a positional value into these cells such that they are guided to their final destination in the embryo? If we assume that there is a time-point (earlier than I have tested so far) at which a single cell can divide asymmetrically to give rise to both olfactory and lens progenitors, then it might be possible to experimentally alter this division to give rise to equivalent progenitors (either only olfactory or only lens) and follow their migratory path under these circumstances.

As a means to this end, it will be essential to determine the molecular players that are involved in the fate specification of daughter cells. Notch, a single pass transmembrane receptor and Numb, a PTB (phosphotyrosine binding protein) domain containing protein, are potential candidates as they have been shown to govern binary cell fate decisions in the developing nervous systems of multiple organisms (Muskavitch, 1994; Chitnis, AB, 1995; Lewis, 1996; Knoblich, 1997; Wakamatsu et al, 2000; Zilian et al, 2001; Roegiers and Jan, 2004; Karcavich, 2005). While Notch signaling plays a decisive role in this process by engaging neighboring cells in "lateral inhibition" (Sternberg, 1988; Cabrera, 1990; Lewis, 1991; Fehon et al, 1991; Kunisch et al., 1994; Schweisguth, 1995; Chitnis, AB, 1995; Heitzler et al, 1996), Numb controls the fate of daughter cells by being exclusively localized to one of these cells and blocking Notch signaling in this cell (Rhyu et al., 1994; Frise et al., 1996; Guo et al., 1996; Spana and Doe, 1996, Verdi et al., 1996, 1999; Zhong et al., 1996, 1997; Wakamatsu et al., 1999). It remains to be seen whether either one or both proteins are expressed in the hypothetical common lens and olfactory progenitor cell and whether they control its asymmetric cell division. If this is indeed the case, it might be possible to force symmetric Numb expression or increase Notch levels uniformly in all daughter cells and consequently determine changes in cell fate and/or cell movements.

Another question of interest with regard to a link between cell division and cell fate is: do lineage-restricted lens and olfactory placode precursors undergo further rounds of symmetric cell division prior to their segregation or do they proliferate only once they have segregated to form homogenous populations of cells? Technical difficulties such as photobleaching and phototoxicity have so far

precluded the possibility of following the division and movements of a single labeled cell and its progeny. One possible approach to overcome this difficulty would be to electroporate a very small population of cells with a histone2B-GFP construct (that would label DNA) and then to follow each of these cells as it divides and contributes to either the olfactory or lens placodes. A potential complication of this experiment is the inability to compare two embryos that have been electroporated in exactly the same location. In chick embryos, cells that are identical by lineage in all embryos need not necessarily occupy the same position at a given stage. So, it is impossible to know whether a cell will always contribute to the same placode or whether there is some plasticity in this decision. However, it should still be possible to study cell division characteristics of the lineage-restricted placode precursors. It will be interesting to note whether some progeny wander off in a direction inappropriate to their fate and subsequently undergo cell death.

5.2B What is the molecular nature of the signal or cohort of signals that sequentially induce placode precursor cells to differentiate into the olfactory epithelium?

FGF family members are likely to play a role in this process. FGFs are small, secreted ligands that bind tyrosine kinase receptors and thereby activate various downstream signaling modules and cellular targets. To date, 23 molecules have been identified as belonging to the FGF family and these have been shown to have multiple roles in cell survival, proliferation, migration and differentiation (Mason, 2003). Of these, FGF4 has been implicated as a chemoattractant both in the movement of cells through the primitive streak (Yang et al, 2002) and for

mesodermal cells in the limb bud (Li and Muneoka, 1999). In contrast, FGF8 appears to function as a chemorepellant during gastrulation (Yang et al, 2002). In addition, FGF-4, -8 and -9 have been implicated in olfactory epithelium development by inducing the Ets family transcription factors, Erm and Pea3, in the chick nasal placode (Firnberg and Neubuser, 2001).

Based on the expression patterns of various FGF family members and their receptors, FGF8 emerges as an excellent candidate to promote the localization or induction of olfactory precursors in the chick embryo at early stages. Between HH stage 6 and 7, FGF8 is expressed in the definitive endoderm underlying the shared olfactory and lens territory (Crossley et al, 2001). At the time when olfactory precursors converge anteriorly and cVax and Dlx3 begin to be expressed in the olfactory territory, strong FGF8 expression is observed in the anterior neural ridge and the overlying surface ectoderm. However, FGF8 is completely absent from the future lens region. While at HH stage 8 all three FGF receptors (FGFR) 1, 2 and 3 are expressed in the common lens-olfactory territory (the anterior neural ridge), by the time olfactory precursors accumulate in the anterior ectoderm (HH stage 10) FGFR1 is the only receptor still expressed in the olfactory precursors (Walshe and Mason, 2000). Even though the binding affinity of the splice form FGF8b is highest for FGFR3 as tested in mitogenic assays (MacArthur et al, 1995), it is capable of binding fairly promiscuously to the other FGF receptors as well. Moreover, all components of the FGF signaling pathway are in place in the olfactory region of the mouse and the pathway is active as assessed by the presence of phosphorylated ERK (MAPK), a downstream kinase in the pathway (Corson et al, 2003). Thus, there is sufficient evidence to prompt the hypothesis that FGF signaling promotes olfactory fate in placode progenitors.

We are addressing the role of FGF signaling in the acquisition of olfactory fate by carrying out gain and loss-of-function studies both in vivo and in vitro. Exposing the common lens and olfactory region at stage 8 to FGF8 coated heparin beads suggests that FGF8 can down-regulate lens markers such as Pax6 in a matter of hours within this territory while correspondingly expanding the expression of markers of olfactory fate, such as Dlx5, Delta and GnRH. Does this initial change of fate affect the later differentiation of this region, or is this effect reversible? If the common presumptive lens-olfactory territory is given a brief pulse of FGF8, which is later washed out, can this region reacquire its original fate? Interestingly, an FGF signal is required later in the lens territory for differentiation of lens fiber cells, suggesting that it is only at early time-points that FGF can affect the binary decision of contributing to the olfactory rather than to the lens placode. Using a dominant-negative FGFR1 construct and the small molecule inhibitor, SU5402, we will block FGF signaling and determine whether this inhibition now biases placode precursors towards a lens fate or simply decreases the number of olfactory progenitors. These studies are likely to shed light on the early decisions placodal precursors make as they begin to differentiate themselves from their neighbours.

5.2C Identifying placode-activated enhancers: the next step in building gene regulatory networks that function during placode induction

With the identification of known and novel signaling pathways that are instrumental in the induction of the olfactory placode, it will become necessary to establish the means by which these signals affect gene expression. Enhancers compute the transcriptional read-out of a gene by integrating all positive (activating)

and negative (inhibitory) signals that impinge on them. Further, an analysis of gene regulation in the context of defined embryological changes can provide unique insights into how cell fate decisions are made.

The differential regulation of Sox2 expression in the various sensory placodes serves to illustrate this point. The Sox2 gene is expressed at differing times in the forming lens, nasal and otic placodes (Kamachi et al, 1998; Groves and Bronner-Fraser, 2000; Uwanogho et al., 1995). Two highly conserved enhancers NOP-1 (323bp) and NOP-2 (374bp) that regulate Sox2 expression both in the chick nasal and otic placodes from stage 10 onwards have been identified (Uchikawa et al., 2003). On the other hand, lens expression of Sox2 is directed by a distinct set of enhancers: N3, N4 and L (unique to chick) (Uchikawa et al., 2003). Therefore with regard to Sox2 expression, signals regulating lens induction are likely to be different from those that regulate early nasal and otic placode induction. This leads to two interesting speculations, a) since the lens and olfactory placode precursors have a spatially indistinguishable origin (Bhattacharyya et al., 2004), differential regulation of Sox2 might be instructive in determining distinct fates from this common domain and b) similar mechanisms may operate to differentiate both olfactory and otic precursors as these two do not share overlapping spatial domains. The Dlx family genes, Dlx3 and Dlx5, are also expressed in both the nasal and otic placodes. The intergenic sequence between Dlx5 and Dlx6 contains a cis-element that drives expression in both the developing forebrain as well as in the olfactory placodes, but not in the otic placodes (Zerucha et al., 2000). It will be interesting to determine the degree of similarity in the upstream molecular mechanisms that control transcription of common markers of the olfactory and otic placodes. The molecular analysis of lens development has revealed the importance of “tissue-specific” enhancers in

identifying important regulatory factors. Such analysis will further uncover the means by which combinatorial transcriptional codes determine different fates. In addition to aiding the search for proteins that are functionally relevant in placode induction and differentiation, “placode-specific” enhancers can also serve as valuable tools for spatial and temporal control in disrupting gene expression in specific placodes and their precursors. In conclusion, rigorous network analysis in conjunction with our knowledge of the embryological parameters of olfactory placode development will provide a holistic understanding of its induction and subsequent differentiation.

Appendix: Cited Literature

Abu-Elmagd, M., Ishii, Y., Cheung, M., Rex, M., Le Rouedec, D. and Scotting, P. J. (2001). cSox3 expression and neurogenesis in the epibranchial placodes. *Dev Biol* **237**, 258-69.

Aota, S., Nakajima, N., Sakamoto, R., Watanabe, S., Ibaraki, N. and Okazaki, K. (2003). Pax6 autoregulation mediated by direct interaction of Pax6 protein with the head surface ectoderm-specific enhancer of the mouse Pax6 gene. *Dev Biol* **257**, 1-13.

Ashery-Padan, R., Marquardt, T., Zhou, X. and Gruss, P. (2000). Pax6 activity in the lens primordium is required for lens formation and for correct placement of a single retina in the eye. *Genes Dev* **14**, 2701-11.

Bachiller, D., Klingensmith, J., Kemp, C., Belo, J. A., Anderson, R. M., May, S. R., McMahon, J. A., McMahon, A. P., Harland, R. M., Rossant, J. et al. (2000). The organizer factors Chordin and Noggin are required for mouse forebrain development. *Nature* **403**, 658-61.

Baker, C. V. and Bronner-Fraser, M. (1997). The origins of the neural crest. Part I: embryonic induction. *Mech Dev* **69**, 3-11.

Baker, C. V. and Bronner-Fraser, M. (2000). Establishing neuronal identity in vertebrate neurogenic placodes. *Development* **127**, 3045-56.

Baker, C. V. and Bronner-Fraser, M. (2001). Vertebrate cranial placodes I. Embryonic induction. *Dev Biol* **232**, 1-61.

Baker, C. V., Stark, M. R., Marcelle, C. and Bronner-Fraser, M. (1999). Competence, specification and induction of Pax-3 in the trigeminal placode. *Development* **126**, 147-56.

Bancroft, M. and Bellairs, R. (1977). Placodes of the chick embryo studied by SEM. *Anat Embryol (Berl)* **151**, 97-108.

Basler, K., Edlund, T., Jessell, T. and Yamada, T. (1993). Control of cell pattern in the neural tube: regulation of cell differentiation by *dorsalin-1*, a novel TGFb family member. *Cell* **73**, 687-702.

Bate, M. and Arias, A. M. (1991). The embryonic origin of imaginal discs in Drosophila. *Development* **112**, 755-61.

Begbie, J., Brunet, J. F., Rubenstein, J. L. and Graham, A. (1999). Induction of the epibranchial placodes. *Development* **126**, 895-902

Begbie, J. and Graham, A. (2001). The ectodermal placodes: a dysfunctional family. *Philos Trans R Soc Lond B Biol Sci* **356**, 1655-60.

Bhasin, N., Maynard, T. M., Gallagher, P. A. and LaMantia, A. S. (2003). Mesenchymal/epithelial regulation of retinoic acid signaling in the olfactory placode. *Dev Biol* **261**, 82-98.

Bhattacharyya, S., Bailey, A. P., Bronner-Fraser, M. and Streit, A. (2004). Segregation of lens and olfactory precursors from a common territory: cell sorting and reciprocity of Dlx5 and Pax6 expression. *Dev Biol* **271**, 403-14.

Blixt, A., Mahlapuu, M., Aitola, M., Pelto-Huikko, M., Enerback, S. and Carlsson, P. (2000). A forkhead gene, FoxE3, is essential for lens epithelial proliferation and closure of the lens vesicle. *Genes Dev* **14**, 245-54.

Bovolenta, P., Mallamaci, A., Puelles, L. and Boncinelli, E. (1998). Expression pattern of cSix3, a member of the Six/sine oculis family of transcription factors. *Mech Dev* **70**, 201-3.

Bronner-Fraser, M. and Fraser, S. (1989). Developmental potential of avian trunk neural crest cells in situ. *Neuron* **3**, 755-766.

Bronner-Fraser, M. and Fraser, S. E. (1988). Cell lineage analysis reveals multipotency of some avian neural crest cells. *Nature* **335**, 161-164.

Brown, S. T., Martin, K. and Groves, A. K. (2003). Molecular basis of inner ear induction. *Curr Top Dev Biol* **57**, 115-49.

Brownell, I., Dirksen, M. and Jamrich, M. (2000). Forkhead Foxe3 maps to the dysgenetic lens locus and is critical in lens development and differentiation. *Genesis* **27**, 81-93.

Cabrera, C. V. (1990). Lateral inhibition and cell fate during neurogenesis in Drosophila: the interactions between scute, Notch and Delta. *Development* **110**, 733-42.

Calof, A. L., Hagiwara, N., Holcomb, J. D., Mumm, J. S. and Shou, J. (1996). Neurogenesis and cell death in olfactory epithelium. *J Neurobiol* **30**, 67-81.

Calof, A. L., Rim, P. C., Askins, K. J., Mumm, J. S., Gordon, M. K., Iannuzzelli, P. and Shou, J. (1998). Factors regulating neurogenesis and programmed cell death in mouse olfactory epithelium. *Ann N Y Acad Sci* **855**, 226-9.

Carpenter, E. (1937). The head pattern in Ambystoma studied by vital staining and transplantation methods. *J Exp Zool* **75**, 103-129.

Cau, E., Casarosa, S. and Guillemot, F. (2002). Mash1 and Ngn1 control distinct steps of determination and differentiation in the olfactory sensory neuron lineage. *Development* **129**, 1871-80.

Cau, E., Gradwohl, G., Casarosa, S., Kageyama, R. and Guillemot, F. (2000). Hes genes regulate sequential stages of neurogenesis in the olfactory epithelium. *Development* **127**, 2323-32.

Cau, E., Gradwohl, G., Fode, C. and Guillemot, F. (1997). Mash1 activates a cascade of bHLH regulators in olfactory neuron progenitors. *Development* **124**, 1611-21.

Chalepakis, G., Wijnholds, J., Giese, P., Schachner, M. and Gruss, P. (1994). Characterization of Pax-6 and Hoxa-1 binding to the promoter region of the neural cell adhesion molecule L1. *DNA Cell Biol* **13**, 891-900.

Chitnis, A. B. (1995). The role of Notch in lateral inhibition and cell fate specification. *Mol Cell Neurosci* **6**, 311-21.

Chow, R. L. and Lang, R. A. (2001). Early eye development in vertebrates. *Annu Rev Cell Dev Biol* **17**, 255-96.

Cohen, B., Simcox, A. A. and Cohen, S. M. (1993). Allocation of the thoracic imaginal primordia in the Drosophila embryo. *Development* **117**, 597-608.

Cohen, S. M., Bronner, G., Kuttner, F., Jurgens, G. and Jackle, H. (1989). Distal-less encodes a homoeodomain protein required for limb development in Drosophila. *Nature* **338**, 432-4.

Collinson, J. M., Hill, R. E. and West, J. D. (2000). Different roles for Pax6 in the optic vesicle and facial epithelium mediate early morphogenesis of the murine eye. *Development* **127**, 945-56.

Collinson, J. M., Quinn, J. C., Hill, R. E. and West, J. D. (2003). The roles of Pax6 in the cornea, retina, and olfactory epithelium of the developing mouse embryo. *Dev Biol* **255**, 303-12.

Corson, L. B., Yamanaka, Y., Lai, K. M. and Rossant, J. (2003). Spatial and temporal patterns of ERK signaling during mouse embryogenesis. *Development* **130**, 4527-37.

Couly, G. and Le Douarin, N. M. (1990). Head morphogenesis in embryonic avian chimeras: evidence for a segmental pattern in the ectoderm corresponding to the neuromeres. *Development* **108**, 543-58.

Couly, G. F. and Le Douarin, N. M. (1985). Mapping of the early neural primordium in quail-chick chimeras. I. Developmental relationships between placodes, facial ectoderm, and prosencephalon. *Dev Biol* **110**, 422-39.

Couly, G. F. and Le Douarin, N. M. (1987). Mapping of the early neural primordium in quail-chick chimeras. II. The prosencephalic neural plate and neural folds: implications for the genesis of cephalic human congenital abnormalities. *Dev Biol* **120**, 198-214.

Crick, F. H. and Lawrence, P. A. (1975). Compartments and polyclones in insect development. *Science* **189**, 340-347.

Crossley, P. H., Martinez, S., Ohkubo, Y. and Rubenstein, J. L. (2001). Coordinate expression of Fgf8, Otx2, Bmp4, and Shh in the rostral prosencephalon during development of the telencephalic and optic vesicles. *Neuroscience* **108**, 183-206.

Cui, W., Tomarev, S. I., Piatigorsky, J., Chepelinsky, A. B. and Duncan, M. K. (2004). Mafs, Prox1, and Pax6 can regulate chicken betaB1-crystallin gene expression. *J Biol Chem* **279**, 11088-95.

d'Amico-Martel, A. and Noden, D. M. (1980). An autoradiographic analysis of the development of the chick trigeminal ganglion. *J Embryol Exp Morphol* **55**, 167-82.

Davis, J., Duncan, M. K., Robison, W. G., Jr. and Piatigorsky, J. (2003). Requirement for Pax6 in corneal morphogenesis: a role in adhesion. *J Cell Sci* **116**, 2157-67.

Davis, J. A. and Reed, R. R. (1996). Role of Olf-1 and Pax-6 transcription factors in neurodevelopment. *J Neurosci* **16**, 5082-94.

DeHamer, M. K., Guevara, J. L., Hannon, K., Olwin, B. B. and Calof, A. L. (1994). Genesis of olfactory receptor neurons in vitro: regulation of progenitor cell divisions by fibroblast growth factors. *Neuron* **13**, 1083-97.

Depew, M. J., Liu, J. K., Long, J. E., Presley, R., Meneses, J. J., Pedersen, R. A. and Rubenstein, J. L. (1999). Dlx5 regulates regional development of the branchial arches and sensory capsules. *Development* **126**, 3831-46.

Dickinson, M. E., Selleck, M. A., McMahon, A. P. and Bronner-Fraser, M. (1995). Dorsalization of the neural tube by the non-neural ectoderm. *Development* **121**, 2099-2106.

Dimanlig, P. V., Faber, S. C., Auerbach, W., Makarenkova, H. P. and Lang, R. A. (2001). The upstream ectoderm enhancer in Pax6 has an important role in lens induction. *Development* **128**, 4415-24.

Dong, P. D., Chu, J. and Panganiban, G. (2000). Coexpression of the homeobox genes Distal-less and homothorax determines Drosophila antennal identity. *Development* **127**, 209-16.

Drapkin, P. T. and Silverman, A. J. (1999). Development of the chick olfactory nerve. *Dev Dyn* **214**, 349-60.

Dulac, C. (1997). Molecular biology of pheromone perception in mammals. *Semin Cell Dev Biol* **8**, 197-205.

Dutta, S., Dietrich, J. E., Aspock, G., Burdine, R. D., Schier, A., Westerfield, M. and Varga, Z. M. (2005). pitx3 defines an equivalence domain for lens and anterior pituitary placode. *Development* **132**, 1579-90.

Esteve, P. and Bovolenta, P. (1999). cSix4, a member of the six gene family of transcription factors, is expressed during placode and somite development. *Mech Dev* **85**, 161-5.

Faber, S. C., Dimanlig, P., Makarenkova, H. P., Shirke, S., Ko, K. and Lang, R. A. (2001). Fgf receptor signaling plays a role in lens induction. *Development* **128**, 4425-38.

Farbman, A. I. (1992). Cellular interactions in the development of the vertebrate olfactory system. In *Molecular Neurobiology of the Olfactory System,* (ed. F. L. Margolis and T. V. Getchell). New York London: Plenum Press.

Farbman, A. I. (1994). Developmental biology of olfactory sensory neurons. *Semin Cell Biol* **5**, 3-10.

Fehon, R. G., Johansen, K., Rebay, I. and Artavanis-Tsakonas, S. (1991). Complex cellular and subcellular regulation of notch expression during embryonic and imaginal development of Drosophila: implications for notch function. *J Cell Biol* **113**, 657-69.

Fernandez-Garre, P., Rodriguez-Gallardo, L., Gallego-Diaz, V., Alvarez, I. S. and Puelles, L. (2002). Fate map of the chicken neural plate at stage 4. *Development* **129**, 2807-22.

Ferrari, D., Sumoy, L., Gannon, J., Sun, H., Brown, A. M., Upholt, W. B. and Kosher, R. A. (1995). The expression pattern of the Distal-less homeobox-containing gene Dlx- 5 in the developing chick limb bud suggests its involvement in apical ectodermal ridge activity, pattern formation, and cartilage differentiation. *Mech Dev* **52**, 257-64.

Firnberg, N. and Neubuser, A. (2002). FGF signaling regulates expression of Tbx2, Erm, Pea3, and Pax3 in the early nasal region. *Dev Biol* **247**, 237-50.

Fornaro, M., Geuna, S., Fasolo, A. and Giacobini-Robecchi, M. G. (2001). Evidence of very early neuronal migration from the olfactory placode of the chick embryo. *Neuroscience* **107**, 191-7.

Fraser, S. E. (1996). Iontophoretic dye labeling of embryonic cells. *Methods Cell Biol* **51**, 147-60.

Frise, E., Knoblich, J. A., Younger-Shepherd, S., Jan, L. Y. and Jan, Y. N. (1996). The Drosophila Numb protein inhibits signaling of the Notch receptor during cell-cell interaction in sensory organ lineage. *Proc Natl Acad Sci U S A* **93**, 11925-32.

Fujiwara, M., Uchida, T., Osumi-Yamashita, N. and Eto, K. (1994). Uchida rat (rSey): A new mutant rat with craniofacial abnormalities resembling those of the mouse Sey mutant. *Differentiation* **57**, 31-38.

Furuta, Y. and Hogan, B. L. (1998). BMP4 is essential for lens induction in the mouse embryo. *Genes Dev* **12**, 3764-75.

Garcia-Bellido, A. and Merriam, J. R. (1969). Cell lineage of the imaginal discs in Drosophila gynandromorphs. *J. Exp. Zool.* **170**, 61-75.

Garcia-Bellido, A., Ripoll, P. and Morata, G. (1976). Developmental compartmentalization in the dorsal mesothoracic disc of Drosophila. *Dev Biol* **48**, 132-147.

García-Castro, M. I., Marcelle, C. and Bronner-Fraser, M. (2002). Ectodermal Wnt function as a neural crest inducer. *Science* **297**, 848-51.

Garcia-Martinez, V., Alvarez, I. S. and Schoenwolf, G. C. (1993). Locations of the ectodermal and nonectodermal subdivisions of the epiblast at stages 3 and 4 of avian gastrulation and neurulation. *J. Exp. Zool.* **267**, 431-446.

Gehring, W. J. (1996). The master control gene for morphogenesis and evolution of the eye. *Genes Cells* **1**, 11-5.

Gordon, M. K., Mumm, J. S., Davis, R. A., Holcomb, J. D. and Calof, A. L. (1995). Dynamics of MASH1 expression in vitro and in vivo suggest a non-stem cell site of MASH1 action in the olfactory receptor neuron lineage. *Mol Cell Neurosci* **6**, 363-79.

Gorfinkiel, N., Morata, G. and Guerrero, I. (1997). The homeobox gene Distal-less induces ventral appendage development in Drosophila. *Genes Dev* **11**, 2259-71.

Goulding, M. D., Lumsden, A. and Gruss, P. (1993). Signals from the notochord and floor plate regulate the region-specific expression of two Pax genes in the developing spinal cord. *Development* **117**, 1001-16.

Graham, A. and Begbie, J. (2000). Neurogenic placodes: a common front. *Trends Neurosci* **23**, 313-6.

Grainger, R. M. (1992). Embryonic lens induction: shedding light on vertebrate tissue determination. *Trends Genet* **8**, 349-55.

Greenwood, A. L., Turner, E. E. and Anderson, D. J. (1999). Identification of dividing, determined sensory neuron precursors in the mammalian neural crest. *Development* **126**, 3545-59.

Grindley, J. C., Davidson, D. R. and Hill, R. E. (1995). The role of Pax-6 in eye and nasal development. *Development* **121**, 1433-42.

Groves, A. K. and Bronner-Fraser, M. (2000). Competence, specification and commitment in otic placode induction. *Development* **127**, 3489-99.

Guillemot, F. (1995). Analysis of the role of basic-helix-loop-helix transcription factors in the development of neural lineages in the mouse. *Biol Cell* **84**, 3-6.

Guillemot, F., Lo, L. C., Johnson, J. E., Auerbach, A., Anderson, D. J. and Joyner, A. L. (1993). Mammalian achaete-scute homolog 1 is required for the early development of olfactory and autonomic neurons. *Cell* **75**, 463-76.

Guo, M., Jan, L. Y. and Jan, Y. N. (1996). Control of daughter cell fates during asymmetric division: interaction of Numb and Notch. *Neuron* **17**, 27-41.

Haggis, A. J. (1956). Analysis of the determination of the olfactory placode in ambystoma punctatum. *J Embryol Exp Morph* **4**, 120-138.

Halder, G., Callaerts, P. and Gehring, W. J. (1995). Induction of ectopic eyes by targeted expression of the eyeless gene in Drosophila. *Science* **267**, 1788-92.

Hamburger, V. and Hamilton, H. L. (1951). A series of normal stages in the development of the chick embryo. *J Morph* **88**, 49-92.

Harland, R. (2000). Neural induction. *Curr Opin Genet Dev* **10**, 357-62.
Harland, R. and Gerhart, J. (1997). Formation and function of Spemann's organizer. *Annu Rev Cell Dev Biol* **13**, 611-67.

Heitzler, P., Bourouis, M., Ruel, L., Carteret, C. and Simpson, P. (1996). Genes of the Enhancer of split and achaete-scute complexes are required for a regulatory loop between Notch and Delta during lateral signalling in Drosophila. *Development* **122**, 161-71.

Hogan, B. L., Horsburgh, G., Cohen, J., Hetherington, C. M., Fisher, G. and Lyon, M. F. (1986). Small eyes (Sey): a homozygous lethal mutation on chromosome 2 which affects the differentiation of both lens and nasal placodes in the mouse. *J Embryol Exp Morphol* **97**, 95-110.

Jacobson, A. G. (1963). The determination and positioning of the nose, lens and ear. III. Effects of reversing the antero-posterior axis of epidermis, neural plate and neural fold. *J Exp Zool* **154**, 293-303.

Jacobson, A. G. (1966). Inductive processes in embryonic development. *Science* **125**, 25-34.

Kamachi, Y., Uchikawa, M., Collignon, J., Lovell-Badge, R. and Kondoh, H. (1998). Involvement of Sox1, 2 and 3 in the early and subsequent molecular events of lens induction. *Development* **125**, 2521-32.

Kamachi, Y., Uchikawa, M., Tanouchi, A., Sekido, R. and Kondoh, H. (2001). Pax6 and SOX2 form a co-DNA-binding partner complex that regulates initiation of lens development. *Genes Dev* **15**, 1272-86.

Kammandel, B., Chowdhury, K., Stoykova, A., Aparicio, S., Brenner, S. and Gruss, P. (1999). Distinct cis-essential modules direct the time-space pattern of the Pax6 gene activity. *Dev Biol* **205**, 79-97.

Karcavich, R. E. (2005). Generating neuronal diversity in the Drosophila central nervous system: a view from the ganglion mother cells. *Dev Dyn* **232**, 609-16.

Kelley, C. G., Lavorgna, G., Clark, M. E., Boncinelli, E. and Mellon, P. L. (2000). The Otx2 homeoprotein regulates expression from the gonadotropin-releasing hormone proximal promoter. *Mol Endocrinol* **14**, 1246-56.

Knoblich, J. A. (1997). Mechanisms of asymmetric cell division during animal development. *Curr Opin Cell Biol* **9**, 833-41.

Knouff, R. A. (1935). The developmental pattern of ectodermal placodes in Rana pipiens. *J. Comp. Neurol.* **62**, 17-71.

Koster, R. W., Kuhnlein, R. P. and Wittbrodt, J. (2000). Ectopic Sox3 activity elicits sensory placode formation. *Mech Dev* **95**, 175-87.

Kozlowski, D. J., Murakami, T., Ho, R. K. and Weinberg, E. S. (1997). Regional cell movement and tissue patterning in the zebrafish embryo revealed by fate mapping with caged fluorescein. *Biochem Cell Biol* **75**, 551-62.

Krull, C. E. and Kulesa, P. M. (1998). Embryonic explant and slice preparations for studies of cell migration and axon guidance. In *Cellular and molecular procedures in developmental biology*, vol. 36 (ed. F. de Pablo A. Ferrus and C. D. Stern), pp. 145-159. San Diego: Academic Press.

Kumar, J. P. and Moses, K. (2001a). The EGF receptor and notch signaling pathways control the initiation of the morphogenetic furrow during Drosophila eye development. *Development* **128**, 2689-97.

Kumar, J. P. and Moses, K. (2001b). Expression of evolutionarily conserved eye specification genes during Drosophila embryogenesis. *Dev Genes Evol* **211**, 406-14.

Kumar, J. P. and Moses, K. (2001c). Eye specification in Drosophila: perspectives and implications. *Semin Cell Dev Biol* **12**, 469-74.

Kunisch, M., Haenlin, M. and Campos-Ortega, J. A. (1994). Lateral inhibition mediated by the Drosophila neurogenic gene delta is enhanced by proneural proteins. *Proc Natl Acad Sci U S A* **91**, 10139-43.

Kurata, S., Go, M. J., Artavanis-Tsakonas, S. and Gehring, W. J. (2000). Notch signaling and the determination of appendage identity. *Proc Natl Acad Sci U S A* **97**, 2117-22.

LaBonne, C. and Bronner-Fraser, M. (1998). Neural crest induction in *Xenopus*: evidence for a two-signal model. *Development* **125**, 2403-2414.

Ladher, R. K., Anakwe, K. U., Gurney, A. L., Schoenwolf, G. C. and Francis-West, P. H. (2000). Identification of synergistic signals initiating inner ear development. *Science* **290**, 1965-8.

Lagutin, O., Zhu, C. C., Furuta, Y., Rowitch, D. H., McMahon, A. P. and Oliver, G. (2001). Six3 promotes the formation of ectopic optic vesicle-like structures in mouse embryos. *Dev Dyn* **221**, 342-9.

LaMantia, A. S., Bhasin, N., Rhodes, K. and Heemskerk, J. (2000). Mesenchymal/epithelial induction mediates olfactory pathway formation. *Neuron* **28**, 411-25.

Lamb, T. M., Knecht, A. K., Smith, W. C., Stachel, S. E., Economides, A. N., Stahl, N., Yancopolous, G. D. and Harland, R. M. (1993). Neural induction by the secreted polypeptide noggin. *Science* **262**, 713-8.

Lawrence, P. A. and Morata, G. (1977). The early development of mesothoracic compartments in Drosophila. *Dev Biol* **56**, 40-51.

Leger, S. and Brand, M. (2002). Fgf8 and Fgf3 are required for zebrafish ear placode induction, maintenance and inner ear patterning. *Mech Dev* **119**, 91-108.

Lewis, J. (1991). Rules for the production of sensory cells. *Ciba Found Symp* **160**, 25-39; discussion 40-53.

Lewis, J. (1996). Neurogenic genes and vertebrate neurogenesis. *Curr Opin Neurobiol* **6**, 3-10.

Li, S. and Muneoka, K. (1999). Cell migration and chick limb development: chemotactic action of FGF-4 and the AER. *Dev Biol* **211**, 335-47.

Liem, K. F., Jr., Tremml, G., Roelink, H. and Jessell, T. M. (1995). Dorsal differentiation of neural plate cells induced by BMP-mediated signals from epidermal ectoderm. *Cell* **82**, 969-79.

Linker, C. and Stern, C. D. (2004). Neural induction requires BMP inhibition only as a late step, and involves signals other than FGF and Wnt antagonists. *Development* **131**, 5671-81.

Mallamaci, A., Di Blas, E., Briata, P., Boncinelli, E. and Corte, G. (1996). OTX2 homeoprotein in the developing central nervous system and migratory cells of the olfactory area. *Mech Dev* **58**, 165-78.

Maroon, H., Walshe, J., Mahmood, R., Kiefer, P., Dickson, C. and Mason, I. (2002). Fgf3 and Fgf8 are required together for formation of the otic placode and vesicle. *Development* **129**, 2099-108.

Mason, I. (2003). Fibroblast growth factors. *Curr Biol* **13**, R346.

Matsuo, T., Osumi-Yamashita, N., Noji, S., Ohuchi, H., Koyama, E., Myokai, F., Matsuo, N., Taniguchi, S., Doi, H., Iseki, S. et al. (1993). A mutation in the Pax-6 gene in rat small eye is associated with impaired migration of midbrain crest cells. *Nat. Gen.* **3**, 299-304.

McLarren, K. W., Litsiou, A. and Streit, A. (2003). DLX5 positions the neural crest and pre-placode region at the border of the neural plate. *Dev. Biol.* **259**, 34-47.

Meise, M. and Janning, W. (1991). Cell lineage and localisation of imaginal disc precursor cells in the early embryo of Drosophila. *Abstract 12th European Drosophila Research Conference*, 25.

Mishima, N. and Tomarev, S. (1998). Chicken Eyes absent 2 gene: isolation and expression pattern during development. *Int J Dev Biol* **42**, 1109-15.

Mombaerts, P., Wang, F., Dulac, C., Vassar, R., Chao, S. K., Nemes, A., Mendelsohn, M., Edmondson, J. and Axel, R. (1996). The molecular biology of olfactory perception. *Cold Spring Harb Symp Quant Biol* **61**, 135-45.

Muskavitch, M. A. (1994). Delta-notch signaling and Drosophila cell fate choice. *Dev Biol* **166**, 415-30.

Muta, M., Kamachi, Y., Yoshimoto, A., Higashi, Y. and Kondoh, H. (2002). Distinct roles of SOX2, Pax6 and Maf transcription factors in the regulation of lens-specific delta1-crystallin enhancer. *Genes Cells* **7**, 791-805.

Oliver, G., Mailhos, A., Wehr, R., Copeland, N. G., Jenkins, N. A. and Gruss, P. (1995). Six3, a murine homologue of the sine oculis gene, demarcates the most anterior border of the developing neural plate and is expressed during eye development. *Development* **121**, 4045-55.

Pandur, P. D. and Moody, S. A. (2000). Xenopus six1 gene is expressed in neurogenic cranial placodes and maintained in the differentiating lateral lines [In Process Citation]. *Mech Dev* **96**, 253-7.

Panganiban, G. and Rubenstein, J. L. (2002). Developmental functions of the Distal-less/Dlx homeobox genes. *Development* **129**, 4371-86.

Parhar, I. (2002). Cell migration and evolutionary significance of GnRH subtypes. In *Progress in Brain Research*, vol. 141 (ed. I. Parhar), pp. 3-17: Elsevier Science.

Pera, E. and Kessel, M. (1999). Expression of DLX3 in chick embryos. *Mech. Dev.* **89**, 189-93.

Pera, E., Stein, S. and Kessel, M. (1999). Ectodermal patterning in the avian embryo: epidermis versus neural plate. *Development* **126**, 63-73.

Phillips, B. T., Bolding, K. and Riley, B. B. (2001). Zebrafish fgf3 and fgf8 encode redundant functions required for otic placode induction. *Dev Biol* **235**, 351-65.

Phillips, B. T., Storch, E. M., Lekven, A. C. and Riley, B. B. (2004). A direct role for Fgf but not Wnt in otic placode induction. *Development* **131**, 923-31.

Quinn, J. C., West, J. D. and Hill, R. E. (1996). Multiple functions for Pax6 in mouse eye and nasal development. *Genes Dev* **10**, 435-46.

Quiring, R., Walldorf, U., Kloter, U. and Gehring, W. J. (1994). Homology of the eyeless gene of Drosophila to the Small eye gene in mice and Aniridia in humans. *Science* **265**, 785-9.

Reza, H. M., Ogino, H. and Yasuda, K. (2002). L-Maf, a downstream target of Pax6, is essential for chick lens development. *Mech Dev* **116**, 61-73.

Reza, H. M. and Yasuda, K. (2004). Roles of Maf family proteins in lens development. *Dev Dyn* **229**, 440-8.

Rhyu, M. S., Jan, L. Y. and Jan, Y. N. (1994). Asymmetric distribution of numb protein during division of the sensory organ precursor cell confers distinct fates to daughter cells. *Cell* **76**, 477-91.

Riley, B. B. and Phillips, B. T. (2003). Ringing in the new ear: resolution of cell interactions in otic development. *Dev Biol* **261**, 289-312.

Roegiers, F. and Jan, Y. N. (2004). Asymmetric cell division. *Curr Opin Cell Biol* **16**, 195-205.

Röhlich, K. (1931). Gestaltungsbewegungen der prasumptiven Epidermis wahrend der Neurulation und Kopfbildung bei Triton taeniatus. *Arch. EntwMech. Org.* **124**, 66-81.

Romanoff, A. L. (1960). The avian embryo. New York: Macmillan.

Rosenquist, G. C. (1966). A radioautographic study of labeled grafts in the chick blastoderm. In *Contributions to Embryology*, vol. 38, pp. 73-110. Washington: Carnegie Inst.

Rosenquist, G. C. (1981). Epiblast origin and early migration of neural crest cells in the chick embryo. *Dev Biol* **87**, 201-11.

Rudnick, D. (1944). Early history and mechanics of the chick blastoderm. *Quart Rev Biol* **19**, 187-212.

Ruiz i Altaba, A., Warga, R. M. and Stern, C. D. (1993). Fate maps and cell lineage analysis. In *Essential Developmental Biology: A practical approach*, (ed. C. D. Stern and P. W. H. Holland), pp. 81-95. Oxford: Oxford University Press.

Sahly, I., Andermann, P. and Petit, C. (1999). The zebrafish eya1 gene and its expression pattern during embryogenesis. *Dev Genes Evol* **209**, 399-410.

Sasai, Y., Lu, B., Steinbeisser, H., Geissert, D., Gont, L. K. and De Robertis, E. M. (1994). Xenopus chordin: a novel dorsalizing factor activated by organizer-specific homeobox genes. *Cell* **79**, 779-90.

Schlosser, G. and Ahrens, K. (2004). Molecular anatomy of placode development in Xenopus laevis. *Dev Biol* **271**, 439-66.

Schlosser, G. and Northcutt, R. G. (2000). Development of neurogenic placodes in Xenopus laevis. *J Comp Neurol* **418**, 121-46
.

Schwanzel-Fukuda, M. and Pfaff, D. W. (1989). Origin of luteinizing hormone-releasing hormone neurons. *Nature* **338**, 161-4.

Schweisguth, F. (1995). Suppressor of Hairless is required for signal reception during lateral inhibition in the Drosophila pupal notum. *Development* **121**, 1875-84.

Selleck, M. A. and Bronner-Fraser, M. (1995). Origins of the avian neural crest: the role of neural plate-epidermal interactions. *Development* **121**, 525-38.

Shah, N. M. and Anderson, D. J. (1997). Integration of multiple instructive cues by neural crest stem cells reveals cell-intrinsic biases in relative growth factor responsiveness. *Proc Natl Acad Sci U S A* **94**, 11369-74.

Shah NM, G. A., Anderson DJ. (1996). Alternative neural crest cell fates are instructively promoted by TGFbeta superfamily members. *Cell* **85**, 331-343.

Shah, N. M., Marchionni, M. A., Isaacs, I., Stroobant, P. and Anderson, D. J. (1994). Glial growth factor restricts mammalian neural crest stem cells to a glial fate. *Cell* **77**, 349-360.

Shimada, N., Aya-Murata, T., Reza, H. M. and Yasuda, K. (2003). Cooperative action between L-Maf and Sox2 on delta-crystallin gene expression during chick lens development. *Mech Dev* **120**, 455-65.

Slack, J. M. W. (1991). From Egg to Embryo: Regional Specification in Early Development. Cambridge: Cambridge University Press.

Smith, J. L. and Schoenwolf, G. C. (1987). Cell cycle and neuroepithelial cell shape during bending of the chick neural plate. *Anat Rec* **218**, 196-206.

Solomon, K. S. and Fritz, A. (2002). Concerted action of two dlx paralogs in sensory placode formation. *Development* **129**, 3127-36.

Soudais, C., Bielinska, M., Heikinheimo, M., MacArthur, C. A., Narita, N., Saffitz, J. E., Simon, M. C., Leiden, J. M. and Wilson, D. B. (1995). Targeted mutagenesis of the transcription factor GATA-4 gene in mouse embryonic stem cells disrupts visceral endoderm differentiation in vitro. *Development* **121**, 3877-88.

Spana, E. P. and Doe, C. Q. (1996). Numb antagonizes Notch signaling to specify sibling neuron cell fates. *Neuron* **17**, 21-6.

Spemann, H. and Mangold, H. (1924). Uber Induktion von Embryonanlagen dürch Implantation artfremder Organisatoren. *Arch. mikr. Anat. EntwMech.* **100**, 599-638.

Stark, M. R., Sechrist, J., Bronner-Fraser, M. and Marcelle, C. (1997). Neural tube-ectoderm interactions are required for trigeminal placode formation. *Development* **124**, 4287-95.

Steiner, E. (1976). Establishment of compartments in the developing leg imaginal discs of *Drosophila melanogaster*. *Wilh. Roux's Arch. Dev. Biol.* **180**, 9-30.

Stern, C. D. and Fraser, S. E. (2001). Tracing the lineage of tracing cell lineages. *Nat Cell Biol* **3**, E216-8.

Stern, C. D., Fraser, S. E., Keynes, R. J. and Primmett, D. R. (1988). A cell lineage analysis of segmentation in the chick embryo. *Development* **104 Suppl**, 231-44.

Sternberg, P. W. (1988). Lateral inhibition during vulval induction in Caenorhabditis elegans. *Nature* **335**, 551-4.

Stoykova, A., Gotz, M., Gruss, P. and Price, J. (1997). Pax6-dependent regulation of adhesive patterning, R-cadherin expression and boundary formation in developing forebrain. *Development* **124**, 3765-77.

Streit, A. (2001). Origin of the vertebrate inner ear: evolution and induction of the otic placode. *J Anat* **199**, 99-103.

Streit, A. (2002). Extensive cell movements accompany formation of the otic placode. *Dev Biol* **249**, 237-54.

Streit, A. (2004). From a common territory to individual identity- sensory placode formation in vertebrates.

Streit, A., Berliner, A. J., Papanayotou, C., Sirulnik, A. and Stern, C. D. (2000). Initiation of neural induction by FGF signalling before gastrulation. *Nature* **406**, 74-8.

Streit, A., Lee, K. J., Woo, I., Roberts, C., Jessell, T. M. and Stern, C. D. (1998). Chordin regulates primitive streak development and the stability of induced neural cells, but is not sufficient for neural induction in the chick embryo. *Development* **125**, 507-19.

Streit, A., Sockanathan, S., Perez, L., Rex, M., Scotting, P. J., Sharpe, P. T., Lovell-Badge, R. and Stern, C. D. (1997). Preventing the loss of competence for neural induction: HGF/SF, L5 and Sox-2. *Development* **124**, 1191-202.

Streit, A. and Stern, C. D. (1999). Neural induction. A bird's eye view. *Trends Genet* **15**, 20-4.

Sunkel, C. E. and Whittle, J. R. S. (1987). Brista: A gene involved in the specification and differentiation of distal cephalic and thoracic structures in Drosophila melanogaster. *Wilh. Roux's Arch. Dev. Biol.* **196**, 124-132.

Szabad, J., Schupbach, T. and Wieschaus, E. (1979). Cell lineage and development in the larval epidermis of *Drosophila melanogaster*. *Dev Biol* **73**, 256-271.

Thery, C. and Stern, C. D. (1996). Roles of kringle domain-containing serine proteases in epithelial- mesenchymal transitions during embryonic development. *Acta Anat* **156**, 162-72.

Tyas, D. A., Pearson, H., Rashbass, P. and Price, D. J. (2003). Pax6 regulates cell adhesion during cortical development. *Cereb Cortex* **13**, 612-9.

Uchikawa, M., Ishida, Y., Takemoto, T., Kamachi, Y. and Kondoh, H. (2003). Functional analysis of chicken Sox2 enhancers highlights an array of diverse regulatory elements that are conserved in mammals. *Dev Cell* **4**, 509-19.

Uwanogho, D., Rex, M., Cartwright, E. J., Pearl, G., Healy, C., Scotting, P. J. and Sharpe, P. T. (1995). Embryonic expression of the chicken Sox2, Sox3 and Sox11 genes suggests an interactive role in neuronal development. *Mech Dev* **49**, 23-36.

van Heyningen, V. and Williamson, K. A. (2002). PAX6 in sensory development. *Hum Mol Genet* **11**, 1161-7.

van Wijhe, J. W. (1883). Uber die Mesodermsegmente und die Entwicklung der Nerven des Selachierkopfes. *Verhandelingen der Koninklijke Akademie van Wetenschappen (Amsterdam)* **22(E)**, 1-50.

Vassar, R., Chao, S. K., Sitcheran, R., Nunez, J. M., Vosshall, L. B. and Axel, R. (1994). Topographic organization of sensory projections to the olfactory bulb. *Cell* **79**, 981-91.

Verdi, J. M., Bashirullah, A., Goldhawk, D. E., Kubu, C. J., Jamali, M., Meakin, S. O. and Lipshitz, H. D. (1999). Distinct human NUMB isoforms regulate differentiation vs. proliferation in the neuronal lineage. *Proc Natl Acad Sci U S A* **96**, 10472-6.

Verdi, J. M., Schmandt, R., Bashirullah, A., Jacob, S., Salvino, R., Craig, C. G., Program, A. E., Lipshitz, H. D. and McGlade, C. J. (1996). Mammalian NUMB is an evolutionarily conserved signaling adapter protein that specifies cell fate. *Curr Biol* **6**, 1134-45.

Verwoerd, C. D. and van Oostrom, C. G. (1979). Cephalic neural crest and placodes. *Adv Anat Embryol Cell Biol* **58**, 1-75.

Wakamatsu, Y., Maynard, T. M., Jones, S. U. and Weston, J. A. (1999). NUMB localizes in the basal cortex of mitotic avian neuroepithelial cells and modulates neuronal differentiation by binding to NOTCH-1. *Neuron* **23**, 71-81.

Wakamatsu, Y., Maynard, T. M. and Weston, J. A. (2000). Fate determination of neural crest cells by NOTCH-mediated lateral inhibition and asymmetrical cell division during gangliogenesis. *Development* **127**, 2811-21.

Walshe, J. and Mason, I. (2000). Expression of FGFR1, FGFR2 and FGFR3 during early neural development in the chick embryo. *Mech Dev* **90**, 103-10.

Walther, C. and Gruss, P. (1991). Pax-6, a murine paired box gene, is expressed in the developing CNS. *Development* **113**, 1435-49.

Wang, F., Nemes, A., Mendelsohn, M. and Axel, R. (1998). Odorant receptors govern the formation of a precise topographic map. *Cell* **93**, 47-60.

Wawersik, S., Purcell, P. and Maas, R. L. (2000). Pax6 and the genetic control of early eye development. *Results Probl Cell Differ* **31**, 15-36.

Wawersik, S., Purcell, P., Rauchman, M., Dudley, A. T., Robertson, E. J. and Maas, R. (1999). BMP7 acts in murine lens placode development. *Dev Biol* **207**, 176-88.

Wetts, R., Serbedzija, G. N. and Fraser, S. E. (1989). Cell lineage analysis reveals multipotent precursors in the ciliary margin of the frog retina. *Dev Biol* **136**, 254-63.

Whitlock, K. E. and Westerfield, M. (2000). The olfactory placodes of the zebrafish form by convergence of cellular fields at the edge of the neural plate. *Development* **127**, 3645-53.

Whitlock, K. E., Wolf, C. D. and Boyce, M. L. (2003). Gonadotropin-releasing hormone (GnRH) cells arise from cranial neural crest and adenohypophyseal regions of the neural plate in the zebrafish, Danio rerio. *Dev Biol* **257**, 140-52.

Wieschaus, E. and Gehring, W. J. (1976). Clonal analysis of primordial disc cells in the early embryo of *Drosophila melanogaster*. *Dev Biol* **50**, 249-263.

Williams, S. C., Altmann, C. R., Chow, R. L., Hemmati-Brivanlou, A. and Lang, R. A. (1998). A highly conserved lens transcriptional control element from the Pax-6 gene. *Mech Dev* **73**, 225-9.

Wilson, S. I. and Edlund, T. (2001). Neural induction: toward a unifying mechanism. *Nat Neurosci* **4 Suppl**, 1161-8.

Wilson, S. I., Graziano, E., Harland, R., Jessell, T. M. and Edlund, T. (2000). An early requirement for FGF signalling in the acquisition of neural cell fate in the chick embryo. *Curr Biol* **10**, 421-9.

Wilson, S. I., Rydstrom, A., Trimborn, T., Willert, K., Nusse, R., Jessell, T. M. and Edlund, T. (2001). The status of Wnt signalling regulates neural and epidermal fates in the chick embryo. *Nature* **411**, 325-30.

Woda, J. M., Pastagia, J., Mercola, M. and Artinger, K. B. (2003). Dlx proteins position the neural plate border and determine adjacent cell fates. *Development* **130**, 331-42.

Wray, S. (2002). Development of gonadotropin-releasing hormone-1 neurons. *Front Neuroendocrinol* **23**, 292-316.

Wright, T. J. and Mansour, S. L. (2003a). Fgf3 and Fgf10 are required for mouse otic placode induction. *Development* **130**, 3379-90.

Wright, T. J. and Mansour, S. L. (2003b). FGF signaling in ear development and innervation. *Curr Top Dev Biol* **57**, 225-59.

Wu, J. and Cohen, S. M. (1999). Proximodistal axis formation in the Drosophila leg: subdivision into proximal and distal domains by Homothorax and Distal-less. *Development* **126**, 109-17.

Xu, P. X., Woo, I., Her, H., Beier, D. R. and Maas, R. L. (1997). Mouse Eya homologues of the Drosophila eyes absent gene require Pax6 for expression in lens and nasal placode. *Development* **124**, 219-31.

Yamada, R., Mizutani-Koseki, Y., Hasegawa, T., Osumi, N., Koseki, H. and Takahashi, N. (2003). Cell-autonomous involvement of Mab21l1 is essential for lens placode development. *Development* **130**, 1759-1770.

Yang, X., Dormann, D., Munsterberg, A. E. and Weijer, C. J. (2002). Cell movement patterns during gastrulation in the chick are controlled by positive and negative chemotaxis mediated by FGF4 and FGF8. *Dev Cell* **3**, 425-437.

Zerucha, T., Stuhmer, T., Hatch, G., Park, B. K., Long, Q., Yu, G., Gambarotta, A., Schultz, J. R., Rubenstein, J. L. and Ekker, M. (2000). A highly conserved enhancer in the Dlx5/Dlx6 intergenic region is the site of cross-regulatory interactions between Dlx genes in the embryonic forebrain. *J Neurosci* **20**, 709-21.

Zhang, X., Friedman, A., Heaney, S., Purcell, P. and Maas, R. L. (2002). Meis homeoproteins directly regulate Pax6 during vertebrate lens morphogenesis. *Genes Dev* **16**, 2097-107.

Zhong, W., Feder, J. N., Jiang, M. M., Jan, L. Y. and Jan, Y. N. (1996). Asymmetric localization of a mammalian numb homolog during mouse cortical neurogenesis. *Neuron* **17**, 43-53.

Zhong, W., Jiang, M. M., Weinmaster, G., Jan, L. Y. and Jan, Y. N. (1997). Differential expression of mammalian Numb, Numblike and Notch1 suggests distinct roles during mouse cortical neurogenesis. *Development* **124**, 1887-97.

Zhu, C. C., Dyer, M. A., Uchikawa, M., Kondoh, H., Lagutin, O. V. and Oliver, G. (2002). Six3-mediated auto repression and eye development requires its interaction with members of the Groucho-related family of co-repressors. *Development* **129**, 2835-49.

Zilian, O., Saner, C., Hagedorn, L., Lee, H. Y., Sauberli, E., Suter, U., Sommer, L. and Aguet, M. (2001). Multiple roles of mouse Numb in tuning developmental cell fates. *Curr Biol* **11**, 494-501.